



NTNU – Trondheim
Norwegian University of
Science and Technology

Modelling and Improvement of Transient Operations in CO₂ Injection Wells

Ole Kristian Gjertsen

Master of Energy and Environmental Engineering

Submission date: June 2014

Supervisor: Philip Ringrose, EPT

Co-supervisor: Gelein de Koeijer, Statoil
Even Solbraa, EPT

Norwegian University of Science and Technology
Department of Energy and Process Engineering

EPT-M-2014-35

MASTER THESIS

for

Student Ole Kristian Gjertsen

Spring 2014

Modelling and Improvement of transient operations in CO₂ injection wells*Modellering og Forbedring av Transiente Operasjoner i CO₂ injeksjonsbrønner***Background and objective**

Utilizing knowledge on transient flow in CO₂ wells is important for the improved operation and design of CO₂ Capture and Storage (CCS) systems. Besides accidents, controlled transient flow occurs during well operations like shut-ins, step-rate tests and leak-offs. These operations are well known in the oil & gas industry and are considered to be useful for deducing reservoir and well properties from the pressure and temperature behaviour over time. The pressure and temperature will respond to these operations in different time-scales, e.g. a pressure wave is much faster than heat transfer. Most information is deduced by operations that enable analysing the physical phenomena at different time scales. However, these operations are not yet systematically studied for CO₂ injection wells. They are expected to be particularly useful for innovations on injecting other components like water, hydrocarbons and N₂ alternating with CO₂. Such co-injections seem promising for enhanced oil recovery or for improving storage capacity. For design of above mentioned operations for these co-injections models are needed. In recent years many models have been published, of which OLGA seems to emerge as a commercially available benchmark. It is aimed to use one or more of these tools for modelling these operations. The purpose of this work becomes to gain more understanding of transient operation in various types of CO₂ injection wells. The study should result in improved operations for getting most useful knowledge for reservoir and fluid characterizations using characteristic timescales of different thermal and pressure phenomena.

The following tasks are to be considered:

1. Literature review of all types on CO₂ injection wells (offshore, onshore, EOR, saline aquifer, depleted gas field, fracking).
2. Literature review of shut-ins and leak-off tests emphasizing on what is special about CO₂ relative to hydrocarbons, mud and water. Describe common practice.
3. Assess tools for simulating transient operations with other components (CO₂ alternating H₂O, hydrocarbon and/or nitrogen). OLGA is a main candidate.
4. Simulate transient behavior in CO₂ injection wells with different components with preferred tool on preferred types of wells:
 - a. Shut-ins
 - b. Simple and extended leak-off tests
 - c. Step-rate tests
5. Assess equations of state to be used for pure CO₂ and mixtures (Span-Wagner, SRK and/or PR)

6. Improve operations for getting most useful knowledge for reservoir and fluid characterizations using characteristic timescales of different thermal and pressure phenomena
7. Uncertainty analysis

-- ” --

Within 14 days of receiving the written text on the master thesis, the candidate shall submit a research plan for his project to the department.

When the thesis is evaluated, emphasis is put on processing of the results, and that they are presented in tabular and/or graphic form in a clear manner, and that they are analysed carefully.

The thesis should be formulated as a research report with summary both in English and Norwegian, conclusion, literature references, table of contents etc. During the preparation of the text, the candidate should make an effort to produce a well-structured and easily readable report. In order to ease the evaluation of the thesis, it is important that the cross-references are correct. In the making of the report, strong emphasis should be placed on both a thorough discussion of the results and an orderly presentation.

The candidate is requested to initiate and keep close contact with his/her academic supervisor(s) throughout the working period. The candidate must follow the rules and regulations of NTNU as well as passive directions given by the Department of Energy and Process Engineering.

Risk assessment of the candidate's work shall be carried out according to the department's procedures. The risk assessment must be documented and included as part of the final report. Events related to the candidate's work adversely affecting the health, safety or security, must be documented and included as part of the final report. If the documentation on risk assessment represents a large number of pages, the full version is to be submitted electronically to the supervisor and an excerpt is included in the report.

Pursuant to “Regulations concerning the supplementary provisions to the technology study program/Master of Science” at NTNU §20, the Department reserves the permission to utilize all the results and data for teaching and research purposes as well as in future publications.

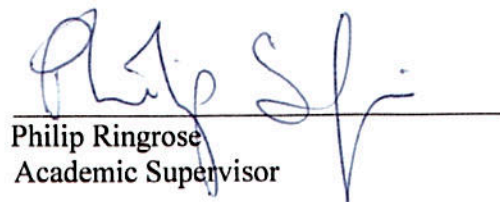
The final report is to be submitted digitally in DAIM. An executive summary of the thesis including title, student's name, supervisor's name, year, department name, and NTNU's logo and name, shall be submitted to the department as a separate pdf file. Based on an agreement with the supervisor, the final report and other material and documents may be given to the supervisor in digital format.

- Work to be done in lab (Water power lab, Fluids engineering lab, Thermal engineering lab)
- Field work

Department of Energy and Process Engineering, 14. January 2014



Olav Bolland
Department Head



Philip Ringrose
Academic Supervisor

Research Advisor:

Even Solbraa, NTNU/Statoil, Gelein de Koeijer, Statoil (main supervisor)

Abstract

Transient well operations such as shut-in, leak-off and step-rate tests are well known in the oil and gas industry, and considered to be useful in deducing reservoir and well properties by studying pressure and temperature behavior over time. Although these tests are routinely used in conventional oil and gas wells, little research on their behavior or possible application to CO₂ storage operations has been performed. The primary aim of this work has been to study shut-in and step-rate tests in CO₂ injection wells. This has been done through collecting and comparing published data and experiences, and by performing simulations. The multiphase flow simulator OLGA was used to build a saline aquifer injection well model, in which shut-in and step-rate tests were simulated. In addition, the OLGA model was used to simulate water alternating CO₂ (WAG) injection, which is used in enhanced oil recovery (EOR). The aim of the WAG simulations was to investigate what pressure and temperature responses can be expected in the well during WAG injection. The published data found on shut-in and step-rate tests showed the importance of the well being thermally stable before the tests are commenced, and enough fluid having been injected before test start to mitigate any near well skin effects. The OLGA model was used to successfully history match the bottom hole data from one step rate test, with partial success in matching wellhead data. It was not found possible to match the bottom hole data of a shut-in test performed on the same well, casting doubt on OLGA's ability to simulation injection well shut-ins. In addition to being a first published attempt of WAG simulations with OLGA, the simulation results highlighted the differences in time scales on which pressure and temperature operates in an injection well. While pressure effects were found to stabilize quickly, temperature effects were found to work on a substantially longer time scale. The literature study and simulations have together resulted in a set of recommendations for how to obtain improved results from from shut-in and step-rate tests.

Sammendrag

Transiente brønn-operasjoner, som "shut-in" og "step-rate" tester, er godt dokumentert innen olje- og gas-industrien og ansett som nyttige for reservoir- og brønnklassifisering gjennom analyse av trykk- og temperatur respons over tid. Selv om disse testene er rutinemessig brukt i konvensjonelle olje- og gassbrønner, har det blitt gjort lite forskning på nytte og mulig bruk for CO₂ lagring. Denne masteroppgaven har hatt som hovedintensjon å studere "shut-in" og "step-rate" tester i CO₂-injeksjonsbrønner. Dette har blitt gjort gjennom å samle og sammenligne publisert data, og gjennom simuleringer. Flerfasestrømningssimulatoren "OLGA" har blitt brukt til å modellere en injeksjonsbrønn, hvor "shut-in" og "step-rate" tester har blitt simulert. OLGA-modellen har også blitt brukt til simulere vann-vekslende-CO₂-injeksjon (WAG), som brukes innen økt oljeutvinning (EOR). Formålet med WAG simuleringene har vært å undersøke hvilke trykk- og temperatur-responser som kan forventes i brønnen under WAG-injeksjon. Tidligere publisert data på "step-rate" og "shut-in" tester viste viktigheten av at brønnen var termisk stabil før testene ble startet, og at nok væske hadde blitt injisert på forhånd til å minimere eventuelle skin-effekter. OLGA-modellen ble med suksess brukt til å replikere målt bunnhullsdata fra en "step-rate" test, med delvis suksess i replikasjon av brønnhodedata. Modellen var ikke istand til å replikere bunnhullsdata fra en "shut-in" utført i samme brønn, noe som sår tvil ved OLGAs evne til å modellere "shut-ins". I tillegg til være et første publisert forsøk på modellering av WAG-injeksjon med OLGA, fremhevet simuleringresultatene forskjellen i tids-skala som trykk og temperatur operer på i en injeksjonsbrønn. Trykkeffektene viste seg å stabiliseres raskt, mens temperatureffektene trengte adskillig mer tid for å stabiliseres. Litteraturstudien har sammen med simuleringene blitt brukt til å utarbeide et sett med anbefalinger for hvordan "shut-in" og "step-rate" tester best kan utføres.

Acknowledgements

I would like to use this opportunity to thank a select few people who, through my work with this thesis, have aided me both academically and on a personal level. First and foremost I would like to thank Statoil and my supervisor Gelein de Koeijer from which I have learned a great deal about CCS, research and academic writing. He has always been able to take time out of a busy schedule to discuss and answer questions. I would also like to thank Olav Hansen for his time and effort in helping me understand the workings of wells. Lastly I would like to thank Tor Arild Melby for his company and the fruitful discussions we have had during the last year.

Contents

| | | |
|----------|--|-----------|
| 1 | Problem Description | 4 |
| 2 | Literature Review | 6 |
| 2.1 | Reservoir Storage Options and CO ₂ Uses in CCS | 6 |
| 2.1.1 | Aquifer Storage | 6 |
| 2.1.2 | Depleted Gas Fields | 8 |
| 2.1.3 | CO ₂ Enhanced Oil Recovery | 9 |
| 2.1.4 | Hydraulic Fracturing of Shale Formations Using CO ₂ | 12 |
| 2.2 | Simulation Tools | 14 |
| 2.2.1 | OLGA | 14 |
| 2.2.2 | LedaFlow | 16 |
| 2.2.3 | TACITE | 16 |
| 2.3 | Shut-In Test | 17 |
| 2.4 | Step-Rate Test | 19 |
| 2.5 | Leak-Off Test | 20 |
| 2.6 | Literature Review Discussion | 21 |
| 3 | Theory | 25 |
| 3.1 | Carbon Dioxide Properties | 25 |
| 3.2 | Equation of State | 25 |
| 3.2.1 | Pure CO ₂ | 25 |
| 3.2.2 | CO ₂ with Impurities | 27 |
| 4 | OLGA Simulations | 32 |
| 4.1 | OLGA Well Model and Properties | 36 |
| 4.2 | Documented Operations at State Charlton | 39 |
| 4.3 | OLGA Simulations Description | 44 |
| 4.4 | Simulation Results | 46 |
| 4.4.1 | Mechanical Integrity Test | 46 |
| 4.4.2 | 2nd Step-Rate Test | 55 |
| 4.4.3 | 2nd Step-Rate Test Heat Sensitivity | 57 |
| 4.5 | Discussion | 60 |
| 4.5.1 | Mechanical Integrity Test | 60 |
| 4.5.2 | 2nd Step Rate Test | 63 |
| 4.5.3 | Second Step-Rate Test Heat Sensitivity | 66 |
| 5 | WAG Injection Simulations | 68 |
| 5.1 | OLGA Simulations Description | 69 |
| 5.2 | Simulation Results | 69 |

| | |
|---|------------|
| 5.3 Discussion | 75 |
| 6 Uncertainty Analysis | 79 |
| 7 Conclusion | 81 |
| 8 Recommendations for Further Work | 84 |
| A Appendix | 95 |
| A.1 Mechanical Injection Test | 95 |
| B | 95 |
| B.1 Two-phase profile plot | 95 |
| B.2 Temperature profile plot of shut-in | 97 |
| C | 98 |
| C.1 BH Temperature Response Shut-In, Variable Cp | 98 |
| D | 99 |
| D.1 Excel-graph re-make | 99 |
| E EOR | 102 |
| E.1 EOS Comparison | 102 |
| E.2 BH Temperature comparison MIT | 102 |
| E.3 24hour injection cycle | 103 |
| E.4 4 hour injection cycle | 105 |
| E.5 WAG Shut-in | 107 |
| E.6 WAG, Water as first injection medium | 108 |
| E.7 H ₂ O and CO ₂ densities. 80[bar], 10-30°C. | 109 |
| E.8 OLGA Input Specifications Report | 110 |

Nomenclature

BH - Bottom Hole

BHP - Bottom Hole Pressure

BOPD - Barrels of Oil Per Day

CCS - CO₂ Capture and Storage

EOR - Enhanced Oil Recovery

IOR - Increased Oil Recovery

MD - Measured Depth

MMP - Minimum Miscible Pressure

OOIP - Original Oil In Place

SWAG - Simultaneous Water Alternating Gas

TVD - True Vertical Depth

WAG - Water Alternating Gas

WH - Well Head

WHP - Well Head Pressure

f_D - Darcy friction factor

h_f - Head loss due to friction

1 Problem Description

CO₂ capture and storage is by many considered to be an important part of achieving a low carbon future and mitigating global climate change. According to the International Energy Agency (IEA) In the International Energy Agency's scenario for reaching a long term global average temperature rise of maximum 2°C, CCS is widely deployed in both power generation and industrial application, and state that "CCS is an integral part of any lowest-cost mitigation scenario where long-term global average temperature increase are limited to significantly less than 4°C, particularly for the 2°C scenario" [62]. Although some large scale CO₂ storage projects already exist, much more is needed if CCS is to be effective in combating climate change. Following IEA's 2°C scenario, CCS needs to be routinely implemented in power generation and industry by 2030. If this is to happen, a solid understanding of flow phenomena in the well and the well-reservoir interface is necessary to improve design and operations of injection wells. Compared to conventional oil & gas wells, the practice of CO₂ injection is relatively new and the amount of published studies and practical experiences are limited.

An important difference between CO₂ and oil, water or hydrocarbon gas is the phase behavior. The CO₂ critical point is at 78.3[bar] and 31.1°C, and can under normal operating well conditions be gas, liquid or supercritical phase. A prime example is the Sleipner injection well, where the CO₂ is gas/liquid two-phase at wellhead and supercritical at bottom hole.

Shut-in and step-rate tests are considered to be useful tools in traditional oil & gas industry to evaluate well and reservoir performance. However, these tests have not yet been systematically studied for CO₂ injection wells. It is therefore considered valuable to examine these tests' applicability for CO₂ injection wells. Expanding knowledge on these tests for CO₂ injection wells can validate their usefulness and help improve operations. History matching of measured data from step-rate and shut-in tests through OLGA simulations can help validate the simulators ability to model these operations. These simulations allow for experimentation, for example to see how different pressures or temperatures affect the tests. Simulations can also help unveil potential problems that might occur and optimize the injection and testing procedures.

In addition to geological storing of CO₂ for environmental purposes, CO₂ injection is also used as a technique for enhancing oil recovery of mature oil fields. CO₂ can act as a solvent by decreasing the viscosity and thereby increasing the flowability of the oil. This extraction method is already in

use and is often combined with water injection. Two active large scale examples of CO₂ and water injection are the Lula field offshore Brasil and the Weyburn field in Canada. The published knowledge on CO₂ combined with water injection is however limited, and studies on how this operation can most effectively be performed can help increase performance.

In this thesis a literature review will be performed, with a main focus on collecting and comparing results and field experiences from performed shut-in and step-rate tests. The literature study will also review different geological storage options for CCS, CO₂ used for enhanced oil recovery, possible numerical simulation tools for CO₂ injection wells and equations of state relevant to CCS operations. Based on the results of the literature review on simulation tools, a simulator will be chosen and used to model different CO₂ injection operations. The simulations will include shut-ins, step-rate tests and WAG injection. The simulators ability to model these operations will be evaluated and the simulation results will also be used to assess possible improvements to test operations.

This thesis aims to expand the current understanding of transient CO₂ injection well operations and the usefulness of simulations in assessing these operations. It is the goal of this work to result in improved practices of transient operations in order to maximize the usefulness of transient operations in CO₂ injection wells.

2 Literature Review

2.1 Reservoir Storage Options and CO₂ Uses in CCS

This section will summarize different uses and storage options of CO₂ related to CCS. The first two subsections discuss two options for pure geological storage: saline aquifers and depleted gas fields. Differences and advantages of the two options will be discussed. The two following subsections will discuss two uses of CO₂ where geological storage can be combined with enhanced hydrocarbon extraction. Published experiences from field tests and simulations of step-rate tests, shut-ins and leak-off tests in CO₂ injection wells will be discussed, focusing on common practices and usefulness of each operation. A review of some relevant multiphase flow simulators will be performed, with a focus on their ability to handle CO₂. The review will conclude with a choice of simulator to be used for the simulations in this thesis.

2.1.1 Aquifer Storage

Most large scale CCS projects to date have used saline aquifers as storage formations, with the Sleipner project in the Norwegian North Sea being an example. Sleipner was the first commercial scale CO₂ storage site, and has been operational since 1996 with a yearly injection rate of approximately $1[\frac{MtCO_2}{year}]$. The produced gas at Sleipner has a CO₂ content of 9 mole%, which has to be reduced to meet export quality specifications. This is done by an amine plant, before the CO₂ is reinjected in the Utsira saline aquifer sandstone formation. The storage reservoir is located approximately 1000[m TVD MSL] and has shown to be well suited for injection with excellent porosity and permeability. The injection well is near vertical down to 600[m TVD RKB], but is from that point highly deviated with a sail angle of 83°. The total length of the well is over 3[km] [27] and has its only gauges installed at WH, where pressure, temperature and flow rate is measured. Due to a relatively low WH pressure and a CO₂ WH temperature of 25°C, the upper part of the well is in two-phase gas/liquid state. It has been estimated that the WH void fraction is 70-85 vol% during normal operating conditions by Gjertsen [22], Lindeberg [40] and Thu [57]. The CO₂ purity is 93-96 vol% , with 0.5-2% hydrocarbons. As of June 2014, the Sleipner CO₂ injection project is still active.

The In-Salah project in Algeria is a onshore CCS project ran by BP, Sonatrach and Statoil. Injection was started in 2004 and 3.8 million tons were stored

before injection was suspended in 2011. As with the Sleipner project, CO₂ is removed from the hydrocarbon production stream by an amine plant to meet export specifications. The CO₂ is compressed and reinjected into the Carboniferous sandstone formation, 1.9[km] below ground level. The storage formation system was low-permeability, faulted and fractured. Three long-reach horizontal injection wells were used. Multiple monitoring techniques were used, including time-lapse seismic, micro-seismic, wellhead sampling of CO₂ gas tracers, down-hole logging and Interferometric Synthetic Aperture Radar (InSAR)[48]. Future injection plans at In-Salah are uncertain [47].

A third large scale CCS project using saline aquifer for geological storage is the Snøhvit project in northern Norway, where CO₂ has been injected since 2008. The natural gas stream contains 5-8 mol% CO₂ and is liquified for transport purposes. Before the liquefaction process, the CO₂ content has to be reduced to less than 50ppm. The separated CO₂ is transported to through a 170[km] long pipeline to a subsea template at the Snøhvit field, 318[m] below sea level. The injection well is deviated, with a maximum inclination of 27°, with both WH and down-hole pressure and temperature gauges. The down-hole gauge is located 1782[m] below sea level, and approximately 800[m TVD] above the perforations. The original storage formation was the Tubåen sandstone formation 2600[m TVD MSL], however due to a rapid pressure increase believed to be caused by salt precipitation, the connection to Tubåen was sealed in 2011. The same well was then re-perforated at a shallower level and backup reservoir, Stø, was utilized. As of 2013, CO₂ was still being re-injected into Stø. The injected CO₂ contains no free water and has only very small amounts of hydrocarbons, and is in supercritical phase from the on-shore CO₂ discharge pump to the geological storage formation. The original plans for the Snøhvit CO₂ storage project was documented by Maldal and Tappel [42]. Hansen et.al. documented the history of the Tubåen injection operation[29].

Combined Sleipner, Snøhvit and In-Salah had by 2010 disposed of over 16[*MtCO*₂], from which Eiken et.al. documented operational experiences and lessons learned. In addition to the before-mentioned active projects the Gorgon project offshore Australia is set to start injection in 2015, and is planned to dispose of a total CO₂ amount of 120[*Mt*] [19].

2.1.2 Depleted Gas Fields

Storing of CO₂ in depleted gas fields is one of the major scenarios being considered for CCS. Using depleted gas fields for storage gives some significant advantages. The geology, sealing properties and capacity of the reservoir is likely to be well known, due to its former use as a natural gas production field. Also, the possibility of using already existing infrastructure can contribute to cost reductions. Depleted gas fields are characterized by low pressures, due to the natural gas that has been removed during the production stage. According to Oldenburg et.al. [44] pressures in depleted gas reservoirs typically 20-50[bar] with temperatures of 27-120[°C].

The theoretical maximum storage capacity of depleted gas fields was in 2000 estimated to be 797[GtCO₂] by the IEA, and in a separate report from 2009 calculated, with 90% certainty, to be within the range of 506-1300[GtCO₂]. The mean of the before-mentioned range was 870[GtCO₂] [36].

The literature review found no active large scale CCS projects with depleted gas field storage. However, two large scale projects using depleted gas field storage with planned injection start before 2020 are reviewed below.

The ROAD project in the Netherlands is planned to start injection of CO₂ into a depleted gas field located off the coast of Rotterdam in 2017. The CO₂ will be sourced from a 1100[MW] coal-fired power plant retrofitted with post-combustion capture technology, aiming to capture 1.1[Mton] per year. The CO₂ will be transported through a 25[km] long insulated pipeline to a off-shore platform. An existing well will be worked-over and re-used for injection. The target storage formation is located at a depth of 3500[m] in a heavily faulted area [2].

The Peterhead CCS demonstration project in the U.K. plans to retrofit the Peterhead natural gas power plant with post-combustion capture technology. Approximately 1[Mton] CO₂ is planned to be captured and stored per year over a 10 year period[43]. A front end engineering design contract was made with the U.K. Government in February 2014, and a final investment decision is expected to be made in 2015. If the project goes through, it is expected to become operational in 2018. The CO₂ is planned to be transported using existing pipelines 100[km] offshore to the Goldeneye depleted gas field [61]. Following the cessation of hydrocarbon production in 2011, a lot of the infrastructure needed is already installed and the reservoir is available. The Goldeneye reservoir is of good quality sandstone and no evidence of gas

chimneys or other escape paths have been observed. The formation is located at a depth of 2500[m] [21].

2.1.3 CO₂ Enhanced Oil Recovery

The production life span of an oil field can be divided into three different phases: primary, secondary and tertiary. During the primary phase, the oil is brought to the surface by the natural pressure in the reservoir alone, or in combination with pumps. Only 10% of the reservoir's OOIP is typically produced during the primary phase [13]. In the secondary recovery phase water or gas is injected in the reservoir in order to drive remaining oil towards production wells. Using these techniques typically results in a recovery factor of 20-40% of the OOIP.

In order to maximize the oil produced from a reservoir, tertiary (or EOR) techniques can be employed, enabling 30-60% of the reservoir's OOIP to be produced. EOR aims to alter the properties of the oil, unlike the secondary techniques which simply aim to "push" out the oil. According to [13] two major categories of EOR have been found to be commercially successful:

- Thermal recovery
 - Consists of injecting hot gas into the reservoir in order to heat the oil, in order to lower its viscosity and thereby ability to flow towards the producing well(s).
- Gas injection
 - Consists of injection hydrocarbon, nitrogen, carbon dioxide (CO₂-EOR) or other gases which dissolve the oil to a lower viscosity and improves mobility. This helps drive the oil to the producing wells.

In the U.S. thermal recovery accounts for $\approx 40\%$ EOR production, while gas injection accounts for $\approx 60\%$. CO₂ is miscible with oil, and has the advantage of being cheaper than similarly miscible fluids. Natural gas, for example, is unlike CO₂ a valuable commodity that will represent a loss to the operator if not all of the injected gas can be retrieved by the end of the production.

The miscibility of CO₂ in oil depends on the reservoir pressure, reservoir temperature and oil composition, where high pressure, low temperature and a light oil composition is generally favorable. Reference [7] provides a correlation for estimating the minimal miscible pressure (MMP) of CO₂ and a

given oil composition for a given reservoir temperature.

So far, CO₂-EOR has predominantly been utilized in onshore projects in the U.S., where in 2010, 280 000 incremental BOPD of incremental oil was produced by 114 active commercial CO₂ injection projects [13]. Most of these projects use CO₂ from naturally occurring reservoirs, but it is also fully possible to use CO₂ captured from industrial processes. One example is the Dakota Gasification Company's plant in Beulah, North Dakota, which delivers CO₂ for EOR to the Weyburn oil field in Saskatchewan, Canada. Large scale offshore CO₂-EOR projects is so far, to the author's knowledge, limited to the Lula project off the coast of Brazil, which in September 2011 started injecting 350 000[$\frac{m^3}{d}$] of a gas mixture containing >80% CO₂ [11]. Statoil has investigated the possibility of utilizing CO₂-EOR at several Norwegian offshore fields, but concluded that "A lack of readily available carbon sources and the high cost of carbon capture and transport have so far meant that carbon injection into fields on the Norwegian continental shelf would be uneconomic (sic) at low to medium oil prices. However, this picture may change in the future if cheaper carbon dioxide becomes available for injection - through governmental incentives or reduced costs - and a rise in long-term oil prices" [1]. Statoil currently uses gas injection of HC gas at several fields offshore for increased recovery.

CO₂-EOR operations often include injection of CO₂ alternated with water, a procedure known as WAG(Water Alternating Gas). The addition of water injection serves two main purposes: it raises the reservoir pressure to improve miscibility and mitigating viscous fingering. As liquid and supercritical CO₂ has substantially lower viscosity than oil, it has a tendency to finger its way ahead of the oil, creating a CO₂ flow channel between the injecting and producing well. This effect is known as viscous fingering, and greatly reduces the effectiveness of the CO₂ injection as any gas injected after the breakthrough will flow directly from the injector to the producer, limiting the contact between oil and CO₂. In this way, WAG injection can increase the sweep of gas injection by using water to control the mobility and stabilize the injected gas front. Christensen et.al. [8] reported in their study of WAG field experiences that "...a common trend for the successful injections is an increased oil recovery of 5 to 10% of the oil initially in place...", and that very few WAG projects had been reported as unsuccessful. Operational problems related to WAG were however not uncommon.

In WAG projects, the water and gas is injected in alternating bulks. Either fluid can be used for the first injection bulk, although with different

effects. Starting with CO₂ would according to Pizarro et.al. [11] lead to a higher recovery factor, as the first contact between oil and injected fluid would be miscible (given that the reservoir pressure is higher than MMP). The injected CO₂ would displace both mobile and residual oil. The following water injection would then displace the miscible bank and act as a mobility controller for the next CO₂ injection. However, WAG has so far usually been implemented on mature fields which have already been water flooded, meaning that water has been the first injection fluid. Water is also more effective than CO₂ for reservoir pressurization due to its low compressibility, and is thereby the most effective if the reservoir needs to be re-pressurized. The CO₂-EOR project at Lula decided to use water as first injection fluid, mainly due to "... time schedule reasons". [11]

Considering CO₂-EOR in a carbon emission perspective, the source from which the CO₂ is acquired is of paramount importance. By 2001, approximately $30[\frac{MtCO_2}{yr}]$ was injected for EOR purposes in the United States. However, a vast majority of this was CO₂ acquired from naturally occurring sources, e.g. pumped up from CO₂ rich underground reservoirs. This does not mitigate GHG release to the atmosphere, as the CO₂ used was already safely stored. For CO₂-EOR to have a climate impact, the CO₂ needs to come from anthropogenic sources, such as gas processing plants, fertilizer plants or fossil energy power plants. In 2001 only $5[\frac{MtCO_2}{yr}]$ of the total stored amount of $30[\frac{MtCO_2}{yr}]$ in the United states came from anthropogenic sources [56].

It is believed that the potential storage capacity for CO₂ is large, these values are however uncertain. The storage potential in the Middle East, Africa, Asia and Latin America has not been properly assessed, but it is believed that a significant storage potential exists in these regions. For the United States, several estimates exist: Ferguson et.al. [18] estimates the economically feasible storage potential for CO₂-EOR to be 10-13[GtCO₂], while Kuuskraa et.al. [35] estimates a economically feasible potential of 10.5[GtCO₂], with an oil price of \$85 per barrel and CO₂ cost of \$45 per ton. However, both point out that these numbers highly depend on oil price, CO₂ price and future technology development. Kuuskraa et.al. predict that with "next generation technology", the numbers might rise to 20[GtCO₂], with similar oil and CO₂ prices. In its 2005 special report on CCS [17], the IPCC estimated a global geological storage capacity for CO₂-EOR of 61-123[GtCO₂]. Moreover, the IPCC report points out that "...as practiced today, CO₂-EOR is not engineered to maximize storage. In fact, it is optimized to maximize revenues from oil production, which in many cases required minimizing the amount

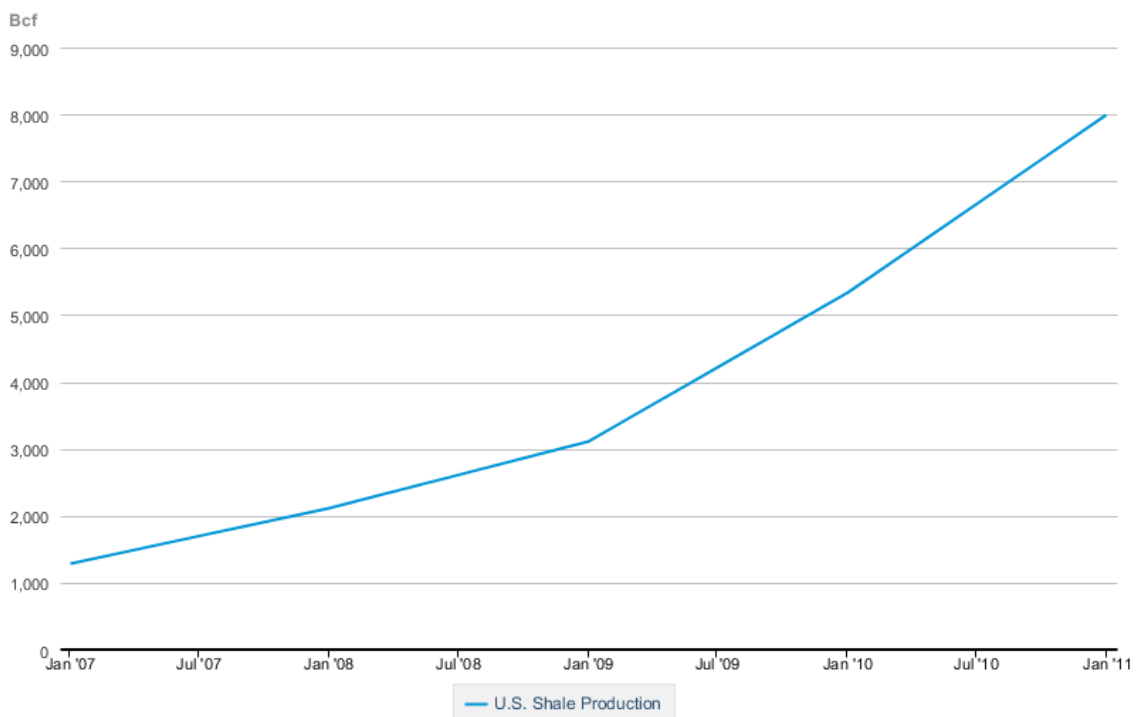
of CO₂ retained in the reservoir. In the future, if storing of CO₂ has an economic value, co-optimizing CO₂ storage and EOR may increase capacity estimates”.

2.1.4 Hydraulic Fracturing of Shale Formations Using CO₂

Shale formations have long been known to contain a large quantity of natural gas, but up until as recent as years ago, very little was considered to be economically viable for production. Increasing natural gas prices along with rapid technology development (e.g. horizontal drilling and hydraulic fracturing) over the last 10-15 years has made vast volumes of natural gas both technically and economically recoverable. In 2010, shale gas accounted for 23% of the U.S. natural gas supply, and the U.S. Energy Information Administration estimates that shale gas production will grow by approximately 4% up to 2030. As shale gas formations usually have a very low permeability, highly pressurized fluids is typically injected in order to fracture the shale formation in order to increase the permeability and release the trapped natural gas, this procedure is known as ”fracking”. The most common fracturing fluid is water mixed with sand and small amounts of various other chemicals. According to Kargbo et.al. deep horizontally drilled wells require 7700-35000[m³] of water to complete the fracturing of each well. Due to the large transportation costs of transporting water, drillers usually extract on-site water from nearby streams or underground water supplies [33]. However, some of the largest sources of shale gas are found in deserts [6], or areas where water is a limited resource. An alternative to water is using CO₂ as fracking fluid. A laboratory experiment conducted at Kyoto University suggests that using liquid or supercritical CO₂ can result in a better network of fractures than what is achieved with water. While water typically creates fractures along a two-dimensional plane, CO₂ was shown to generate a three dimensional network of fractures, with supercritical CO₂ yielding even better fractures than liquid CO₂ [32].

A second advantage of CO₂ over water is the increased amount of fluid flowing back to the surface when the natural gas is produced. In conventional fracking with water, roughly half the amount of water injected stays in the formation. This water can block the path of significant amounts of natural gas, leading to slower production, and possibly a lower total amount of produced gas. As a majority of the injected CO₂ flows back to surface, the natural gas will be able to flow more freely and not block in as much natural gas as water does [6].

Shale Gas Production



 Source: U.S. Energy Information Administration

Figure 1: U.S. Shale Gas Production 2007-2011. [14]

As with CO₂-EOR, CO₂ enhanced shale gas production has the possibility of reducing storage costs in CCS, as the natural gas production adds an economic incentive. However, as most of the CO₂ injected for fracking flows back to the surface with the natural gas, the CO₂ will have to be re-injected before the well is abandoned if CO₂ assisted shale gas production is to act as an efficient storage method. The amount of CO₂ that can be stored in shale gas reservoirs is uncertain, but the IPCC state that "...the large volumes of shale suggest that storage capacity may be significant". However, due to the low permeability nature of shale, high injection rates might be hard to achieve [17].

2.2 Simulation Tools

In this section some commonly used industrial flow simulators will be described, and their ability to perform simulations with CO₂ will be assessed. The section will conclude with a choice of simulator in which the simulations in this thesis will be performed.

2.2.1 OLGA

OLGA is a one-dimensional transient multiphase simulator designed for flow in pipelines, and is short for "Oil And Gas Simulator". The development of OLGA started as a project for Statoil in 1983 with a goal of simulating the slow transient behaviors associated with mass transfer in pipes and meet the demand for a multiphase flow simulator in the oil and gas industry. The first working version was ready in 1983, but development continued by a joint research project between the Institute for Energy Technology and SINTEF in order to widen the empirical basis of the model and possible applications. The model is still under continuous development and improvement, with Schlumberger being the current license holder after their acquisition of SPT Group in 2012. [22] [5]

The workings of the, at that time, current OLGA version was thoroughly described by Bendiksen et.al. in 1991 [5]. As OLGA is a commercial software, detailed information on recent versions is not available. The current standard OLGA version solves for a three-phase mixture of gas, oil and water using nine conservation equations. "Five equations describe conservation of mass in the bulk of the phases as well as oil droplets immersed in gas and gas bubbles immersed in oil. There are three momentum equations and one

mixture equation” [3].

OLGA is a spacially one-dimensional simulator, meaning that it only uses one calculation point for each length of the well. This means that properties calculated are independent of radii, and only change with length in the well and time. A well model in OLGA is divided into several ”pipes”, which consist of multiple ”sections”. For each section and time step OLGA calculates the average values of properties of the flow, such as pressure and temperature, using an iterative approach. The number of pipes and sections, and thereby spacial grid size, are determined by the user. OLGA also allows for the user to decide the maximum and minimum time-step length for each simulation.

The standard OLGA version uses externally generated pressure-temperature(P-T) tables in order to calculate fluid properties for a given mixture. This method was originally designed for multicomponent hydrocarbon fluids, which usually have wide two-phase envelopes in P-T diagrams and thereby allows for a gradual transition in fluid properties with changes in pressure or temperature. Fluid mixtures dominated by a single component will typically have a narrow phase envelope, possibly leading to large changes in properties such as density or gas-liquid fraction in the two-phase area for small changes in pressure or temperature. Due to this numerical approach, standard OLGA may become unstable when performing simulations on fluids with narrow phase envelopes. According to Monica Håvelsrud of SPT Group, standard OLGA should be able to handle mixtures consisting of up to 80% of a single component, given that the fluid mixture has a significantly wide two-phase envelope [57]. This limits OLGA’s range of application, and excludes CO₂ dominated mixtures with small amounts of impurities.

A useful addition to OLGA with respect to CO₂ transport is the single component module. It allows for simulations of pure CO₂, without importing externally supplied tables for thermodynamic properties. It uses six conservation equations: three for mass, two for momentum and one mixture energy equation. The single component module uses the Span-Wagner equation of state to generate the necessary tables of fluid properties, instead of importing externally generated tables. A drawback of the single component module is that it does, as of now, only support pure CO₂, meaning that it is not able to handle the presence of impurities [3].

2.2.2 LedaFlow

LedaFlow is a transient multiphase simulator for wells and flow-lines, designed to solve multiphase transport challenges in the oil and gas industry. Development started in the early 2000s as a collaboration between Total ConocoPhillips and SINTEF, with Kongsberg joining as the commercialization partner in 2009. The first commercial version was released in June 2011. LedaFlow is designed to have both one-dimensional(1D) and quasi-three-dimensional(Q3D) capabilities, with the 1D simulator being the "work horse" of the program, "sufficient for perhaps 80% of the simulation work that would be done." [9]. As of February 2014, "The Q3D model is being validated and further developed" [63].

As LedaFlow has been developed for the oil and gas industry, it has primarily been designed to solve for three-phase oil-gas-water mixtures. This mixture "may exhibit up to 9 fields: three continuous fields(water, oil and gas) and up to 6 dispersed fields..." [9], with "field" referring to the the description of the motion of a particular form of the fluid [9]. An example of a dispersed field is water droplets in the continuous oil field. In the case of 9 fields, LedaFlow 1D solves 15 transport equations: nine conservation of mass equations for the continuous and dispersed fields, three conservation of momentum equations and three energy equations. LedaFlow uses the Suave-Redlich-Kwong (SRK) and Peng-Robinson(PR) equations of state for the thermodynamics [3].

Although oil-gas-water is LedaFlow's main area of application, "the framework and formulation is general for multiphase flow, and can in principle be applied to CO₂ transport. This would require "implementation of closure relations relevant to CO₂ and the relevant impurities" [3]. According to Bjørn Tore Løvfall of SINTEF, LedaFlow is, as of March 2014, not facilitated for CO₂ simulations and would require minor alterations to the code and "... consistent PVT data" [41].

2.2.3 TACITE

The TACITE multiphase flow simulation tool was developed by Elf Aquitaine/Total in the early 1990s, and was primarily developed for natural gas transport simulations. The TACITE model and underlying equations are described by Pauchon et.al. [45]. It handles eight different flow regimes, with the characterization of and transition between these regimes being highly dependent on the fluid. TACITE has been validated for natural gas transport, but its

”validity to CO₂ is unclear” [3].

Choice of simulator for this thesis Based on the information revealed in this simulation tools literature review, OLGA has been chosen for the simulations that are to be performed in this work. It is the only one of the studied simulation tools which has found to be validated for CO₂ simulations. LedaFlow is in its current form not facilitated for CO₂ transport simulations, and no information on TACITE’s ability to perform CO₂ simulations was found. The facts that OLGA has a ”single component module” for pure CO₂ using the Span-Wagner EOS and the simplicity with which oil wells can be modeled in OLGA also speak in its favor. A drawback of OLGA is its inability to simulate mixtures with impurities unless the CO₂ content is >80% .

2.3 Shut-In Test

The term shut-in refers to sealing off a well, stopping production or injection. Wells are commonly shut in for inspection or repairs, or to conduct well or reservoir tests. Depending on the reason for the shut-in, the well can be sealed off either at the well head, bottom hole or any other part of the well.

The Midwestern Regional Carbon Sequestration Partnership (MRCSP) conducted field assessments of injectivity and containment at three locations between 2007-2010, with the goal of contributing to establish a set of best practices for CCS storage and validation. Shut-in tests were conducted at at least two of the sites. The pressure fall-off curves were used to determine key reservoir properties, including transmissivity and permeability. At one site, the State Charlton 4-30 well in the Michigan basin, a total of four shut-in tests were conducted after different amounts of CO₂ had been injected, where bottom hole pressure and temperature were logged for the entire test period:

- February 2008 after injection of 1 125 tons of CO₂
- March 2008 after injection of 10 000 tons of CO₂
- May 2009 after injection of 25 000 tons of CO₂
- July 2009 after injection of 50 000 tons of CO₂

The February 2008 was monitored for a little over 74 hours, while for the three later shut-ins the BH pressure was monitored for 240 hours. The pressure fall-off curves exhibited the same general shape, but with different magnitudes of pressure change. The tests indicated ”a complicated pressure

response with wellbore storage, skin effects, outer boundary effects, and a dual porosity system with pseudo steady-state flow from the matrix to the fractures” [31]. The BH pressure response during the February 2008 test was successfully used to estimate the formation permeability [53], with the following three tests indicated little change in reservoir permeability over the 17 months separating the first and last test. Lessons learned and implications for commercial deployment from the entire MRCSR project were reported in Gupta et.al. [26], while experiences from the State Charlton well specifically have been documented by Sminchak et.al. [53] and in a comprehensive final project report by Batelle [31].

Hansen et.al. [29] reported experiences from the offshore Snøhvit CO₂ storage project, including multiple shut-ins of various length. Between startup in 2008 and permanent shut-in in 2011, more than 1 Mt CO₂ was injected to the primary target formation of Tubåen at 2582[m] TVD SS through a 7” tubing. The well included a set of down-hole pressure and temperature gauges, located 800[m] TVD above the target formation, but has no bottom hole gauges. Regular short shut-ins of ”a few minutes” were performed to estimate the near well reservoir pressure from the well gauges and ”evaluate potential skin development”. These tests were kept short ” in order to neglect temperature effects”. The reservoir pressure estimated in these tests were later confirmed to be correct ”within a few bars” by a well intervention performed in 2011. The pressure fall-off analysis of the longer shut-ins were used in reservoir mapping, where it was found that a reservoir flow barrier 3000[m] from the well had to be added to the reservoir model used in order to match the measured pressure fall-off from the gauges. Regarding the longer shut-ins, it was also found that due to ”The shallow location of the down-hole pressure gauge (800m above the reservoir), changing fluid properties of CO₂ with changing pressure and temperature, affect the pressure measured by the permanent pressure gauge. First after about 100 hours, stable conditions are obtained and reservoir behavior can be recognized”. The down-hole gauges were successfully used to estimate the bottom-hole flowing and stagnant pressure, and regarding the placement of the gauges it was found that ”The shallow location of the pressure gauge does not really influence our ability to predict the near wellbore reservoir pressure. However,[...], it has a major impact on the transient analysis of any fall-off, and normal transient fall-off analysis cannot be utilized for reservoir property estimation due to temperature transient in the CO₂”. [29].

Gjertsen [22] performed a simulation study of the CO₂ injection well at Sleipner, with a primary goal of investigating ”if bottom hole conditions of a two-

phase well can be estimated from the transient pressure and temperature response at well head to a shut-in/leak-off test". The upper portion of the Sleipner well is two-phase gas/liquid CO₂, with the remainder of the well being in the supercritical phase. Results showed that the pressure response at well head during shut-in and leak-off tests were affected by the bottom hole pressure, and could in theory be used to estimate bottom hole conditions. However, sensitivity analysis revealed that the results were "highly sensitive to the heat transfer modeling, indicating that a more thorough modeling of heat transfer is necessary to achieve accurate simulation results". The shut-in simulations, with the fluid in the well being stagnant, were found to be especially sensitive to heat modeling.

2.4 Step-Rate Test

In petroleum engineering, the term "step rate test" most commonly refers to a procedure used in preparation for hydraulic fracturing of a reservoir. In this test, fluid is injected through a well in a pre-defined time series with increasing pump rates. The main goal of this operation is to identify key parameters of the fracturing operation such as the formation fracture pressure and maximum injection rate, but also to demonstrate the integrity of the injection well.

The MRCSP conducted two documented step-rate tests at their CO₂ injection well in the Michigan basin (State Charlton 4-30 well). The first step-rate test was conducted as a part of an "underground injection control mechanical integrity test" program, where CO₂ injection was stepped up from an initial flow rate of 10417 $[\frac{kg}{h}]$ to 20833 $[\frac{kg}{h}]$ in 2083 $[\frac{kg}{h}]$ increments. Each rate was sustained for approximately two hours. This was the first injection of CO₂ in this well. The measured data provided insight on the "hydraulic behavior of the reservoir system" [25], and suggested a maximum injection rate possible. The injection rate during this test was manually adjusted and difficult to stabilize at lower injection rates, and the BH pressure increase over this test was considered difficult to interpret, with only a 2[bar] increase from 10417 $[\frac{kg}{h}]$ to 20833 $[\frac{kg}{h}]$. Results and analysis of this step-rate test are provided in Gupta et.al.(2009) [25], Sminchak et.al.[53] and the State Charlton final report [31].

A second step rate test was performed in State Charlton 4-30 well approximately one month after the first. Injection rate was stepped down from an initial rate of 28167 $[\frac{kg}{h}]$ to 12500 $[\frac{kg}{h}]$ through a first step of 3167 $[\frac{kg}{h}]$ followed

by three steps of $4167[\frac{kg}{h}]$. Unlike the first test, which was a virgin injection, CO₂ had been continuously injected for 19 days before the second step-rate test. This caused a lower and more stable BH temperature during the test [31].

Regarding the results from the step-rate and shut-in(fall-off) tests in the State Charlton well, Gupta et.al.(2011) remark: "The pressure falloff curves provided a better idea of overall reservoir behavior than step-rate and injection tests, which could be irregular due to inconsistent injection rates, CO₂ phase behavior, and other factors.

A second demonstration of a step rate test is described in Schechter et.al. [50], on a CO₂ injection well for EOR in a mature oil field. Water was used as injection fluid, with the goal the goal of the test being to determine the maximum safe injection pressure without fracturing the reservoir rock.

2.5 Leak-Off Test

Leak-off test commonly refers to a test performed during drilling operations to determine the formation fracture pressure. It is usually conducted immediately after drilling below a new casing shoe, after which the well is shut-in and fluid is pumped in to the wellbore in order to increase the pressure that the formation experiences. At a certain pressure, the fluid will "leak-off" from the well bore into the formation, either by finding permeable paths or by fracturing the formation. This test is conducted to determine the maximum pressure that may safely be applied to a well during drilling operations. A more thorough explanation is provided by Raaen et.al. in [46]. However, this kind of leak-off different from what intended to be performed in this thesis, where CO₂ would be vented at WH to investigate the systems pressure and temperature response.

Gjertsen [22] performed a simulation study on the Sleipner two-phase injection well, including simulations of leak-off tests. Constant injection was first simulated for 50 hours in order for the well to approach steady state. Injection was then stopped for 10 hours, before CO₂ was allowed to escape through a 0.005[m] circular valve at WH. The simulation results were not found to provide any significant information of the well and/or reservoir, and did not provide any information not already gained through shut-in tests. Gjertsen also remarks on the impracticalities related to the test procedure, with injection needed to be stopped and possible installation of additional equipment

at wellhead.

No published field experiences of leak-off tests were found, and except for Gjertsen's work described in the previous paragraph, no simulation work or theoretical studies were found. Due to this it was impossible to evaluate or compare existing practices. The lack of published measured data from leak-off tests also limits the accuracy and relevance of performing OLGA simulations, as there the simulation results can not be validated against measured data. In addition, the simulations performed by Gjertsen were found to, by his assessment, not provide any information on the system not already gained through shut-in tests. Based on this, it was decided to not perform leak-off simulations and rather focus on shut-in and step-rate tests.

2.6 Literature Review Discussion

Saline Aquifer Storage This literature review has shown that large scale CO₂ storage in subsurface saline aquifers is fully possible, however at both Snøhvit and In-Salah there have been operational challenges. Important lessons have been learned from the three projects described, but it is also clear that more research is needed to ensure successful and operationally stable CCS projects in the future. The literature has also shown that bottom hole well gauges have only been used at the In-Salah wells. Snøhvit had gauges installed 800[m] above the original target formation Tubåen, while the Sleipner well has no down hole instrumentation. All three projects have wellhead gauges. Saline formations have a very large storage potential with estimates of global capacity ranging between 1000[GtCO₂] and 10000[GtCO₂] [17]. A drawback of saline formations is that a significant amount of mapping of the formations are required before they can be used, which takes time and can be expensive. Even with the formation being well studied before injection start, it's capacity and performance can not be fully known until after injection has commenced. The Tubåen formation at Snøhvit is an example of this, where it was found after three years of injection that the formation was not able to take the required flow rate.

Depleted Gas Field Storage Although depleted gas field storage does not offer the same theoretical global storage capacity as saline formations, nor the economic incentives associated with CO₂-EOR or CO₂-fracking, it has several advantageous properties making it a viable scenario for CCS. The geology, capacity and sealing properties of depleted gas fields are usually well

known, as a result of it being a former natural gas production field. This minimizes the need for further mapping of the storage site, and provides confidence storage security. In both the ROAD and Peterhead project existing infrastructure is planned to be re-used for storage operations, contributing to cost reduction of the operation.

CO₂-EOR CO₂ injection has been proved to be a successful way of boot-boosting reservoir pressure and increasing oil production. This provides an economic incentive for CO₂ injection and possible storage. CO₂-EOR is already in use at multiple locations in the U.S., and the world wide potential is believed to be large. However, there are multiple challenges related to CO₂-EOR as a method of reducing green house gas emissions. As practiced today, the CO₂-EOR is designed to maximize oil production revenue, which in can entail minimizing CO₂ storage since the CO₂ has to be bought. Also, the CO₂ needs come from anthropogenic sources if CO₂-EOR is to have a positive environmental impact. In 2001, only 5 out of 30[Mt CO₂] used in CO₂-EOR came from anthropogenic sources. The environmental benefit of injecting CO₂ has to be weighed against the CO₂ released from consuming the additional oil extracted due to CO₂ injection.

Hydraulic Fracturing of Shale using CO₂ The literature review on CO₂ as a fracking fluid revealed some advantages CO₂ has over water. Laboratory experiments suggest that CO₂ can create better fracture networks, increasing the hydrocarbon gas production. Also, large shale gas reserves are located in "dry" areas, where CO₂ can be used to not put further strain on already scarce water supplies. However, from a CO₂ storage perspective there are several challenges. When CO₂ is used as a fracking fluid, most of the injected CO₂ will flow back to the surface as the hydrocarbon gas is retrieved. The CO₂ then has to be re-injected afterwards. The storage capacity of shale formations are unknown, and due to the low permeability nature of shale, high injection rates might be hard to achieve.

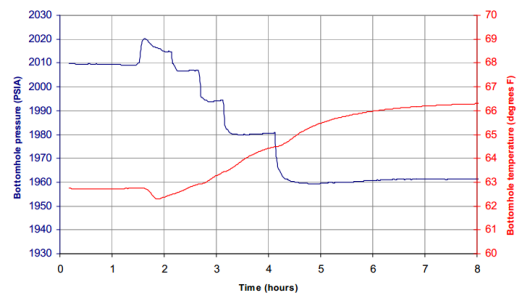
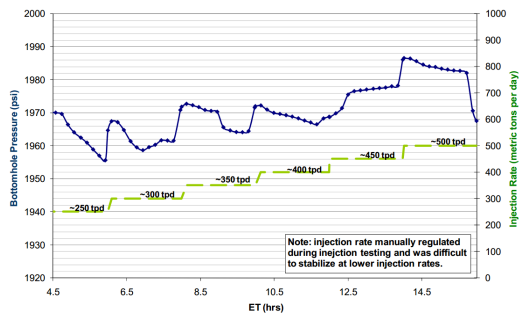
Shut-in Tests In the State Charlton well shut-ins were successfully used to estimate injectivity, formation permeability and gain information on the other aspects of the reservoir. Repeated shut-in tests were used to monitor the reservoir performance over time. In the Snøhvit well, regular shut-ins of various lengths were performed. The shorter shut-ins were used to estimate

the near well reservoir pressure and evaluate skin development over time. Information gained from pressure fall-off analysis of the longer shut-ins was used in mapping of the reservoir. This shows that shut-ins and pressure fall-off analysis is a useful tool for gaining information on the reservoir, both near well and on a larger scale.

The down hole gauges in the Snøhvit well are not located at the bottom, but, due to operational issues during completion, sits 800[m TVD] above the perforations and target formation. This was not found to affect the estimation of near well reservoir pressure. However, the gauge placement was considered to have "a major impact" [29] on shut-in pressure fall-off analysis. During the first hours of shut-in, the measured pressure was found to be strongly affected by CO₂ density changes due to fluid temperature changes. If pressure data from the gauges during the first 100 hours of simulation were to be used, a temperature correction function would have to be applied, this would however make the fall-off analysis dependent on the accuracy of the correction function [28]. First after 100 hours of shut-in, stable temperature conditions were reached, and reservoir behavior could be interpreted. Based on this, it is considered advisable to have down hole gauges installed as close to the perforation as possible, in order to maximize the information gain from shut-in pressure fall-off analysis.

In the State Charlton well both multiple shut-in and step-rate tests were performed, and according to the experiences of Gupta et.al.(2011)[26], pressure fall-off analysis of BH pressure provided a better understanding of the reservoir than step-rate tests.

Step-rate Tests Two documented step-rate tests were performed in the State-Charlton well. The first test was performed as the first injection in the well, while the second was performed one month later, and was preceded by 18 days of continuous injection of CO₂. A comparison of the BH pressure responses of the two tests revealed significant differences. The first test has an irregular pressure response, and except for a short pressure rise after 4/5 of the step-ups in injection rate, no clear pattern emerges. This makes it difficult to interpret or draw any knowledge from the test. The second test shows a much more consistent BH pressure response, with each injection change rate resulting in a pressure drop before quickly stabilizing. A possible explanation for the difference in BH pressure response between the two tests, is that the first step-rate test is the first CO₂ injection in the well. This could



(a) BH Pressure of first step-rate test from St.Charlton well. (b) BH Pressure of second step-rate test from St.Charlton well.

lead to significant skin effects from sediments and other debris that has to be washed away before stable conditions can be expected. A second factor is the high BH temperature gradient during the first step rate test (as seen in figure 6). As the CO₂ in the well rapidly cools during the step-rate test the CO₂ density changes and thereby the weight of the fluid column in the well. The injection of relatively cold CO₂ will also cool the target reservoir, causing changes in near-well reservoir behavior and possibly performance.

3 Theory

3.1 Carbon Dioxide Properties

The thermodynamic properties of pure CO₂ have been thoroughly studied, and can be considered to be well known. The phase diagram for CO₂ is given in figure 3, showing the three different fluid phases, triple and critical point, and the supercritical phase. The triple point is located at -56.60°C and 5.18[bar], while the critical point is located at 30.9782°C and 73.773[bar]. The triple point is the one single thermodynamic state where CO₂ exists as liquid, vapor and solid in equilibrium. CO₂ with a pressure higher than 73.773[bar] and temperature higher than 30.9782°C is considered to be supercritical, and the fluid phases are indistinguishable. Supercritical CO₂ can be said to have approximately the viscosity of a gas and the density of a liquid, making it a beneficial phase for transport. CO₂ is non-combustible and colorless in gas phase. In small concentrations it is odorless, but has an acidic odor at higher concentrations. In addition to its use in the oil industry for EOR, it is also used as a coolant in nuclear reactors and heat pumps. It exists in small amounts in the earth's atmosphere and is normally considered to be harmless. However, at large concentrations it can cause unconsciousness.

3.2 Equation of State

An equation of state (EOS) is a thermodynamic equation describing the properties of a fluid under a specified set of physical conditions. It provides a mathematical relationship between two or more state functions, such as temperature, pressure and molar volume, and can be used to predict phase transitions for fluids. Being able to accurately predict the properties and vapor liquid equilibrium (VLE) of CO₂ and CO₂ mixtures is of great importance for CCS operations, as the temperature-pressure range of operation in many instances, including CCS, encompass the the gas-liquid transition conditions.

Multiple families of equations of state exist, and here a brief overview is given.

3.2.1 Pure CO₂

For pure CO₂ a large amount of experiments have been conducted, and the thermophysical properties can be considered to be well know. The Span-

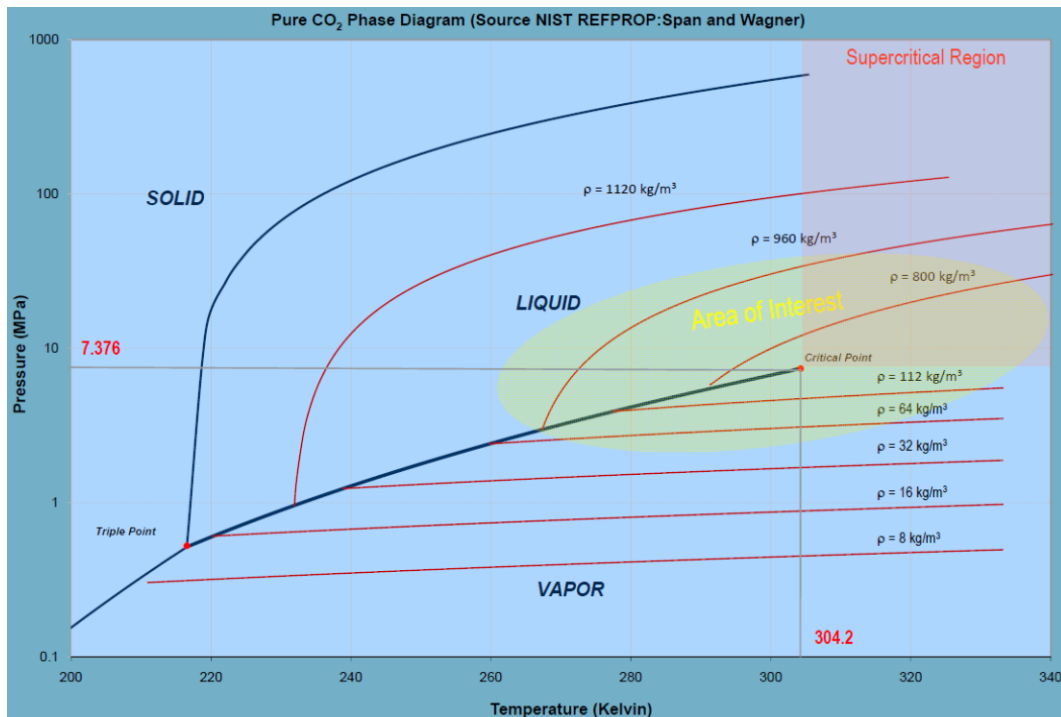


Figure 3: Phase diagram for pure CO₂. Taken from Pekot et.al. [16]

Wagner EOS is considered the reference EOS for pure CO₂ [3] [58]. It covers the temperatures from 216[K] up to 1100[K] and pressures up to 800MPa, which is a sufficient range for CO₂ transport and geological storage operations. In regard to the equations accuracy, Span and Wagner claim that "In the technically most important region up to pressures of 30[MPa] and up to temperatures of 523[K], the estimated uncertainty of the equation ranges from $\pm 0.03\%$ to $\pm 0.05\%$ in the density, $\pm 0.03\%$ to 1% in the speed of sound, and $\pm 0.15\%$ to $\pm 1.5\%$ in the isobaric heat capacity" [55].

A drawback of the Span-Wagner EOS is that it contains 42 terms, of which 8 are complex exponential terms. This requires significantly more computational power than for example a cubic EOS, and may affect the computational time of simulations. To combat this, Kim [34] proposed a simplified version containing 30 terms, claiming to be "...less accurate than Span and Wagner in the gas and liquid region but more accurate in the critical region" [34].

Li et.al. [39] evaluated a set of commonly used cubic EOSs performance in estimating the vapor-liquid equilibrium(VLE) for pure CO₂ and binary mixtures of CO₂ with common impurities in CCS. The equations of state evalu-

ated were: Redlich-Kwong(RK), Redlich-Kwong-Soave(SRK), Peng-Robinson(PR), Patel-Teja(PT) and 3P1T. For pure CO₂ all of the models, except RK, were found "...capable of calculating the saturation pressure with an absolute average deviation(AAD) less than 3%". "SRK EOS was found to be more accurate than the others over the whole range of tested conditions, with AAD of 1.05%". RK was found to not be appropriate for calculating VLE of pure CO₂ for temperatures below 290[K].

Wilhelmsen et.al. [58] evaluated multiple EOSs relevant for carbon capture and storage modeling, with a purpose of finding an EOS which is accurate, consistent and computationally fast for CO₂-mixtures. The equations evaluated were SRK, SRK with Peneloux correction (SRK-P), Peng-Robinson, Lee-Kesler (LK), SPUNG/SRK and GERG-2004. For pure CO₂, the equations were evaluate for four different regions: vapor, liquid, critical (defined as $300 < T < 308\text{K}$ and $70 < p < 78[\text{bar}]$), and supercritical. 1000 random temperature/pressure points across all regions were calculated with each of the equations and the results were then compared to the Span-Wagner equation, which was used as a baseline. SRK was outperformed by SRK-P on density prediction in all regions, but SRK-P still yielded above 10% AAD in the critical region. SRK-P yielded <1% AAD in density in the liquid and vapor region, outperforming both LK and PR. Only SPUNG/SRK and GERG-2004 gave accurate predictions of the density (< 2% ADD) in the critical region, with GERG-2004 outperforming the other equations for all regions in density prediction. LK performed. SPUNK/SRK and GERG-2004 were the most accurate in specific heat capacity calculation in the supercritical and vapor regions, but SRK and SRK-P were found to be "surprisingly accurate in the liquid phase area" [58]. SRK, SRK-P, LK and PR performed similarly in the liquid and supercritical region, none of the before-mentioned equations were able to predict specific heat capacity within 10% AAD in the critical region. SRK, SRK-P and PR yielded >20% AAD in the critical region.

3.2.2 CO₂ with Impurities

Impurities The type and amount of impurities in the CO₂ mixture depends on the source of the CO₂, and will effect the behavior of the mixture. Li et.al. [38] performed a review of existing theoretical models for estimating thermodynamic properties of CO₂ mixtures relevant for CCS, where they list possible impurities and impurity concentration for some possible sources of anthropogenic CO₂. The tables from Li et.al. have been re-produced in tables 1 and 2.

CO₂ from naturally occurring CO₂ reservoirs have extensively been used in

| Description | Possible Impurities |
|---|---|
| CO ₂ captured from natural gas sweetening | CH ₄ , amines, H ₂ O |
| CO ₂ captured from heavy oil production and upgrading | H ₂ S, N ₂ , O ₂ , CO H ₂ O, H ₂ , COS, Ar, SO _x NO _x |
| CO ₂ captured from power plant using post combustion capture | N ₂ , amines, H ₂ O, O ₂ , NH ₃ , SO _x , NO _x |
| CO ₂ captured from power plant using oxy-combustion capture | N ₂ , O ₂ , SO ₂ , H ₂ S, Ar |
| CO ₂ captured from power plant using pre-combustion capture | H ₂ , CO, N ₂ , H ₂ S, CH ₄ |

Table 1: Table of common impurities from some anthropogenic CO₂ sources.
From reference [38]

| Component | Min. mol% | Max. mol% |
|------------------------|-----------|-----------|
| CO ₂ | 75 | 99 |
| N ₂ | 0.02 | 10 |
| O ₂ | 0.04 | 5 |
| Ar | 0.005 | 3.5 |
| SO ₂ | <0.0001 | 1.5 |
| H ₂ S + COS | 0.01 | 1.5 |
| NO ₂ | 0.0002 | 0.3 |
| CO | 0.0001 | 0.02 |
| H ₂ | 0.06 | 4 |
| CH ₄ | 0.7 | 4 |

Table 2: Impurity concentrations. From reference [38].

the onshore EOR industry in the U.S. The composition and impurities in these CO₂ sources vary from reservoir to reservoir, but primarily relatively pure CO₂ sources have been used [51]. A list of three long distance pipeline systems transporting naturally sourced CO₂ for EOR are listed in table 3. The fluid composition of these pipelines are also listed, showing a CO₂ purity of > 95% with the main impurities being CH₄ and N₂.

| | Central Basin | Sheep Mountain | Cortez |
|------------------|----------------|----------------|----------------|
| CO ₂ | 98.50% | 96% | 95% |
| CH ₄ | 0.20% | 1.70% | 1-5% |
| N ₂ | 1.3% | 0.9% | 4% |
| C ₂ + | - | 0.60% | Trace |
| H ₂ O | 257 ppm weight | 129 ppm weight | 257 ppm weight |
| Length [km] | 278 | 660 | 808 |
| Capacity [Mt/yr] | 20 | 9.5 | 19.3 |

Table 3: Existing long distance CO₂ pipelines with naturally sourced CO₂. From reference [51]

Statoil currently have two large scale CCS operations running in Norway: the LNG plant Snøhvit and the gas processing plant at Sleipner. In addition, it was a partner in the CCS operation at the gas processing plant at In Salah in Algeria. Eiken et.al. have published a paper [15] briefly summarizing Statoil's experiences from their CCS operations, stating that all three sites have a CH₂ content of 0.5-2% and that the In Salah and Snøhvit operations have a water content of less than 50ppm. De Visser et.al. [12] give a more detailed description of the CO₂ stream at Sleipner, listed in table 4.

| Component | |
|--|--------------------|
| CO ₂ (vol.%) | 93-96% |
| Total hydrocarbons | 0.5-2% |
| Non-condensable gases (N ₂ ,H ₂ ,Ar) | 3-5% ^{a)} |
| H ₂ S (ppm) | Up to 150 |
| H ₂ O | Saturated |

Table 4: CO₂ stream content at Sleipner. From de Visser et.al. [12].

a) The non-condensable content is not expected to increase above 3% during normal operation, even though 5% non-condensable is stated as design basis.

Information on the injected fluid composition at the Lula oil field in Brasil is limited, however Pizarro et.al. [11] reported that between April 2011 and

September 2011 "The[injected] gas was mainly HC with some CO₂ content". From September 2011 "The injection well started to inject mainly CO₂...with concentrations higher than 80%...". This leaves room for an impurity concentration of up to 20%, with hydrocarbon gas most likely being the main impurity.

Table 2 shows N₂, O₂, H₂ and CH₄ being the largest contamination chemicals from the anthropogenic sources listed in table 1. CH₄ is the main impurity in the streams from the gas processing plants at Sleipner and In Salah, and the LNG plant at Snøhvit. Table 3 shows CH₄ and N₂ being the main contamination chemicals from natural sources. Based on this, it's reasonable to focus on EOSs that handle CO₂ mixtures with these impurities well.

EOS for Impurities Li et.al.'s article on experimental data and equations of state relevant for CCS operations reviewed multiple EOS of different complexity. The cubic equations of state are the simplest and are popular in engineering applications due to their simplicity. Li investigated seven cubic equations, and compared their performance in estimating the VLE and density for CO₂ mixtures including CH₄, N₂, O₂, H₂S, SO₂ and Ar. The equations examined were Peng-Robinson(PR), Redlich-Kwong(RK), Soave-Redlich-Kwong(SRK), Patel-Teja(PT), 3P1T, Peng-Robinson-Peneloux(PR-P), Soave-Redlich-Kwong-Peneloux (SRK-P) and the improved Soave-Redlich-Kwong, and found that all gave an Absolute Average Deviation(AAD) of within 5% for VLE calculations and 6% for density calculations for all mixtures, except CO₂/SO₂.

A previous study by Li and Yan [39] on cubic EOSs for CO₂ and CO₂-mixtures relevant to CCS examined five cubic equations performance in VLE calculation. PR, PT, RK, SRK and 3P1T were six different binary CO₂ mixtures, including CO₂/CH₄, CO₂/O₂ and CO₂/N₂. For the CO₂/CH₄-mixture PR, PT and SRK performed well in estimating the VLE at 219.26[K] and 270[K]. PR, PT and SRK were also found to have similar accuracy in calculating the saturation pressure and CO₂ saturated mole fraction in vapor phase, with PR being the most accurate of the three.

For the CO₂/O₂-mixture PR, PT, SRK and RK were found to have quite similar performance in VLE calculation, but 3P1T was better. All models performed better for higher CO₂ concentrations.

For the CO₂/N₂-mixture, PT was found to be more accurate in calculations

of saturation pressure and saturated CO₂ molar fraction in vapor phase with AADs of 1.62% and 2.17% respectively. However, all models except RK were found to have better accuracy for high concentrations of CO₂, with the deviations of PR,PT and SRK being within 2.5% at 270[K] when CO₂ mole fraction in liquid phase was >85%.

Li and Yan [39] conclude that "For the VLE properties of of binary CO₂ mixtures, PR, PT and SRK are generally superior to RK and 3P1T. Comparatively PR is recommended to the calculations of CO₂/CH₄ and CO₂/H₂S; PT is recommended to the calculations of CO₂/O₂, CO₂/N₂ and CO₂/Ar..."

4 OLGA Simulations

In this section OLGA simulations of step-rate tests and shut-tests will be performed. The OLGA well model is based on the State Charlton well, which is documented in the State Charlton final report [31]. The goal of the simulations is to validate OLGA's ability to simulate these operations by matching pressure and temperature data from the simulation to measured data. Simulations investigating the effect of heat transition during step-rate tests will also be performed.

The State Charlton well was chosen for this work as it was the only project found that had published data from both step rate and shut-in tests for a CO₂ injection well. Flow rate, bottom hole pressure and temperature data was published for the shut-in and one of the two step rate tests performed. For the second step rate test flow rate, well head and bottom hole pressure and temperature were published. However, this data is only given through figures which has to be manually read, thus limiting their accuracy.

OLGA Reservoir Model Equations OLGA offers multiple one-equation models for modeling of the reservoir for injection wells. The two most relevant to liquid phase CO₂ injection are the "linear reservoir equation" and "non-linear reservoir equation", both given below (with units in brackets):

$$G_w \left[\frac{kg}{s} \right] = A \left[\frac{kg}{s} \right] + B \left[\frac{kg}{s * Pa} \right] \cdot (P_{BH} - P_{Res}) [Pa] \quad (1)$$

$$A [Pa^2] + B \left[\frac{s * Pa^2}{kg} \right] \cdot G_w \left[\frac{kg}{s} \right] + C \left[\frac{s^2 * Pa^2}{kg^2} \right] \cdot G_w^2 \left[\frac{kg^2}{s^2} \right] = P_{BH}^2 - P_{Res}^2 [Pa^2] \quad (2)$$

In both equations "A", "B" and "C" are constants. G_w is the mass flow rate into the reservoir, P is pressure with "BH" denoting bottom hole and "Res" reservoir. In the both equations, "A" gives "the minimum pressure difference required for the fluid to start to flow from the well into the reservoir" [23]. In the linear equation "B" is the injectivity index, while the OLGA user manual gives no explanation for "B" and "C" for the non-linear equation.

The State Charlton 4-30 Well The Midwest Regional Carbon Sequestration Partnership (MRCSP) is a partnership of more than 30 organizations

from the energy industry, research community, non-governmental organizations and the U.S. government. The MRCSP is lead by Battelle Memorial Institute and has as it's objective to "...test the safety and effectiveness of carbon sequestration and to further understand the best approaches to carbon sequestration in the midwest USA through a series of focused field tests of sequestration technologies" [31]. One of the field tests performed in Otsego County, Michigan, where a well identified as State Charlton 4-30 was drilled in 2006. The project was temporary in nature and designed to inject a relatively small amount of high purity CO₂, with the purpose of advancing the understanding of CO₂ storage and public acceptance. The project is documented in a article by Sminchak et.al. [53] and a comprehensive final project report prepared by Battelle, from here on referred to as State Charlton final report [31].

The injection well was completely vertical with a tubing inner diameter of 7.3025[cm] and was perforated from 1049-1071[m] in the Bass Island Dolomite formation. The lithology surrounding the well is given in figure 5, and is shown to consist of mainly shale, dolomite and limestone. A pre-injection baseline temperature log from 610[m](2000[ft]) to 1036[m](3400[ft]), shown as the blue line in figure 4, was given in the final report [31]. This shows a near linear temperature gradient of $15.63 \frac{\text{°C}}{\text{km}}$ in this interval.

The target rock formation for the CO₂ injection was the Bass Islands Groups, situated at a depth of 1049[m TVD] to 1128[m TVD] in the injection well. It "consists mostly of light brown to buff dolostone and anhydrite present in the lower sections"[31]. While the interval below 1071[m TVD] consists of high density anhydrite not likely suited for injection, rock core tests indicated that the 1049-1071[m TVD] interval consisted mainly of porous and permeable dolostone. This section is considered the main injection zone and is "characterized by interbedded, laminated algal dolomudstone, minor-crossbedded and sandy dolograinstone, intraclast beds, and disrupted karstic breccia zones"[31]. Rock core tests suggest that the 22[m] dolostone interval has a average permeability of 22[md] and a porosity of 13% [53].

The CO₂ used for injection was a byproduct from nearby natural gas production. The produced natural gas contained 10-15% CO₂, which had to be lowered to meet commercial natural gas purity requirements. This was done by using an amine absorption system, resulting in a high purity CO₂ stream. A gas sample taken of the injectate composed, on a mole basis, of 99.42% CO₂ and 0.48% CH₄ [31]. The injection wellhead CO₂ temperature was dependent on the upstream transport and surrounding temperatures,

Michigan Basin State-Charlton 4-30 Injection Well Downhole Temperature Logging

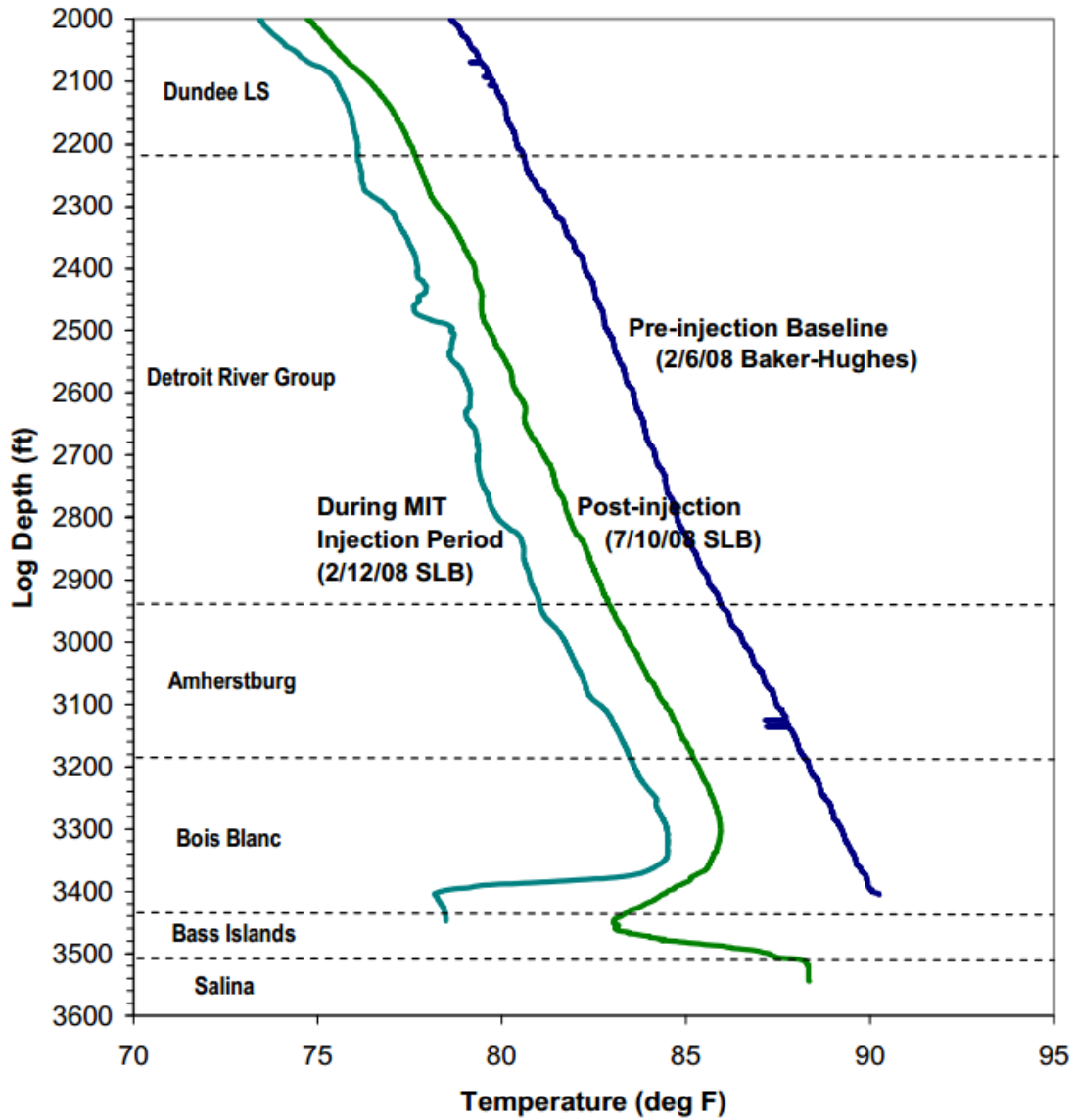


Figure 4: State Charlton Injection well(4-30) downhole temperature log. From Michigan Basin Phase II Final Report [31]

| Formation | Depth (feet) | | Comments |
|-----------------------------|----------------------|----------------------|---------------------------------------|
| | State-Charlton 4-30 | State-Charlton 3-30 | |
| Kelly Bushing | +13 (1201 ft msl) | +13 (1183 ft msl) | Drilling floor elevation |
| Surface | 0 (1188 ft msl) | 0 (1170 ft msl) | |
| Base Glacial Drift | 665 | 663 | Unconsolidated glacial till |
| Coldwater Shale | 665 | 663 | |
| Sunbuy Shale | 735 | 727 | |
| Ellsworth Shale | 745 | 735 | |
| Antrim Shale | 805 | 810 | |
| Dark Antrim | 1112 | 1105 | |
| Traverse Fm | 1270 | 1240 | |
| Traverse Lm | 1303 | 1292 | |
| Bell Shale | 1942 | 1935 | |
| Dundee Fm | 2003 | 1997 | |
| Detroit River Gp | 2238 | 2225 | Top Lucas Fm |
| Amherstburg Fm | 2942 | 2930 | Filer SS Member between 3085' - 3121' |
| Bois Blanc Fm | 3190 | 3160 | Intermediate storage zone |
| Bass Islands Gp – dolomite | 3442 | 3425 | Top of injection interval |
| Bass Islands Gp – anhydrite | 3515 | 3495 | Base of injection interval |
| Salina | NA | 3852 | |
| Niagaran | NA | 5300 | EOR target |
| Total Depth | 5800 | 5746 | |

Figure 5: State Charlton Injection well(4-30) and monitoring well(3-30) lithology. From Michigan Basin Phase II Final Report [31]

with fluid temperature varying with the time of day. However, 4.44°C was found to be an approximately average wellhead CO₂ temperature.

4.1 OLGA Well Model and Properties

The OLGA model used for simulations of the State Charlton will be described in this section, with explanations for the choices made in building the model given where found necessary. Important elements when constructing an injection well model in OLGA include wellbore material properties, temperature and properties of the rock formations surrounding the well, reservoir pressure and reservoir modeling. The density(ρ), heat capacity(C_p) and conductivity (k) of the well material and surrounding formation are key in deciding the heat conduction between the fluid in the well and surrounding rock formation. The reservoir modeling equation and reservoir pressure are key in determining pressure phenomena and flow properties in the well.

Well Geometry The full well specification, casing program and cementation of the State Charlton well is described in the State Charlton final report [31]. The OLGA model does not take the casings or cementation into consideration, but models the 7.3025[m] diameter injection liner only. The well reaches to 1071[m TVD] and is completely straight. An "OLGA well module" is installed in OLGA at 1050[m TVD], which connects the well to the reservoir. An OLGA "mass flow source" is installed at WH, from which injection fluid is supplied.

Wellbore material Neither Sminchak et.al. [53] or the State Charlton final report [31] state the heat properties of the material used in the well construction. Due to the corrosive nature of CO₂ and water, it is common to use stainless steel alloys with high chromium content to prevent corrosion. For the CO₂ injection well at Sleipner, which operates at similar pressures and temperatures as the State Charlton well, it was found necessary to use 25% chrome duplex stainless steel for the tubulars and the exposed parts of the casing. 22% chrome duplex steel for the topside equipment, although the precise steel classification used at Sleipner is not mention [4]. For this modeling of the State Charlton injection well, AISI 304 steel will be used, which is a high quality stainless steel with a chrome content of 18-20%. This does not match the documentation from Sleipner precisely, but the approximation

is considered to be sufficient. The relevant properties of AISI 304 are listed in table 5, with values taken from Incropera et.al. [30]. The properties listed in table 5 were used in the OLGA model.

| | Density(ρ) $\frac{kg}{m^3}$ | Heat Capacity(C_p) $\frac{kJ}{kg*K}$ | Heat Transfer Coefficient(k) $\frac{W}{m*K}$ |
|----------|---------------------------------------|---|---|
| AISI 304 | 7900 | 0.477 | 14.9 |

Table 5: Properties of AISI 304 Stainless Steel. From Incropera et.al. [30]

Lithology A simplified model of the lithology in figure 5 was created for the OLGA model. Each formation was listed according to their primary rock type and thickness in table 6. The thicknesses and properties listed in table 6 were used in the model. A shale layer from 591-610[m] was neglected due to its small thickness.

| Rock Type | Intervall [m] | Heat Capacity (C_p) $\frac{kJ}{kg*K}$ | Thermal Conductivity(k) $\frac{W}{m*K}$ | Density $\frac{kg}{m^3}$ |
|--------------|------------------|--|--|-----------------------------|
| Glacial till | 0-202.7 | 1.000 | 2.9 | 2000 |
| Shale | 202.7-387.1 | 0.7950 | 3.4 | 2600 |
| Limestone | 387.1-682.1 | 0.8368 | 2.9 | 2500 |
| Dolomite | 682.1-972.3 | 0.9200 | 4.5 | 2850 |
| Limestone | 972.3-1049.1 | 0.8368 | 2.9 | 2500 |
| Dolomite | 1049.1-1071.4 | 0.9200 | 4.5 | 2850 |

Table 6: Simplified lithology of St.Charlton Injection well

Although both heat capacity(C_p) and thermal conductivity(k) of rocks depend on multiple parameters, the goal of this evaluation is to create a simple model of the rock surrounding the well and its thermal properties. Due to this, the heat capacities were considered to be independent of temperature and evaluated at a single temperature of 25°C. Heat capacities for limestone and shale were taken from "Thermal properties and temperature-related behavior of rock/fluid systems" [54], while the value for dolomite was taken from Engineering Toolbox [60]. The heat capacity and thermal conductivity values for glacial till were taken from reference [20]. For thermal conductivity of limestone, shale and dolomite, the rocks were assumed to have a porosity of 10% with water filled pores at a temperature of 300[K] and pressure

of 50[bar]. Values were taken from reference [49], a U.S. Geological Survey on thermal properties of rocks. For shale, a quartz content of 30% was assumed. Densities of the rocks were taken from www.edumine.com [59]. For the glacial till, density of "wet earth" was assumed.

Reservoir Pressure The background reservoir pressure was measured pre-injection to be 103.42[bar] [31]. This value was used in the OLGA well component.

Geothermal Gradient The linear temperature gradient of $15.63 \frac{\text{°C}}{\text{km}}$ from figure 4 was extrapolated to the entire length of the well to form a continuous geothermal gradient for the entire well. Although the top part of the soil will hold a lower temperature due to cooling from the atmosphere, this portion is small and is assumed negligible.

CO₂ purity and injection temperature Due to the high purity, the single component module using 100% pure CO₂ was used in the OLGA simulations. This module uses the Span-Wagner EOS for calculation of fluid properties. The injection source temperature was set to 4.44°C, as this was found to be an approximate average WH fluid temperature.

Spacial grid Gjertsen [22] performed a OLGA CO₂ injection simulation of the Sleipner two-phase well. In his work he performed a Spacial Grid Sensitivity analysis in OLGA, which focused on determining the effect of the spacial grid length (section length) on simulation results and time. Lengths between 4[m] and 20[m] were investigated. It was found that the differences in results were small, with a 0.25% difference in gas/liquid fraction between the 4[m] and 20[m] simulations being the largest discrepancy. The grid length was found to have a significant impact on the time it took to perform each simulation, with simulation times ranging from approximately one hour for the 20[m] grid to approximately 10 hours for the 4[m] simulation. Based on this, it was decided to keep the section lengths below 20[m] for the simulation work in this thesis. The maximum and minimum section lengths used were 18.45[m] and 11.5[m], with the average section being 17[m].

Temporal grid Gjertsen [22] also performed an analysis of the effect of maximum time step length in OLGA simulations on the Sleipner two-phase well. The same simulation was run multiple times, with the maximum time step length being the sole difference. Time steps between 0.1[s] and 8[s] were investigated. The most prominent difference was that the longer step times were seen to cause instabilities at the two-phase gas/liquid to supercritical transition point in the well. No instabilities was seen in the 0.1[s] simulation. The different time steps were also found to yield different results for WH & BH pressure and temperature. Based on this, a maximum time step length of 0.1[s] has been chosen for the simulations in this thesis.

4.2 Documented Operations at State Charlton

Mechanical Integrity Test, February 7-13th Before the main injection was started, the well was required to perform a Mechanical Integrity Test(MIT) by the U.S. Environmental Protection Agency, which was completed February 7-13, 2008. This included a step rate injection test, followed by period of constant injection and a shut-in. Bottom hole pressure and temperature data recorded during the mechanical integrity test was published and is displayed in figure 6. Zoom-ins of the step rate test and the shut-in test are given in figure 7 and 8.

The State Charlton final report describes the procedure of the MIT: "Injection rates were stepped up from 250 to 500 metric tons of CO₂ per day(10416.6-20833.3 $[\frac{kg}{h}]$) in 50 ton per day (2083.3 $[\frac{kg}{h}]$) increments [...] Each rate was sustained for 2 hours". The step rate test was followed by a 60 hour period of constant injection at 18750.0 $[\frac{kg}{h}]$ before injection was stopped and the well was shut-in for 75 hours for monitoring. It is noted in the report that "No formation breakdown was encountered and bottom hole pressure limits(approximately 2 500psi(172.4[bar])) were not approached. During the step rate test, only a 30psi(2.1[bar]) pressure increase was observed from 250 to 500 metric tons per day, making it difficult to interpret pressure trends".

As the primary injection commences, the bottom hole pressure sees a spike to over 138[bar](2000[psi]), before rebounding to \approx 135[bar] at the start of the step rate test. The bottom hole temperature drops from the original 31.7°C to 29.5°C. During the step rate test the bottom hole pressure rises from a minimum of 134.8[bar] during injection at 10416.6 $[\frac{kg}{h}]$ to a maximum of 136.9[bar] at the step-up from 18750.0 to 20833.3 $[\frac{kg}{h}]$, resulting in a pressure rise of 2.1[bar] over 10 hours. The behavior of the bottom hole pressure

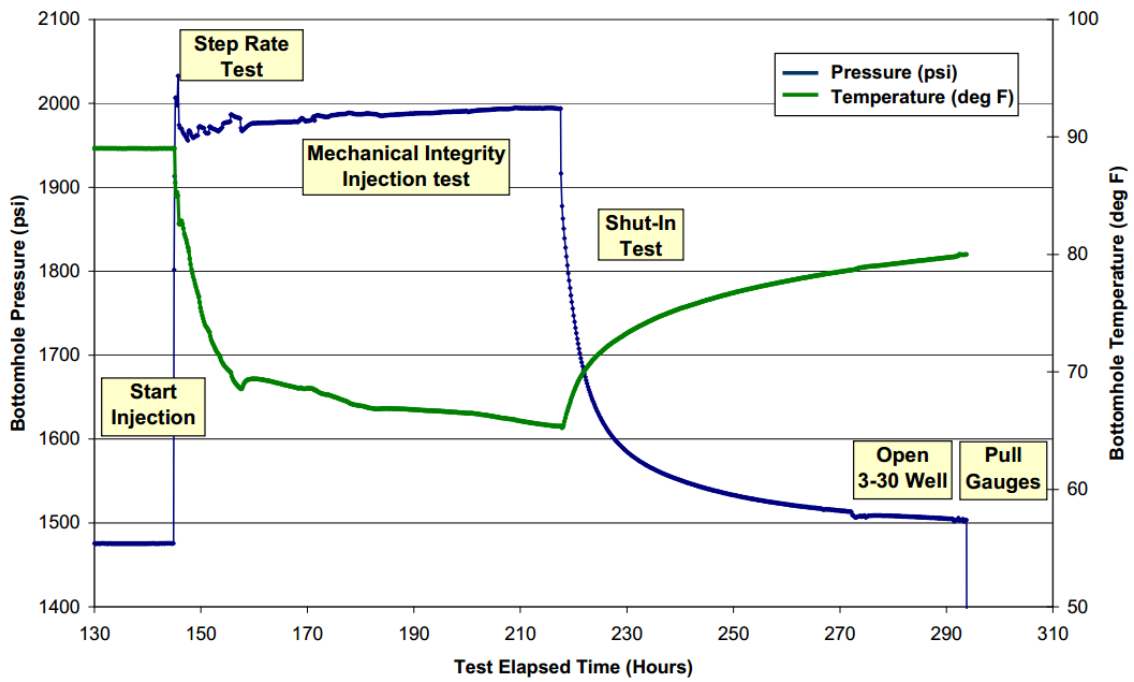


Figure 6: Bottom hole pressure and temperature data from the State Charlton 4-30 mechanical integrity test. From State Charlton Final Report [31]

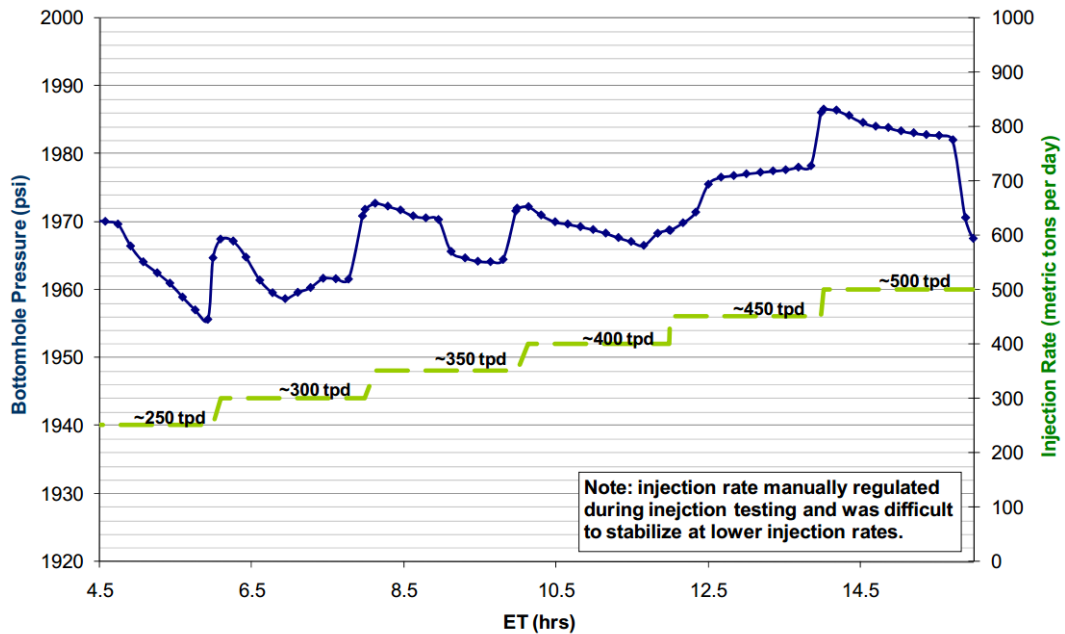


Figure 7: Bottom hole pressure and injection rate data from the State Charlton 4-30 step rate test. From Michigan Basin Phase II Final Report [31]

during the step rate test is irregular, with an inconsistent response to the injection rate step-ups. The bottom hole temperature drops sharply during the step rate test from 29.5°C to 20.4°C. At the end of the step rate test the injection rate is lowered from 20833.3 $[\frac{kg}{h}]$ resulting in a pressure drop and temperature rise.

During the constant injection period, the bottom hole pressure rises in a near linear fashion by 1.2[bar] over 60 hours. The temperature drops from 20.4 degrees to its minimum of 18.5°C.

At the shut-in, the bottom hole pressure sees a rapid drop of $\approx 7[bar]$, before following a smooth inverse-exponential decline approaching the original reservoir pressure of 103.42[bar]. The BH temperature follows a logarithmic rise, reaching a value of 26.7°C after the 75 hours of shut-in. Moreover, at the end of logging, 75 hours post shut-in, the BH temperature is still rising.

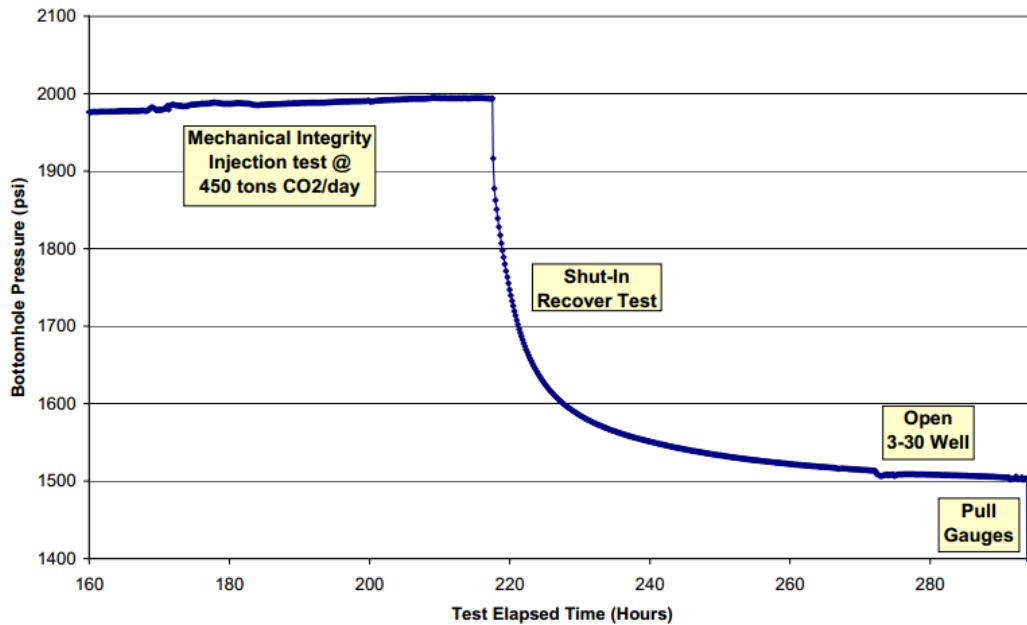


Figure 8: Pressure data from the State Charlton 4-30 shut-in test. From State Charlton Final Report [31]

To be able to compare the measured data to data from simulations, the graphs in figures 6, 7, 8 were transcribed to an Excel sheet. As this was done by manually plotting data points, the Excel plots are not exact re-makes. The Excel plots of the before-mentioned figures can be found in appendix D.1.

Second Step Rate Test, March 5th March 5th 2008, three weeks after the end of the MIT, a second step rate test was performed in the State Charlton 4-30 injection well. The sole published documentation on this test is figures 9 and 10. The data had to be manually read from the figures, limiting its accuracy.

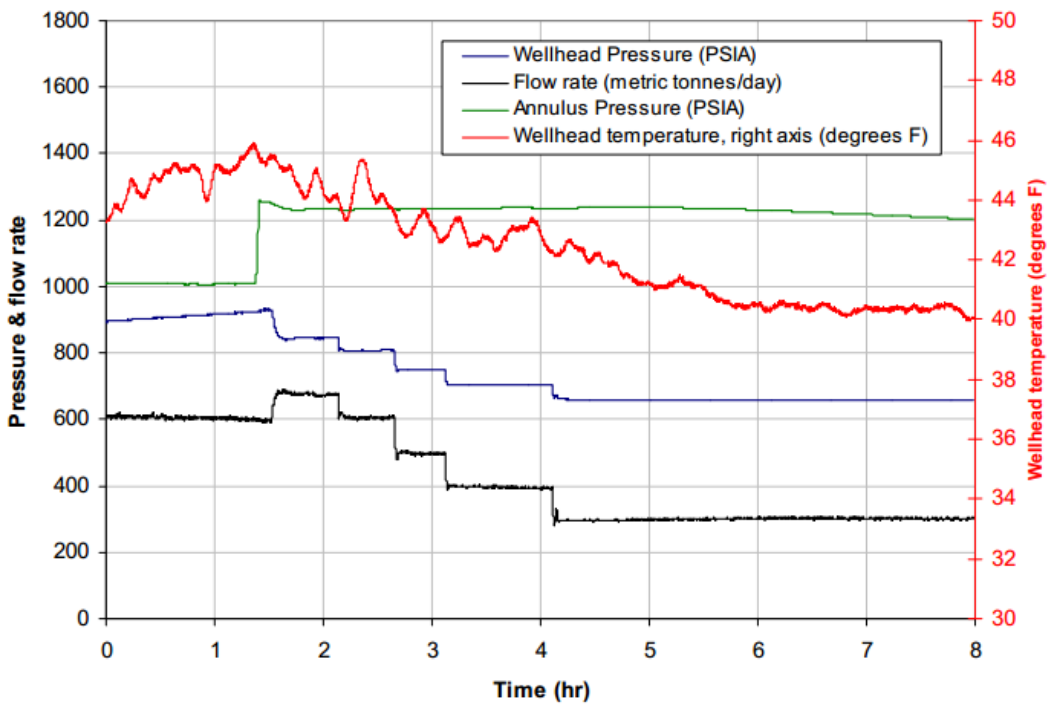


Figure 9: WH pressure, flow rate, annulus pressure and WH temperature data from the State Charlton 4-30 2nd step rate test performed March 5th. From State Charlton Final Report [31]

Ahead of the March 5th test, it was suspected that physical restrictions in the injection tubing was causing an elevated WH pressure and decreased flow rate. In an attempt to combat this, methanol was added to the CO₂ injectate at approximately 1.5 hours in figure 10 and 9. The methanol injection caused the WH pressure to drop while flow rate increased, indicating less restricted flow. Separately, the annulus pressure was boosted to maintain a sufficient pressure differential between the annulus and injection tubing.

The step rate test is performed by lowering the injection rate in distinct steps, with each injection rate being held constant for 0.5-1 hour. The injection rate and the resulting WH and BH pressures for each step are given in

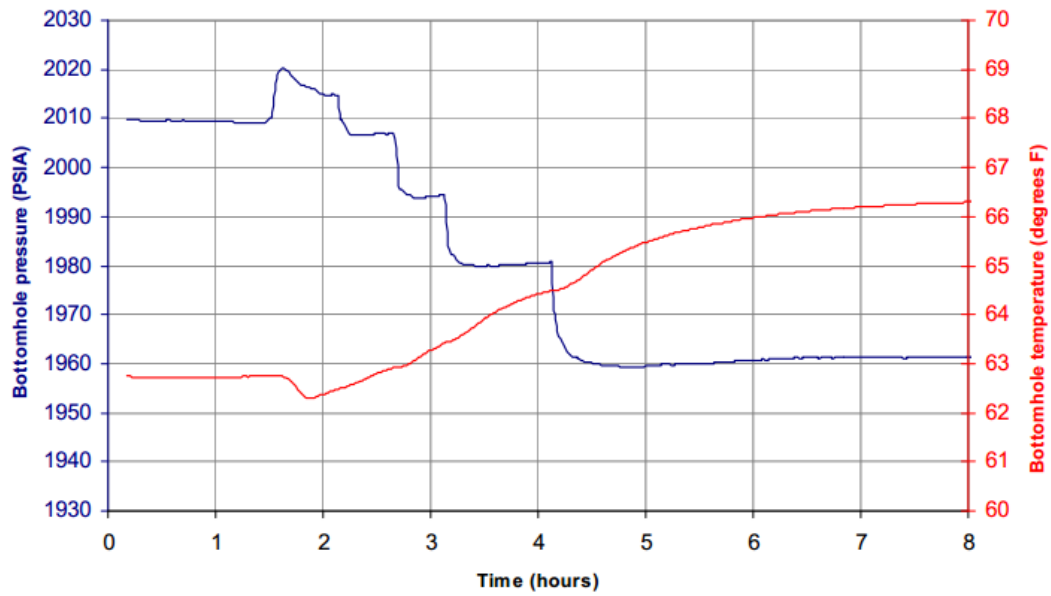


Figure 10: BH pressure and temperature data from the State Charlton 4-30 2nd step rate test performed March 5th. From State Charlton Final Report [31]

| Time hours | WH Pressure [bar] | BH Pressure [bar] | Flow rate [$\frac{ton}{day}$] |
|------------|-------------------|-------------------|---------------------------------|
| 1.53-2.10 | 58.4 | 139.3-138.9 | 676 |
| 2.10-2.60 | 55.8 | 138.4 | 600 |
| 2.60-3.04 | 51.5 | 137.5 | 500 |
| 3.04-4.04 | 48.4 | 136.5 | 400 |
| 4.04-8.00 | 45.2 | 135.2 | 300 |

Table 7: WH pressure, BH pressure and flow rate of March 5th step rate test. Taken from figure 10 and 9.

table 7.

During the test, the WH temperature varies between 7.8°C and 4.4 °C, with a declining trend over the 8 hours of the test. The WH pressure drops in distinct steps with the flow rate, and stabilizes quickly after each injection rate decrease. The WH pressure has a starting value of 58.4[bar] around 2 hours and an ending pressure of 45.2[bar], resulting in a total pressure differential of 13.2[bar] over the test. For each of the 4166.7 $[\frac{kg}{h}]$ steps, the WH pressure drops by $\approx 3.2[bar]$.

The BH temperature is constant at 17.1°C for the first 1.5 hours of the test, before dipping to 16.9°C as a result of the flow rate increase at 1.5hours. As the flow rate is lowered from 27791.7 $[\frac{kg}{h}]$ (667 $\frac{ton}{day}$) to 12500.0 $[\frac{kg}{h}]$ (300 $\frac{ton}{day}$) the temperature increases in a near linear fashion between 2 and 5 hours. As the flow rate is held constant at 300 $\frac{ton}{day}$ the BH temperature approaches $\approx 19.2[^\circ C]$, following a logarithmic curve. The BH pressure has a starting value of 138.9[bar] and an ending value of 135.2[bar] resulting in a total pressure differential of 3.7[bar]. During the first injection interval at 27791.7 $\frac{kg}{h}$ the pressure drops from 139.3[bar] to 138.9[bar]. However, during the four following injection intervals, the BH pressure quickly stabilizes after the injection rate step down and is constant for the remainder of the interval. The pressure drop over the first injection interval could be linked to the preceding methanol injection. For each of the 4166.7 $[\frac{kg}{h}]$ steps, the BH pressure drops between 0.9 and 1.3[bar].

To be able to compare the measured data to simulation data, figures 9 and 10 were transcribed to an Excel sheet. As this was done by manually reading the graphs and plotting the data points the Excel plots are not exact re-makes. The Excel plots can be found in appendix D.1.

4.3 OLGA Simulations Description

Mechanical Integrity Test A full simulation of the Mechanical Integrity Test was performed in OLGA, following the description given in section 4.2. The first simulation of the mechanical integrity test used the injectivity of $1.937 \times 10^{-6} \frac{kg}{s * Pa}$ (at a rate of 25000.0 $\frac{kg}{hour}$) estimated in the final report of the State Charlton well, along with no minimum pressure difference between well and reservoir for flow to start, defined in the following linear reservoir equation:

$$G_w = A + B(p_{wf} - p_{res}) = 0 + 1.937 \times 10^{-6} \cdot (p_{wf} - p_{res}) \quad (3)$$

| Rock type | Interval [m] | Thermal conductivity (k) $\frac{W}{m \cdot K}$ |
|--------------|-----------------|---|
| Glacial till | 0-202.7 | 2.32 |
| Shale | 202.7-387.1 | 2.72 |
| Limestone | 387.1-682.1 | 2.32 |
| Dolomite | 682.1-972.3 | 3.6 |
| Limestone | 972.3-1049.1 | 2.32 |
| Dolomite | 1049.1-1071.4 | 3.6 |

Table 8: Modified rock thermal conductivity. Modified k-values=80% of original k-values

This equation will be referred to as the original reservoir equation.

The simulation using this reservoir equation resulted in too high of a BH pressure response to the injection rate increases, and a $\approx 10[bar]$ too low BH pressure during the constant injection period. Due to this, the injectivity suggested in the report was abandoned and new simulations were ran using a different equation. The reservoir equation found to best reproduce the measured data from the MIT step-rate test and constant injection period is given below, and will be referred to as the modified reservoir equation. The values of the constants in the equation were found by trial and error through matching simulation BH pressure response from step rate test to the measured data.

$$G_w = -34.7 \left[\frac{kg}{s} \right] + 1.16 \times 10^{-5} \left[\frac{kg}{s * Pa} \right] \cdot (p_{wf} - p_{res}) \quad (4)$$

The primary simulations revealed that BH temperatures in the simulations were higher than the measured values. Due to this, alterations were made to the thermal conductivity of the rock formations surrounding the well, with conductivity being lowered to 80% of the values provided in table 6 in section 4. This setting will be referred to as the "modified rock conductivity", and uses the conductivity values given in table 8.

Finally, attempts to match the BH pressure and temperature response during shut-in were made. For the pressure, a wide array of injectivity coefficients were tested for the linear reservoir equation in an attempt to recreate the pressure response measured, but none of these attempts were successful and the results are not reported. In a separate simulation attempting to match the BH pressure a time dependent reservoir equation with "B"= 1.16×10^{-5}

and a time variable "A" were used. For matching the BH temperature response to shut-in, simulations were ran with altered reservoir temperature, heat capacity and heat conductivity for the formation rock.

Second Step Rate Test OLGA was used to simulate the March 5th step rate test, using information gathered from figures 10 and 9. Flow rate was adjusted according to the information in table 7. The simulation used the same reservoir model (equation 4) as used to match the MIT. The results from this simulation was matched against the measured BH and WH pressures and temperatures.

The second step rate test was preceded by 18 days of constant injection, causing both BH pressure and temperature to be stable before the methanol injection and step-rate test. To replicate this, 100 hours of constant injection at $25000[\frac{kg}{h}]$ was simulated before the step-rate test was commenced. This ensured that simulation BH temperature and pressure were stable before the test commenced.

To investigate the effects of formation-to-wellborefluid heat conduction during the step-rate test, two more versions of the second step-rate test were simulated. The results were compared to the simulation described in the previous paragraph, labeled in the result figures as "matched simulation". The first is a completely adiabatic well, where no heat is conducted from the formation to the wellbore. In the second simulation only 1.5hours of constant injection is performed before the step-rate test is commenced. This leads to a high influx of heat from the formation to the well as the near-well formation temperature is almost at virgin conditions, which is significantly warmer than the CO₂ supplied at WH. The aim of these simulations is to compare two extreme cases of heat conduction, to investigate the possible effects this may have on step-rate test results. This will show what results can be expected when performing a step-rate test in a well that is thermally stable, compared to one that is not.

4.4 Simulation Results

4.4.1 Mechanical Integrity Test

Original reservoir equation Figure 11 shows the BH pressure of the simulation using reservoir equation 3 versus the measured BH pressure.

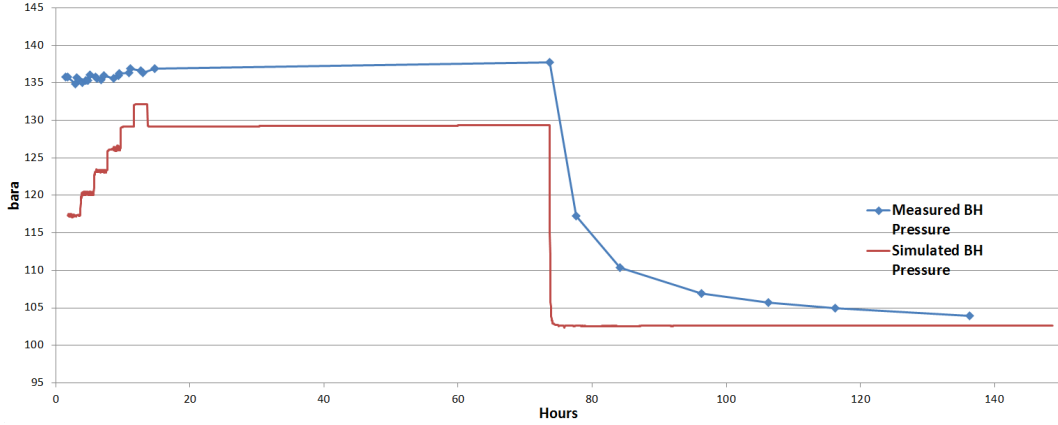


Figure 11: Mechanical integrity test simulation with original reservoir equation and rock properties. Simulated versus measured BH pressure. Linear reservoir equation constants from equation 3

From figure 11 we see that the BH holds a pressure of 117.3[bar] during the first injection period with $10416.7[\frac{kg}{h}]$. For each of the five following $2083.3[\frac{kg}{h}]$ step-ups in injection rate, the BH pressure increases by $\approx 3[bar]$. This results in a BH pressure of 132.2[bar] at the highest injection rate of $20833.3[\frac{kg}{h}]$, and a total pressure rise of 14.9[bar] over the step rate test. Following each injection rate change, the pressure changes and stabilizes quickly at its new level. At the end of the step rate test the injection rate is lowered to $18750[\frac{kg}{h}]$, causing a pressure drop of 3[bar] down to 129.3[bar]. The BH pressure stays constant at this value for the duration of the 60 hour constant injection period.

The BH temperature (figure 12) is $31.1^{\circ}C$ at the start of the step rate test, and falls throughout to a value of $21.5^{\circ}C$ at the end of the step rate test. The temperature rises slightly for about one hour after the injection rate is lowered after the end of the step rate test. Following this, the BH temperature drops steadily during the constant injection period to $19.8^{\circ}C$ before the shut-in.

As the CO_2 injection is stopped, the BH pressure rapidly drops from 129.3[bar] to 103.6[bar], where it's stable for the remainder of the simulation. The BH temperature rises from the start of shut-in, following a logarithmic curve to $30.7^{\circ}C$ after 70 hours of shut-in.

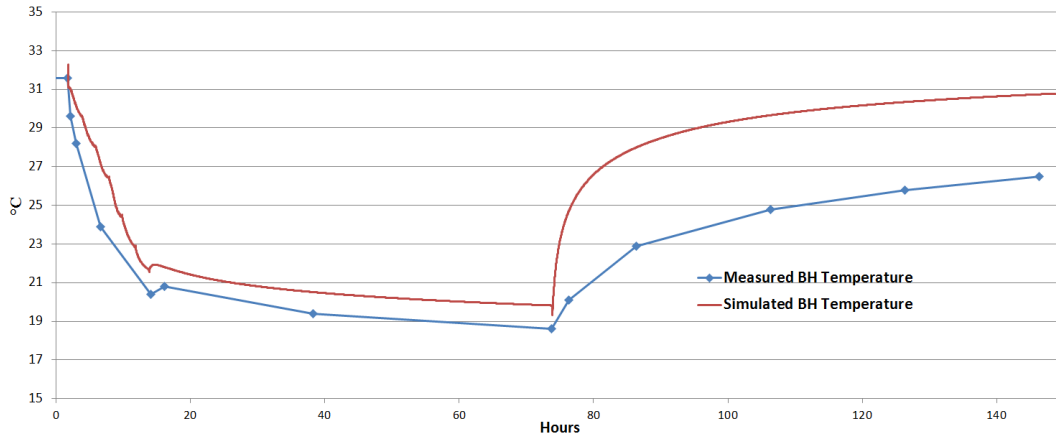


Figure 12: Mechanical integrity test simulation with original reservoir equation and rock properties. Simulated versus measured BH temperature. Linear reservoir equation constants from equation 3

Modified Reservoir Equation and Rock Conductivity The results from the simulation using the modified reservoir equation and modified formation rock conductivity are given in figures 13 and 14. With figure 15 being a zoom-in of figure 13.

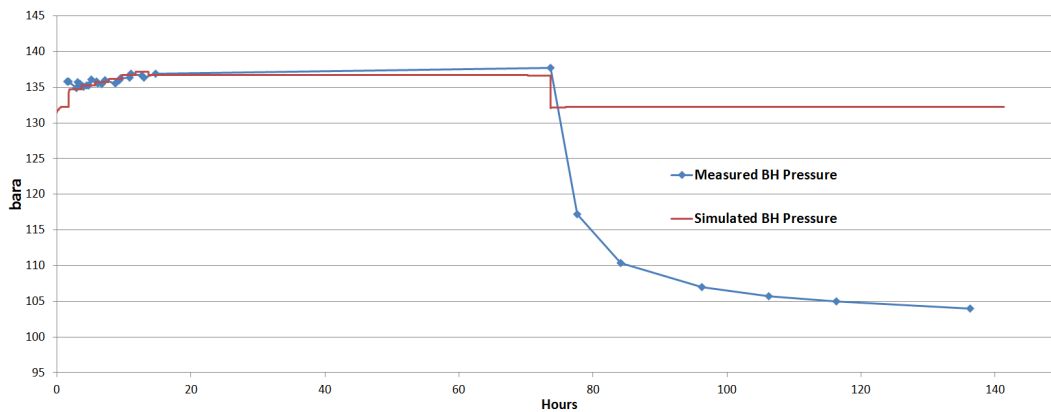


Figure 13: Measured and simulated BH pressure. Modified reservoir equation and rock conductivity.

During the step rate test, the BH pressure rises by 0.49-0.50[bar] for each of the five $2083.3 \frac{kg}{h}$ step ups. This results in a 2.47[bar] BH pressure rise over the full step rate test, from 134.7[bar] at $10416.7 \frac{kg}{h}$ to 137.2[bar] at $20833.3 \frac{kg}{h}$. After the step rate test, the injection rate is lowered to $18750 \frac{kg}{h}$, resulting

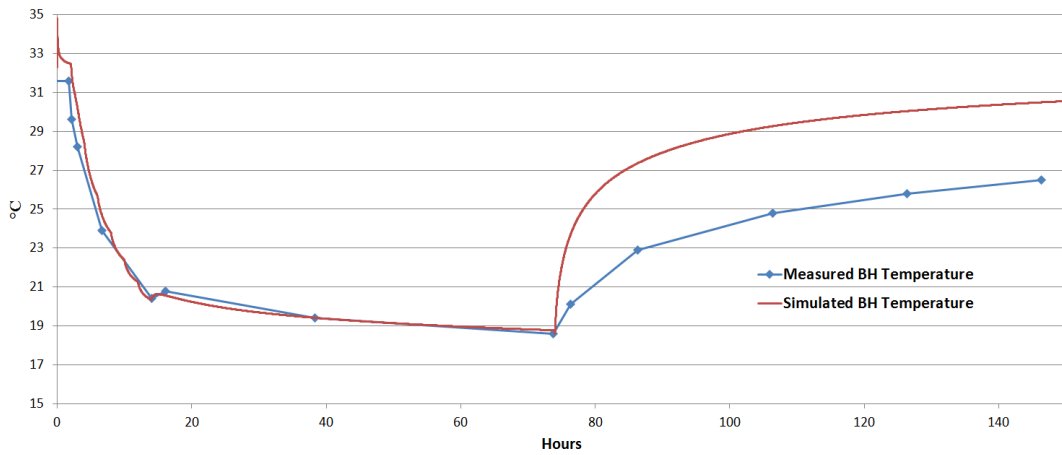


Figure 14: Measured and simulated BH pressure. Modified reservoir equation and rock conductivity.

in a pressure drop down to 136.7[bar]. During the following 60 hour constant injection period, the BH pressure stays constant at this value.

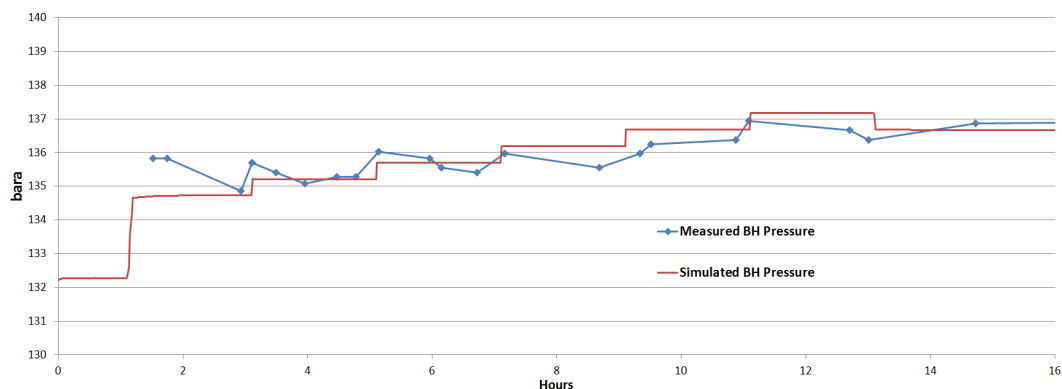


Figure 15: Measured and simulated BH pressure, step rate test zoom-in. Modified reservoir equation and rock conductivity.

The BH temperature follows the same trend as with the original reservoir equation and rock conductivity, but has a larger temperature drop during the step rate test and generally a lower value for the entire simulation. The temperature is 32.4°C at the start of the step rate test, and 20.3°C at the end. At the end of the constant injection period the BH temperature is 18.8°C. The temperature then sees a rise over the shut-in period, leaving it at 30.4°after 70 hours of shut-in.

As the well is shut-in, the BH pressure rapidly drops from 136.7[bar] to 132.2[bar], leveling off and staying constant for the following time of the simulation. This BH pressure is 28.8[bar] higher than the reservoir pressure.

Variable Reservoir Equation In an attempt to fit the BH pressure response of the shut-in to the measured data, reservoir equation with a time dependent "A" was used. This simulation is equivalent to the "Modified Reservoir Equation" simulation up till the point of shut-in. From this point, the two simulations have different reservoir equations. While the "Modified Reservoir Equation" uses a constant value of $-34.7[\frac{kg}{s}]$ for "A", the "Variable Reservoir Equation" uses a time series shown in figure 16, with the discrete points given in table 9. The "A"-values in table 9 were found using a trial-and-error approach, where each "A"-value was adjusted until simulated BH pressure approximately matched measured.

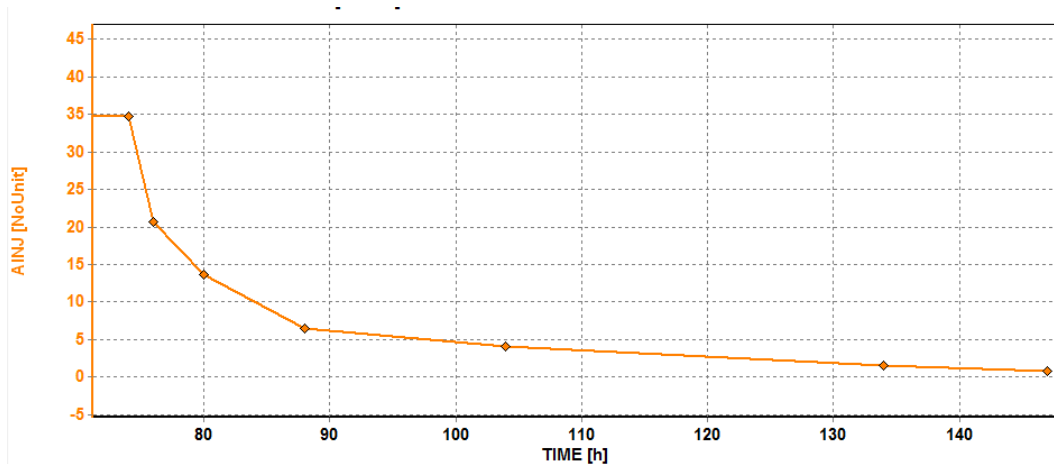


Figure 16: "A" values used in "Variable Reservoir Equation" simulation.

Measured and simulated BH pressure response during shut-in is shown in figure 17.

The BH temperature response is the same as in "Modified Reservoir Equation" simulation, while the BH pressure differs distinctly due to the introduction of a time dependent "A".

Shut-In BH Temperature Matching As was seen in figure 14, the simulation of the MIT using the modified reservoir equation and rock conductivity

| Simulation Time hours | A [$\frac{kg}{s}$] |
|--------------------------|-------------------------|
| 74 | -34.7 |
| 76 | -20.7 |
| 80 | -13.7 |
| 88 | -6.4 |
| 104 | -4.1 |
| 134 | -1.6 |
| 147 | -0.8 |

Table 9: "A" value for simulation "Variable Reservoir Equation". Shut-in commences at 74 hours simulation time.

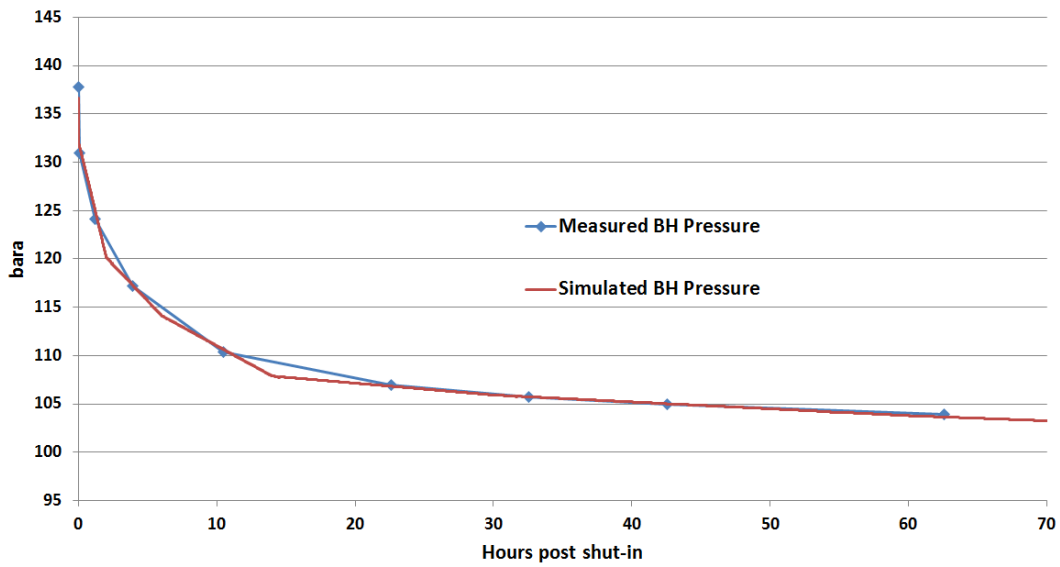


Figure 17: Measured and simulated BH pressure from "Variable Reservoir Equation" simulation.

was able to match the BH temperature during the step-rate test and constant injection period, but the simulated BH temperature did not match the measured during shut-in. In this section, changes to the simulation will be made in an effort to investigate what alterations need to be made to match the measured BH temperature response, if at all possible.

The injection of cold CO₂ has a distinct effect on the temperature of the storage reservoir, which can be seen in figure 4. To investigate how this effected BH temperature response to shut-in, a simulation where the surrounding rock formation temperature of the interval 972[m TVD]-1072[m TVD] was changed from the linear geothermal gradient described in section 4, to a constant 25°C for the full interval. The chosen interval incorporates both the Bois Blanc and Bass Islands formations, and the value of 25°C was chosen as this is the lowest reservoir temperature recorded in figure 4 during injection. This change had to be added manually, as OLGa does not correct for the reservoir cooling due to injected CO₂ automatically.

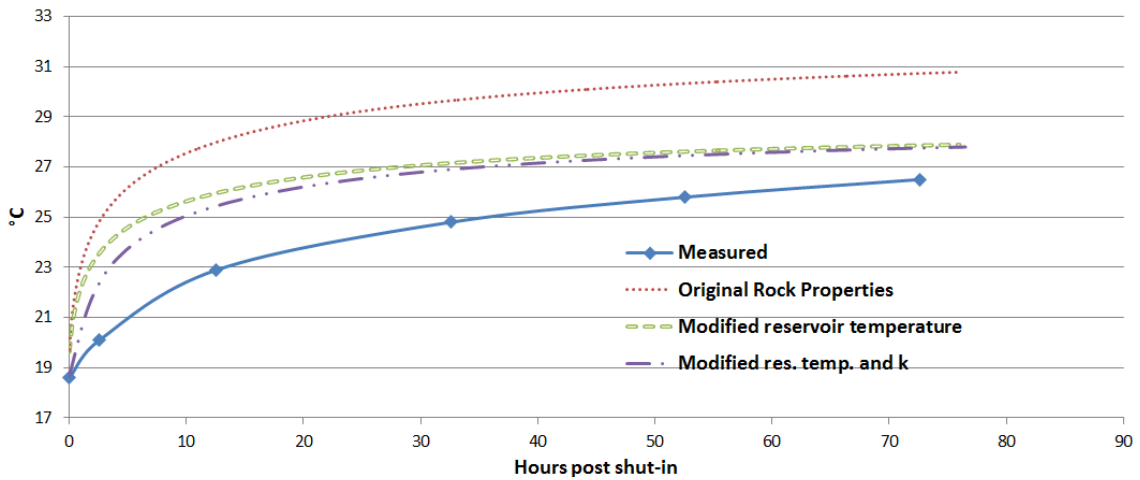


Figure 18: Comparison of shut-ins with different different reservoir temperature and rock properties to the measured BH temperature response to shut-in.

Figure 18 compares the BH temperature response to shut-in for three different heat transfer settings to the measured values. One uses the geothermal gradient and original rock conductivity described in section 4. Both of the other simulations use a reservoir temperature of 25°C, but one uses the original formation rock conductivity while the second uses the modified rock conductivity from table 8. It can be seen that none of the simulations are

able to match the measured BH temperature response to shut-in. The stark-
 est difference in between measured and simulated temperature is the rate of
 increase during the first 15 hours after shut-in.

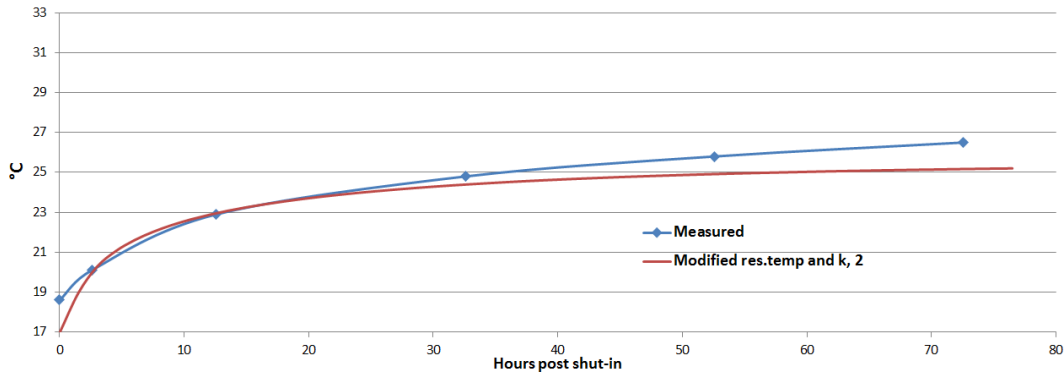


Figure 19: Shut-in BH temperature comparison of measured data to sim-
 ulation with reservoir temperature of 18°C, and dolomite and limestone
 $k=1.5 \frac{W}{m \cdot K}$

As the change of reservoir temperature to 25°C and using the "modified rock
 thermal conductivity" was found to not reproduce the measured BH tem-
 perature response, a more extreme change was tested. The values chosen
 for reservoir temperature and rock conductivity in this simulation were not
 meant as a realistic representation of the conditions surrounding the State
 Charlton well, but more a test to see if OLGA can possibly reproduce mea-
 sured values and specifically the response during the first hours of shut-in.
 The surrounding rock formation temperature in the interval 972[m TVD]-
 1072[m TVD] was lowered to 18°C, and the heat conductivity of limestone
 and dolomite (387.1-1071.4[m TVD]) was lowered to $1.5 \frac{W}{m \cdot K}$. These conduc-
 tivity values are $\frac{1}{3}$ and $\approx \frac{1}{2}$ of the original values for dolomite and limestone
 respectively. The results are shown in figure 19. Due to the changes done,
 the simulation has a 1.63°C lower BH temperature than the measured value
 after the step rate test and constant injection period preceding the shut-in.
 After ≈ 3 hours of shut-in the simulated temperature has risen 3.3°C com-
 pared to the 1.6°C measured, leaving both at 20.2°C. From this point, the
 simulated value rises by 5°C to 25.2°C over the following 70 hours, com-
 pared to the measured value of 6.3°C to 26.5°C. Figure 20 shows a comparison of
 the full mechanical integrity test.

It was also tested how increasing or decreasing the heat capacity of the
 limestone and dolomite by a factor of two would effect the BH temperature

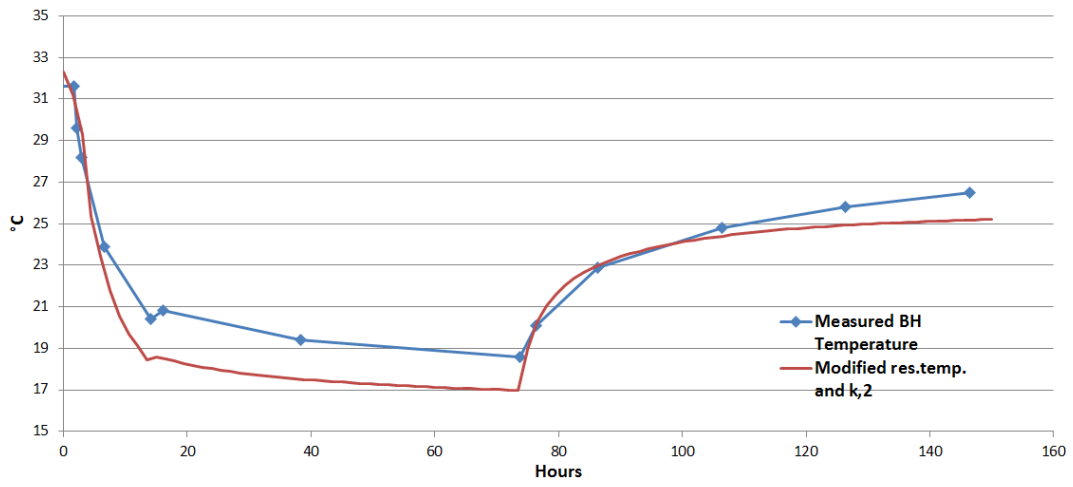


Figure 20: MIT BH temperature comparison of measured data to simulation with reservoir temperature of 18°C, and dolomite and limestone $k=1.5 \frac{W}{m \cdot K}$

response. However, these changes were shown not to be very impactful on the temperature gradient in the first hours after shut-in, and have therefore only been included in appendix C.

4.4.2 2nd Step-Rate Test

Figures 22 and 21 show the main results of the simulation of the March 5th step rate test. This simulation used equation 4 to model the reservoir. Table 10 summarizes WH and BH pressures from the simulation, and compares them to the measured values.

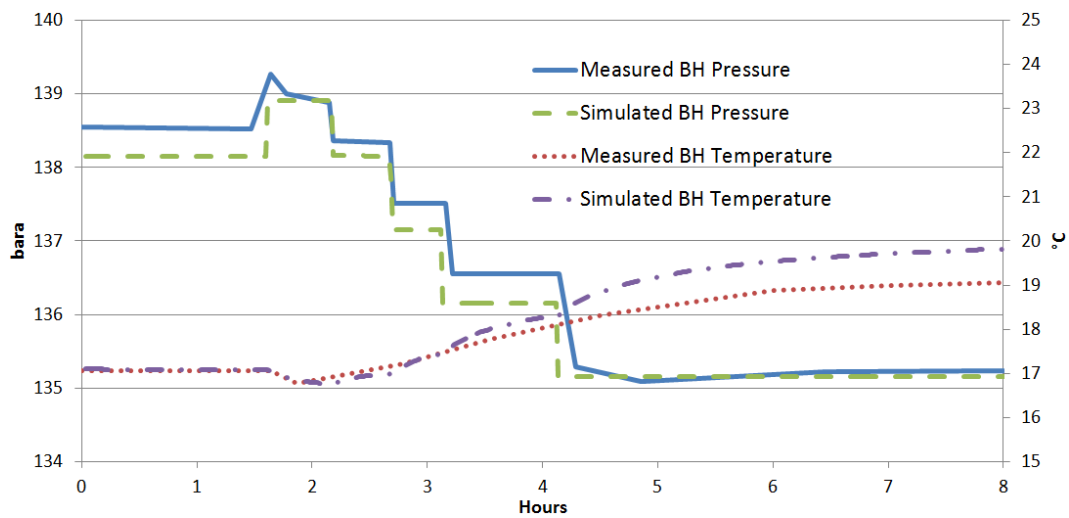


Figure 21: Measured and simulated bottom hole temperature and pressure for March 5th step rate test simulation.

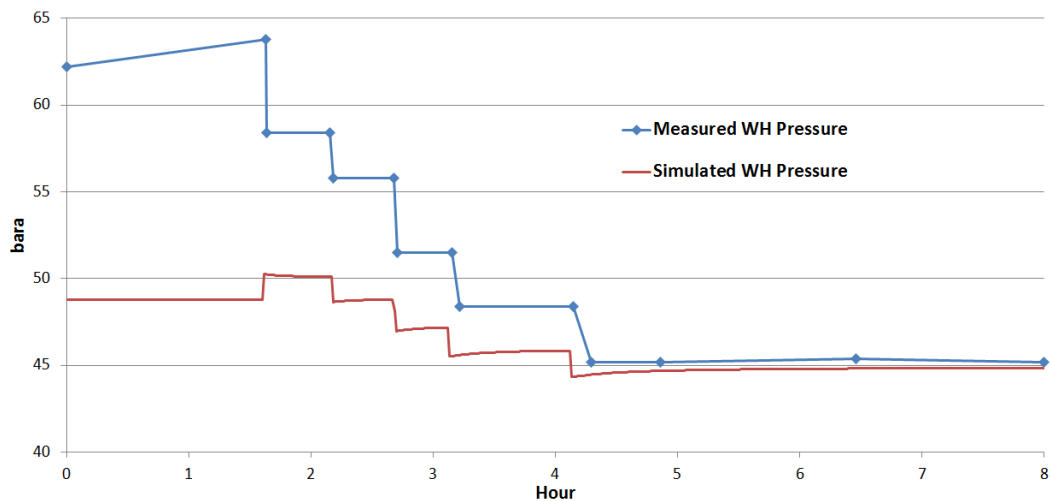


Figure 22: Simulated and measured wellhead pressure for March 5th step rate test simulation.

| Time hours | Flow rate [$\frac{ton}{day}$] ($[\frac{kg}{h}]$) | Simulated Values | | Measured Values | |
|---------------|---|----------------------|----------------------|----------------------|----------------------|
| | | WH Pressure [bar] | BH Pressure [bar] | WH Pressure [bar] | BH Pressure [bar] |
| 1.53-2.10 | 676 (28125) | 50.2-50.1 | 138.9 | 58.4 | 139.3-138.9 |
| 2.10-2.60 | 600 (25000) | 48.7-48.8 | 138.2 | 55.8 | 138.4 |
| 2.60-3.04 | 500 (20833) | 47.0-47.2 | 137.2 | 51.5 | 137.5 |
| 3.04-4.04 | 400 (16667) | 45.5-45.8 | 136.2 | 48.4 | 136.5 |
| 4.04-8.00 | 300 (12500) | 44.3-44.9 | 135.2 | 45.2 | 135.2 |

Table 10: Approximate WH and BH pressures for the given injection rate, from step rate test simulation. Measured values in the two right columns.

Mass flow rate As the mass flow rate is given as input in the simulation, the measured and simulated value match very well. The first step from 25 000 $\frac{kg}{s}$ to 28 125 $\frac{kg}{s}$ reflects the flow rate increase due to the methanol injection. The first step is back down to 25 000 $\frac{kg}{s}$, followed by three more down steps, each of 4167 $\frac{kg}{hour}$.

Wellhead temperature In the simulations, the well head temperature is constant at 4.44[°C] as explained in section 4.

Wellhead Pressure The first injection step with a flow rate of 28125 $[\frac{kg}{hour}]$ gives a WH pressure of 50.1[bar], while the WH pressure at the end of the test stabilizes at 44.9[bar]. This gives a total pressure drop of 5.2[bar]. The down steps in flow rate causes the well head pressure to rapidly drop, before stabilizing at a new value. Over each injection step period, the WH pressure rises slightly, with the largest increase being 0.52[bar] between 4 and 8 hours. The first 4167 $[\frac{kg}{hour}]$ step causes a pressure drop of 1.8[bar], while the following steps cause drops of 1.7[bar] and 1.6[bar].

Bottom hole Temperature For the first 1.5hours, the temperature is constant at 17.1°C. As the flow rate is increased, the temperature drops slightly down to 16.7°C over the first injection period, before increasing to 18.3°C over the next 2 hours. During the constant injection period from 4-8hours the temperature approaches a value of 19.8°C .

Bottom hole Pressure During the constant injection period prior to the step rate test, the BH pressure is constant at 138.2[bar]. As the test starts, mass flow is changed from 26 000 $[\frac{kg}{hour}]$ to 28 125 $[\frac{kg}{hour}]$ causing a BH pressure

rise of .75[bar]. The first step down brings the flow rate and pressure back down to $26\,000\left[\frac{kg}{hour}\right]$ and 138.2[bar]. This is followed by three more steps of $4166.7\left[\frac{kg}{hour}\right]$, each resulting in a 1[bar] BH pressure drop, resulting in an ending pressure of 135.2[bar] at a flow rate of $12500\left[\frac{kg}{hour}\right]$. This gives a total pressure drop of 3.7[bar] for the step rate test.

4.4.3 2nd Step-Rate Test Heat Sensitivity

The BH temperatures of the simulations comparing different heat transfer options for the second step-rate test are given in figure 23, while WH pressures are given in figure 24. The BH pressures were found to be largely unaffected by the thermal stability of the well, with the differences in BH pressure between the "virgin conditions" and "adiabatic conditions" being 0.1[bar] at highest.

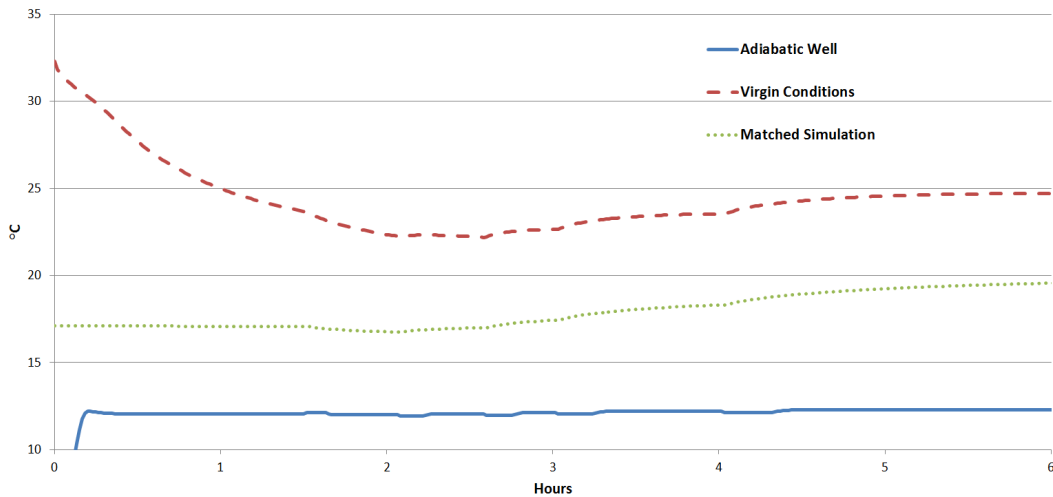


Figure 23: BH temperature comparison of second step-rate test simulations with different heat transfer.

The BH fluid temperatures were clearly affected by the length of the constant injection period preceding the step-rate test. The "virgin conditions" simulation BH temperature drops to a low of 22.2°C at 2 hours, before leveling off throughout the test and rising to 24.7°C at 6 hours, resulting in a 2.5°C during the test. The "matched simulation" has a low of 16.8°C at 2 hours, and rises to 19.6°C at 6 hours, resulting in a 2.8°C change during the test. The adiabatic well simulation has a constant BH temperature of 12.1°C .

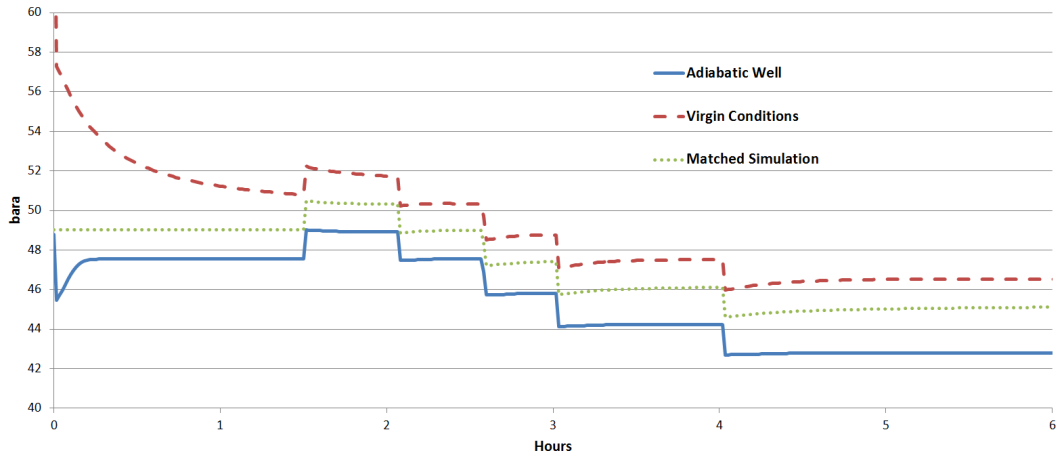


Figure 24: WH pressure comparison of second step-rate test simulations with different heat transfer.

The WH pressure of the virgin conditions simulation drops significantly over the 1.5 hour injection period leading up to the step-rate test, and drops by 0.5[bar] over the first injection step of the test. The following steps-downs in flow rate result in distinct pressure drops for all simulations and re-adjusting to a new level for the new flow rate. Throughout the simulation, the virgin conditions simulation constantly holds a higher pressure than the matched simulation, which again constantly holds a higher pressure than the adiabatic simulation.

The wellhead temperature of all simulations was equal and constant throughout the step-rate test. This is due to fluid injection temperature being given as an input variable in OLGA.

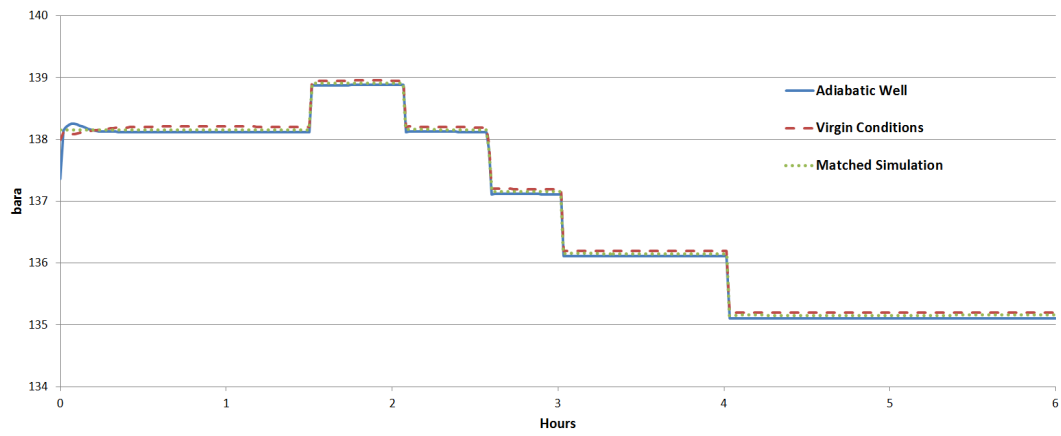


Figure 25: BH pressure comparison of second step-rate test simulations with different heat transfer.

4.5 Discussion

4.5.1 Mechanical Integrity Test

Original Reservoir Equation The simulation using the reservoir equation given in equation 3, based on the injectivity value provided in the State Charlton final report [31] was not able to replicate BH pressure response seen in figure 7 of the step rate test. The simulation gives a pressure rise of 14.9[bar] compared to the measured value of ≈ 2 [bar]. Based on this, a modified reservoir equation was adopted to better match the measured shut-in data.

Modified Reservoir Equation The modified reservoir equation has a pressure rise of 2.47[bar] over the step rate test, which is higher than the actual rise measured, but a significant improvement over the original reservoir equation. Shape of the simulated and measured response differs significantly. While the simulation value has a consistent response to each step-up in injection rate, there is no clear and consistent pattern in the measured response to each step-up.

During the step rate test and constant injection period, the simulated values of the BH temperature follow the same trend as the measured values, with a sharp drop during the step rate test and a slower temperature drop during the constant injection phase. Table 11 gives a comparison of the bottom hole temperatures at the end of the constant injection period, the start and end of the step rate test. The measured values from the State Charlton 4-30 well test were acquired by reading off figure 6, making their accuracy limited.

| | Simulation Value | Measured Value |
|----------------------------------|------------------|----------------|
| Start of step rate test | 32.4°C | 31.6°C |
| End of step rate test | 21.4°C | 20.3°C |
| End of constant injection period | 19.7°C | 18.6°C |
| 70 hours post shut-in | 30.7°C | 26.1°C |

Table 11: Comparison of simulated and measured bottom hole temperature values during step rate test and constant injection.

During the shut-in period, the BH temperature response in the simulation recovers much quicker than the actual response seen in figure 6. After a shut-in period of 70 hours, the simulated BH temperature has almost rebounded

to pre-injection level at 30.7°C, while the measured BH temperature in the State Charlton well was only 26.1°C. The BH temperature in the simulation reaches 26.1°C after only five hours.

The simulated BH pressure response to shut-in differs significantly from the measured response. Due to the "A" value of $-34.7[\frac{kg}{s}]$ flow between the well and reservoir stops as the BH pressure drops to 132.2[bar]. This is shown below, where an estimated $p_{wf} = 133.3[bar]$ has been used to account for the elevation difference between the point where BH pressure is measured and the point where the reservoir perforation is defined.

$$\begin{aligned}
 G_w &= A + B \cdot (p_{wf} - p_{res}) \\
 G_w &= -34.7 + 1.16 \times 10^{-5}((133.3 - 103.4) \cdot \times 10^5) \\
 G_w &= -34.7 + 1.16 * 29.9 = -.016 \\
 G_w &\approx 0 \frac{kg}{s}
 \end{aligned}$$

Variable Reservoir Equation By using a time variable linear reservoir equation, it was possible to match the BH pressure response to shut-in. The match is not perfect, but could be improved by using a higher definition time series. The BH temperature is seemingly not affected by the change in reservoir equation, and has the same values as for the "Modified Reservoir Equation". Using the variable reservoir equation was the only way found to match the measured pressure with OLGA. However, this method requires the measured response to be known beforehand, so that reservoir equation can be tuned according to it. Due to this, the method can not be used to predict shut-in response and it useless as a predicative method.

Shut-In BH Temperature Matching The comparison of measured BH temperature response to the simulation with the original rock properties and geothermal gradient given in section 4 in figure 18 shows that this simulation is not able to recreate the BH temperature response to shut-in measured in the State Charlton 4-30 well. The simulation over-predicts the temperature gradient in the first hours of shut-in. The reservoir formation rock temperature was lowered to 25°C in an attempt to account for the cooling of the reservoir due to injection of cold CO₂ and the formation rock heat conductivity adjusted to 80% of the values given in Lithology in section 4. This lowered the ending shut-in BH temperature to $\approx 1^\circ\text{C}$ over the measured value. However, the temperature gradient in first hours following shut-in is

still much higher in the simulation than measured, and the general shape of the two graphs differ. This shows that adjusting the thermal properties of the formation within what was considered a reasonable boundary, it was not possible to achieve a match between the simulated and measured BH temperature response to shut-in.

The best match to the measured values was found by setting reservoir temperature to 18°C and, the limestone and dolomite conductivity to $1.5 \frac{W}{m \cdot K}$. However, there are still differences between simulated and measured response, and figure 20 shows that adjusting the reservoir temperature and formation properties to best match the shut-in response, results in a poor match of BH temperature during the step rate test and constant injection period. This result shows that even when freely adjusting the formation properties, it was not possible to re-create the measured temperature response using OLGA.

No good explanation to why it was not deemed possible to match the BH shut-in temperatures was found, it does however raise questions regarding OLGA's ability to handle heat transfer in injection well shut-ins. It is worth noting that OLGA does not support natural convection based flows [24]. This probably does not play an important role during injection, as the flow is then largely dominated by forced convection, but could be an important factor during shut-in. As the well is shut-in, the density difference between WH and BH is $\approx 12 \frac{kg}{m^3}$ which possibly could cause a natural convection based flow with lower density CO₂ rising and high density CO₂ sinking. If this is the case, then OLGA not accounting for this effect could be a reason to the disparity between measured and simulated BH temperature response.

Shut-in BH Pressure Matching The simulation was unable to re-create the measured BH pressure to shut-in. The linear reservoir equation (equation 4) was used to represent the reservoir, and the simulations showed that this reservoir modeling option was not able to match the shut-in. OLGA offers the possibility of using a quadratic one-equation model for reservoir modeling, which was not tested. It is possible that this model could provide improved results for BH pressure matching. However, in the author's opinion it is questionable if any one-equation model of the simplicity offered by the linear and quadratic equation will be able provide a sufficient modeling of the reservoir. OLGA is primarily designed to be a multiphase pipe flow simulator, and has only very limited reservoir modeling capabilities.

4.5.2 2nd Step Rate Test

The OLGA simulations of the March 5th step rate test used a the linear reservoir model with the constants given in equation 4 to match OLGA simulations to measured data from the State Charlton CO₂ injection well. These values differ significantly from the suggested injectivity value in the State Charlton final report of $1.937 \times 10^{-6} [\frac{kg}{s*Pa}]$. It was attempted to match the simulations using this injectivity value, but this value resulted in too large drops in BH pressure from the injection rate drops. The injectivity value (B) of $1.16 \times 10^{-5} [\frac{kg}{s*Pa}]$ was found to give the correct BH pressure "sensitivity" to flow rate changes. With this B-value, it was necessary to add an "A" of $-34.7 [\frac{kg}{s}]$ to raise the BH pressure to the measured value. The "A" in the linear reservoir equation gives the minimum pressure difference required for flow to start from the well to the reservoir. The necessity of a minimum pressure difference to start flow is supported by the State Charlton final report which notes that "...it appears that a pressure increase of approximately 500psi (34.5[bar]) was necessary to initiate injection".

Bottom hole Pressure The simulation successfully matched the starting and ending BH pressure using the given reservoir equation constants. Table 12 shows a comparison of the BH pressure response to each of the four steps. Please note that the first step down is of $3166.7 [\frac{kg}{h}]$ while the following three steps are of $4166.7 [\frac{kg}{h}]$.

| Measured Δp [bar] | Simulated Δp [bar] |
|------------------------------|-------------------------------|
| -0.5 | -0.7 |
| -0.9 | -1.0 |
| -1.0 | -1.0 |
| -1.3 | -1.0 |

Table 12: Comparison of measured to simulated BH pressure response to mass flow step down.

The measured values from State Charlton show that none of the steps yield the same change in BH pressure. A trend of increasing Δp_{BH} for each step is observed, indicating that Δp_{BH} from a mass flow rate change is not only a function of the step size, but also the absolute value of the flow rate. This behavior is not captured in the simulations, where the BH pressure drops

by 1[bar] for each of the $4166.7[\frac{kg}{h}]$ mass flow down steps, indicating that the simulation BH pressure is only dependent on the step size and not the absolute value of the mass flow rate. However, it is important to note that due to there only being three identical steps to compare, it is hard to identify if the variable Δp_{BH} response to each step is an actual general trend.

Bottom hole Temperature Both the measured and the simulated bottom hole temperature follow the same general trend with a dip after the flow rate increase at $\approx 1.5hours$, followed by a temperature increase during the injection rate test. Both simulated and measured BH temperature seem to be approaching a steady state value during the constant injection period from 4-8 hours. However, the simulated value exceeds the measured value for the throughout the documented period, and also has a steeper incline during the step rate test. Before the step rate test commences the simulated value exceeds the measured value by $0.7^{\circ}C$, and at the end of the documented period the simulated value is $1.8^{\circ}C$ higher than the measured value. This indicates that the heat transfer from the formation rock to the fluid in the wellbore is set too high.

Wellhead Pressure Table 13 gives a comparison of the simulated and measured WH pressures during the step rate test. It can be seen that the simulated WH pressure has a smaller sensitivity to the flow rate decrease than the actual measured WH pressure, with a total Δp_{WH} of only 5.2[bar], compared to the measured value Δp_{WH} of 13.2[bar]. Measured and simulated have a similar ending pressure at $12500[\frac{kg}{h}]$ of 45.2 and 45.1[bar], but the measured value supersedes the simulated by 8.1[bar] at the start of the step rate test.

| Flow rate [$\frac{ton}{day}$] ([$\frac{kg}{h}$]) | Measured WH Pressure [bar] | Simulated WH Pressure [bar] |
|---|-------------------------------|--------------------------------|
| 676 (28125) | 58.4 | 50.3 |
| 600 (25000) | 55.8 | 49.0 |
| 500 (20833) | 51.5 | 47.4 |
| 400 (16667) | 48.4 | 46.0 |
| 300 (12500) | 45.2 | 45.1 |

Table 13: Comparison of the measured and simulated values of the WH pressure during March 5th step rate test.

The simulations were not able to produce the correct pressure difference between WH and BH for the higher flow rates. While the measured data from State Charlton shows a pressure difference of $\Delta p_{Well} = p_{BH} - p_{WH} = 80.5[bar]$ for an injection rate of $28125[\frac{kg}{h}]$, the simulation gives $\Delta p_{Well} = 88.6[bar]$. The pressure difference between WH and BH is in this instance caused by hydrostatic pressure and frictional losses, given by equations 5 and 6.

$$\Delta p = \rho \cdot g \cdot \Delta h \quad (5)$$

$$h_f = f_D \cdot \frac{L}{D} \cdot \frac{\rho \bar{V}^2}{2} \quad (6)$$

The most probable sources for the simulations miscalculation of the Δp_{Well} at high flow rates is a under prediction of the friction factor or an over prediction of the fluid density. However, the fact that the simulations give a correct Δp at lower flow rates indicate that either the fluid density is highly sensitive to the relatively small pressure and temperature differences separating the $28125[\frac{kg}{h}]$ and the $12500[\frac{kg}{h}]$ simulations, or that the friction factor in the simulations is an important cause. The well operates near the critical conditions of CO_2 ($73.77[bar], 30.98^\circ C$), which is a known problematic area for most equations of state. A miscalculation of CO_2 density by the Span-Wagner EOS used for this simulation is a probable contributor to the simulations erroneous WH pressure. It is also relevant to recall that the simulation assumes that the injected fluid is pure CO_2 . Although it in section 4 was documented that samples taken of the injectate showed very high CO_2 purity, this is not the same as 100% pure CO_2 and will be a source of error. Finally, the possibility of the errors in the measured values or the well description given in the State Charlton final report [31] must be considered.

| Measured Δp [bar] | Simulated Δp [bar] |
|------------------------------|-------------------------------|
| -2.6 | -1.3 |
| -4.3 | -1.6 |
| -3.1 | -1.4 |
| -3.2 | -0.9 |

Table 14: Comparison of measured to simulated WH pressure response to mass flow step down.

The WH Δp response to each step for both measured and simulated is shown in table 14. The values measured at State Charlton show no obvious trend from the four injection steps, with the second step yielding the highest pressure drop, and step two and three yielding almost similar pressure drops. Even when accounting for the fact that the flow rate change in the first step is only 76% of the last three steps, the Δp of the first step is lower than the second. The simulated Δp show a decreasing trend over all four steps when the lower amplitude of the first step is accounted for.

4.5.3 Second Step-Rate Test Heat Sensitivity

The comparison of step-rate tests with different reservoir-to-fluid heat conduction showed the differences in BH & WH pressures and temperatures that can be expected between a thermally stabilized well and a thermally "unstable" well. The adiabatic well simulation represents a perfectly stable well, where no heat is conducted from the surrounding rock formation to the fluid in the wellbore. Although an adiabatic well is unrealistic, it is a good baseline for comparison. Of the four parameters measured, only BH temperature and WH pressure were found to be affected by the thermal stability of the well. A maximum difference of 0.1[bar] was seen on BH pressure and this parameter can thereby, according to the simulations, be considered to be independent of the thermal stability of the well. WH temperature was given as an input parameter in the simulations and was therefore constant for all simulations.

The BH temperature of the "virgin conditions" simulation dropped significantly (10°C) during the 1.5 hour injection period preceding the step rate test, unlike the "matched simulation" and the adiabatic simulation which had constant temperatures. However, during the step-rate test itself the "virgin conditions" simulation BH temperature rose by 2.5°C, comparable to the 2.8°C in the "matched simulation". The temperature rise during the test can be related to the flow rate being lowered during the test. The heat influx from the wellbore wall [$\frac{W}{m^2 \cdot s}$] is likely to be quite constant throughout the test, causing a higher BH temperature as each fluid particle spends more time in the well due to the lowered flowrate and thereby fluid velocity. Contrarily, an increased temperature drop could be expected if the flow rate was increased, instead of decreased in the step-rate test. The adiabatic well BH temperature is constant at 12.1°C throughout the simulation and unaffected by the changes in flow rate. The temperature rise of 7.7°C between WH and BH can likely be attributed to the Joule-Thomson effect, which describes temperature changes of gases or liquids that undergo an adiabatic pressure

change.

The "virgin conditions" simulation consistently holds a higher WH pressure than the "matched", which again has a higher pressure than the adiabatic simulation. As described in the previous paragraph, simulations have different fluid temperatures, causing a difference in CO₂ density. Lower density results in lower weight of the fluid column separating BH and WH, and thereby causes higher WH pressure. Over the first period of the step-rate test, between 1.5-2.0 hours, the flow rate has been increased and the "virgin conditions" simulation sees a drop in WH pressure of 0.5[bar], compared to 0.1[bar] for the "matched" simulation. For the remainder of the simulation time, where flow rate is decreased, the difference in WH pressure between "virgin" and "matched" is near constant at 1.4[bar].

According to the simulations, the thermal stability of the well has no impact on the BH pressure. This indicates that thermal stability may not be an important factor in a step-rate tests if the BH pressure is used for analysis. Differences in WH pressure were observed, most distinctly during the first step, where flow rate is increased. The increase in flow rate increased the difference in fluid temperature between "virgin" and "matched", and thereby the difference in WH pressure. Conversely, during the following four step-downs in flow rate only resulted in a 0.3°C difference between the two simulations, which was reflected in the WP pressure responses being very similar over this period. From these results, it can be suggested that if a step-rate test is to be performed in a well that is "thermally unstable", it is advisable to step the flow-rates down instead of up.

5 WAG Injection Simulations

In this section, WAG injection simulations will be performed. No comparable simulations were found during the literature study, meaning that this could be a first published attempt of WAG-simulation with OLGA. The simulations aim to investigate what pressure and temperature responses can be expected in the well during a WAG injection, and how the injection cycle period length, meaning the time for which one medium is injected before switching to the other, affects the well conditions.

In the WAG simulations, CO₂ was first injected at 18750 $[\frac{kg}{h}]$ for a given time period, before instantaneously turning the CO₂ injection off and at the same time starting the water injection at 18750 $[\frac{kg}{h}]$. As the WAG simulations uses both CO₂ and water, it was not possible to use the pure CO₂ module in OLGA. Therefore, a file containing the thermodynamic properties of CO₂ and water was imported from the program "PVTsim". This PVT-file was created using the SRK-Peneloux EOS. "PVTsim" provided a limited set of EOSs, including SRK, SRK-P, PR and Peng-Robinson-Peneloux. The Wilhelmsen et.al paper [58] showed SRK-P to outperform SRK in density prediction over the total examined PT-range. Following the region classification provided by Wilhelmsen et.al. [58], the well conditions are most likely in the liquid and supercritical regions for the most of the time, although critical conditions might occur during the startup of injection. SRK-P yielded better results on specific heat capacity prediction than PR in both liquid and supercritical regions, and also on density prediction in the liquid region. PR-P was not considered based on a lack of data on its performance in CCS-applications.

The simulations were performed using the same settings as described in section 4, except for the surrounding rock formation heat conductivity. The history matching simulations performed in section 4 showed that the best match between measured and simulated BH temperatures for step rate test and constant injection period was achieved when using the thermal rock conductivity given in table 8. Figure 43 in appendix E.2 shows a BH temperature comparison of measured versus simulated with rock conductivity given in table 8.

To perform the EOR simulations, a second mass flow source was added in the OLGA model, leaving one source to inject pure CO₂ and one to inject water. When switching from one medium to the other, the mass flow rate of the first source is linearly decreased from 18750 $[\frac{kg}{h}]$ to 0 $[\frac{kg}{h}]$ over a 36 second

period, while the flow rate from the second source is simultaneously increased linearly from $0[\frac{kg}{h}]$ to $18750[\frac{kg}{h}]$.

5.1 OLGA Simulations Description

A simulation of the full MIT using 100% pure CO₂ was performed to compare the Span-Wagner model to the SRK-Peneloux model. The Span-Wagner model uses the "singleoptions" setting, where OLGA creates the required tables of thermodynamic properties using the Span-Wagner EOS. The SRK-Peneloux model imports the required tables from PVTsim. Except of this, the simulations are identical, and serve as a comparison of the two equations of state.

Both CO₂ and water are injected at a rate of $18750[\frac{kg}{h}]$ and at a temperature of 4.44°C.

Simulations with different injection time lengths were performed and compared to each other. Equally long simulations with cycle lengths between 4 and 24 hours were ran to investigate the effect of the injection cycle length. In this work, "injection cycle length" refers to the time period of constant injection of each medium before switching to the other medium. Simulations investigating the effects of using CO₂ or water as the first injection medium were also performed.

To investigate BH temperature development over a longer time period than the ≈ 120 hour simulation times used for the 4-24 hour injection cycle simulations, a simulation consisting of a single 800hour CO₂ cycle, followed by a single 800 hour water cycle was performed.

5.2 Simulation Results

Equation of State Figure 42 in appendix E.1 shows a plot of the BH temperature and pressure for the simulation using Span-Wagner and SRK-Peneloux equation of state. There is only a minor difference in pressure between the two simulations, with the SRK-Peneloux model predicting a $\approx 0.1[\text{bar}]$ higher BH pressure for the entire simulation. The differences in BH temperature are somewhat higher, reaching a maximum at the end of the constant injection period where the SRK-Peneloux model predicts a 0.4°C

higher BH temperature.

WH temperature, and mass flow rate Figure 44 in appendix E.3 shows the WH temperature for the simulation with 24 hour injection cycles. During all six injection cycles, WH temperatures are between 4.50°C and 4.47°C . Spikes in temperature up to 50°C occur when switching from CO_2 to water, and up to 7.5°C when switching from water to CO_2 . These spikes last ≈ 90 seconds. Similar spikes are seen in the mass flow rate plot in appendix E.3. It is noteworthy that the largest injection rate spikes reach more than three times the standard injection rate of $18750[\frac{\text{kg}}{\text{h}}]$. It was attempted to lower the maximum time step in the simulations from $0.1[\text{s}]$ to $0.01[\text{s}]$, but this was not found to affect the the spikes.

BH pressure Figure 46 in appendix E.3 shows the BH pressure from the simulation with 24 hour injection cycles. During CO_2 injection the pressure is $136.9[\text{bar}]$, while it is $136.7[\text{bar}]$ during water injection. No change in BH pressure is seen between the first and last CO_2 cycle, or the first and last water cycle.

WH Pressure The WH pressure of the 24 hour injection cycle simulation is shown in figure 26. During the first CO_2 injection cycle, the pressure drops from an initial value of $\approx 61[\text{bar}]$ to $53.5[\text{bar}]$. The pressure is more stable during the following two CO_2 injection cycles, with a ending pressure of $53.1[\text{bar}]$ at 74 hours and $52.9[\text{bar}]$ at 122 hours. At the switch from CO_2 to water as injectate 26 hours into the simulation, BH pressure drops to $36.4[\text{bar}]$ over a 15 minute period. During all three water injection cycles, the BH pressure is stable at $36.4[\text{bar}]$. For all of the cycles, the difference in pressure between CO_2 and water was $\approx 17[\text{bar}]$.

To evaluate the difference in frictional loss between CO_2 and water, a simulation with shut-in of both water injection and CO_2 injection was performed, and the WH pressure plot of this simulation is included in 51 in appendix E.5. The difference in frictional loss can be estimated by evaluating the WH pressure difference right before and after a shut in. It was found that the water injection has a pressure difference of $6.7[\text{bar}]$ between flowing and stagnant conditions, while CO_2 has $5.6[\text{bar}]$.

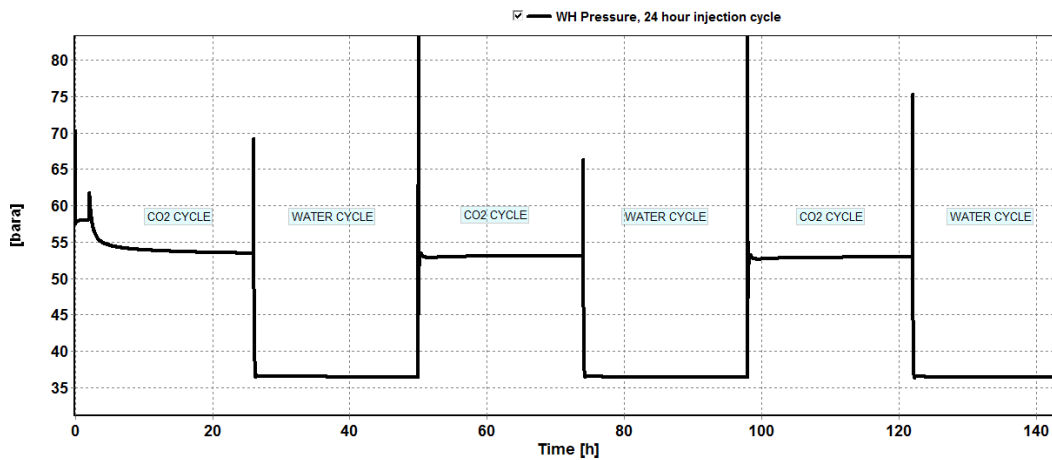


Figure 26: Wellhead pressure, 24 hours injection cycle simulation.

BH Temperature Figure 27 shows the BH temperature of the 24 hour injection cycle simulation. A sharp drop in BH temperature from 32.6°C to 20.6°C is seen during the first CO_2 injection period. The first water cycle starts 26 hours into the simulation, causing a rapid drop in temperature to 11.3°C at 28 hours and 9.7°C at the end of the cycle at 50 hours. As the second CO_2 injection cycle is started, the BH temperature rises to 17.2°C at 50.5 hours, and continues to rise 19.4°C at the end of the second CO_2 cycle. At the end of the second water cycle the BH temperature is 9.3°C , and 9.1°C at the end of the third. At the end of the third CO_2 cycle BH temperature is 18.9°C . A BH temperature plot from an extended 310hour simulation with 24 hour injection cycles has been added in appendix E.3 figure 47. This plot confirms that the BH temperature continues to drop for each cycle beyond the 150 hours shown in figure 27.

Figure 28 shows the BH temperature of the 4 hour injection cycle simulation. As with the 24 hour injection cycle, the most significant temperature drop occurs over the first injection cycle. However, temperature continues to drop for each cycle, and has not completely stabilized at the end of the simulation. At the end of each cycle, the temperature is still changing; with -0.15°C during the last hour of the final water cycle, and 0.2°C during the final hour of the final CO_2 cycle.

The 4 hour simulation and 24 hour simulation can be compared at 102 hours of simulation time. Both simulations switch from water to CO_2 at 98 hours, and have therefore been injecting CO_2 continuously for four hours at the 102 hour mark. The 4 hour injection cycle simulation has a BH temperature

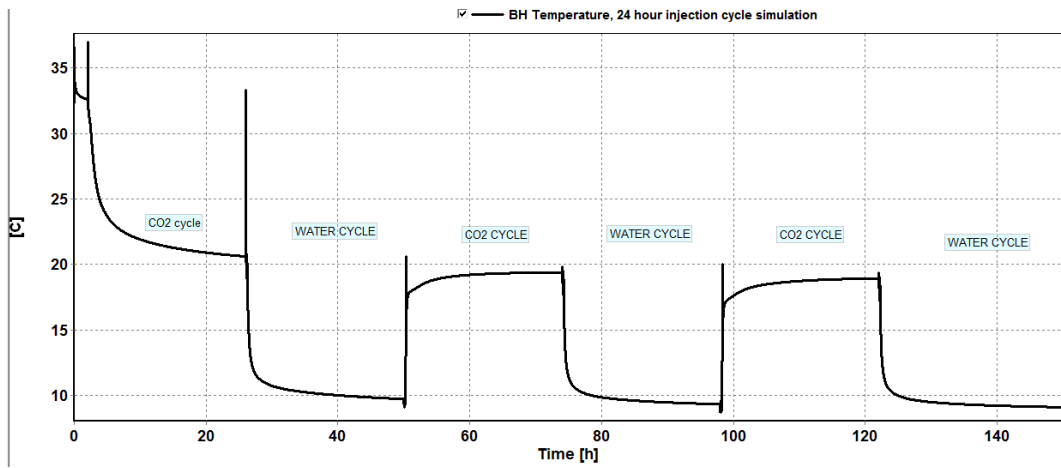


Figure 27: Bottom hole temperature, 24 hours injection cycle simulation.

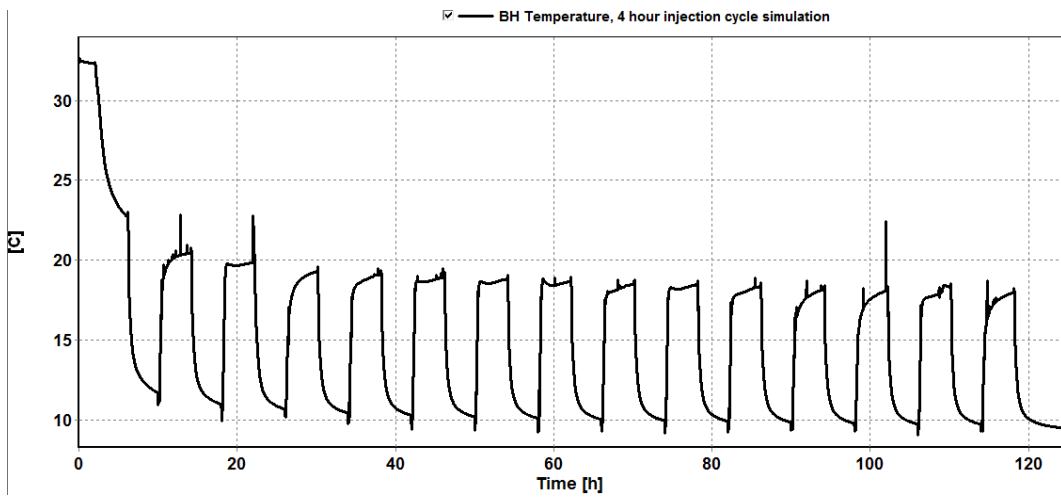


Figure 28: Bottom hole temperature, 4 hours injection cycle simulation.

of 18.05°C, compared to 18.13°C for the 24 hour injection cycle simulation. This can be compared to the 800 hour cycle simulation (figure 29), where pure CO₂ was injected for the first 800 hours. After 102 hours of only CO₂ injection, the BH temperature was 20.30°C.

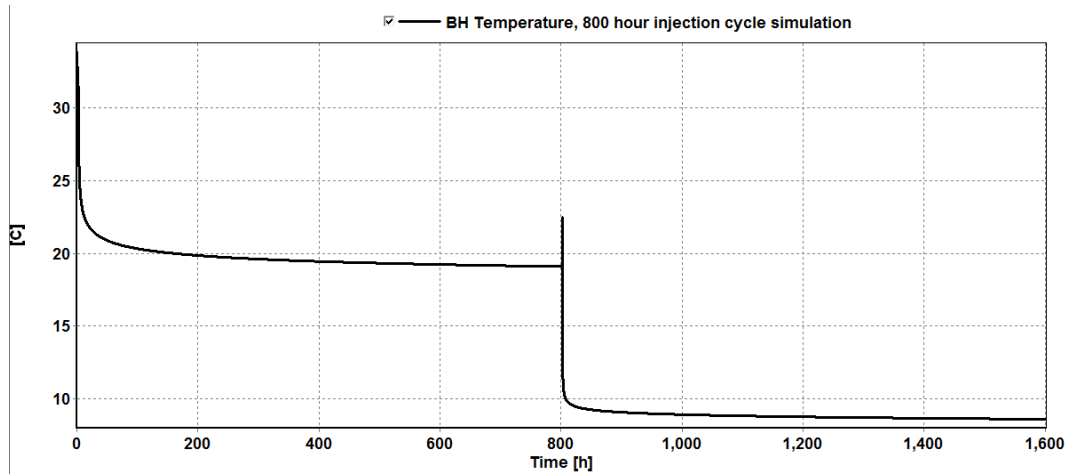


Figure 29: Bottom hole temperature, 800 hours injection cycle simulation.

As seen in the 24 hour cycle simulation, WH pressure, WH temperature and BH pressure stabilize quickly after injection medium switch and are thereby unaffected by the injection cycle length being 4 or 24 hours. Due to this, these variables will not be further discussed, but the plots from the 4 hour cycle simulation have been included in appendix E.4.

Water as first injection medium Figures 30 and 31 show the BH temperature and WH pressure of a simulation using water as the first injection medium, with 24 hour cycles. The BH pressure and WH temperature plots are given in appendix E.6.

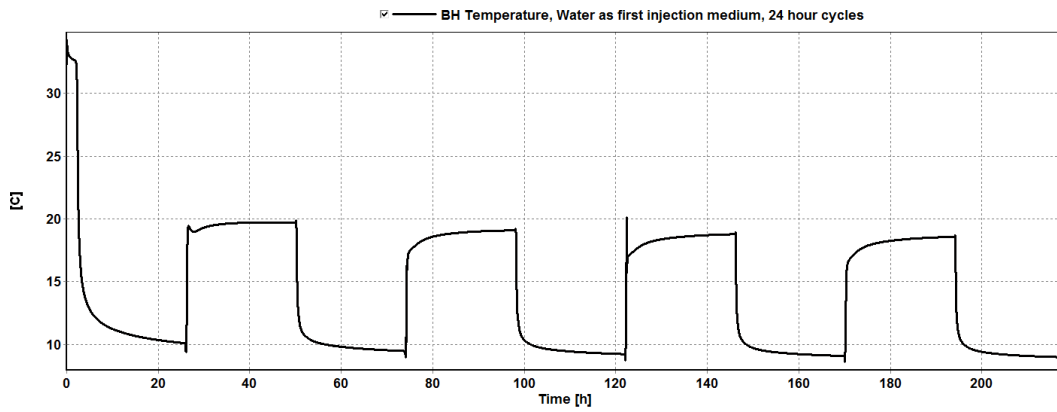


Figure 30: Bottom hole temperature, water as first injection medium, 24 hour injection cycle simulation.

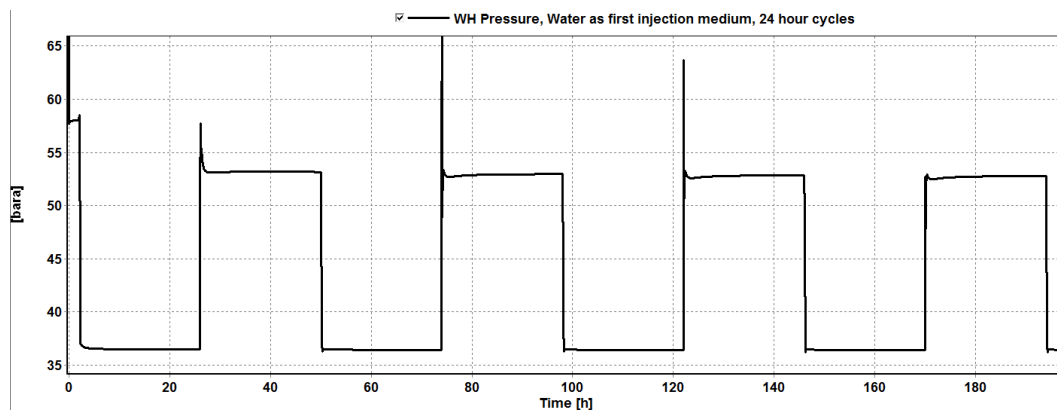


Figure 31: Wellhead pressure, water as first injection medium, 24 hour injection cycle simulation.

5.3 Discussion

Flow rate, pressure and temperature spikes Spikes in mass flow rate pressure, temperature and were observed in the simulations when switching between water and CO₂ as injection medium. The OLGA model operates with two mass flow sources, both having a maximum flow rate of 18750 $[\frac{kg}{h}]$. The two sources are never operating simultaneously at maximum flow rate, but even if this was the case, a flow rate of 55000 $[\frac{kg}{h}]$ as seen in figure 45 in appendix E.3 would not be possible. The reason for the spikes is unknown, but since the flow rate spikes exceed the theoretical maximum, it is considered unlikely to be an actual flow phenomena, but rather a simulation related problem. This makes it impossible to interpret any actual flow phenomena that might occur during the injection medium switch, as these are masked by the likely simulation related spikes. It is reasonable to assume that the pressure and temperature spikes are related to the mass flow spikes, and hence the reason or implications of the any of the spikes will not be further discussed.

WH temperature and BH pressure The simulations did not reveal any interesting information regarding the WH temperature, as this is controlled by the fluid temperature of the mass source, which in this case is set to a constant of 4.44°C for both CO₂ and water. The BH pressure only changes by 0.2[bar] when switching between CO₂ and water, and is near constant for each medium over the entire duration of the simulation. It's worth noting that in the OLGA simulation, BH pressure is governed by the model's reservoir pressure, mass flow rate and reservoir model equation. As all these parameters are equal for both the CO₂ and water injection, no major change in pressure was expected.

WH pressure While the BH pressure is near equal for water and CO₂, the difference in WH pressure is ≈ 17 [bar]. The primary reason for the WH pressure density difference between CO₂ and water, but also a difference in frictional losses between CO₂ and water. However, as it was estimated that water frictional loss ≈ 1 [bar] larger than CO₂, the hydrostatic pressure difference between CO₂ injection and water injection is ≈ 18 [bar]. This results in a average density difference between water and CO₂ in the well of:

$$\rho_{H_2O} - \rho_{CO_2} = \frac{p_{H_2O} - p_{CO_2}}{g \cdot h} = \frac{18 \times 10^5}{9.81 \cdot 1048} = 175[\frac{kg}{m^3}]$$

Except for a pressure drop during startup of the first CO₂ injection cycle, the WH pressure was stable during all injection cycles. A pressure difference of 0.5[bar] is observed between the end of the first and third CO₂ injection cycle. This is likely related to the CO₂ in the wellbore holding a lower temperature during the third cycle. This increases the CO₂ density and the hydrostatic pressure difference between WH and BH.

BH temperature While both water and CO₂ hold the same temperature at WH, the BH temperature plots clearly show that CO₂ holds a higher temperature than water by the time the fluid reaches BH. The primary reason for this is the difference in heat capacity between the two substances. As an illustration, the C_p of water at 15°C and 80[bar] is $4.16[\frac{kJ}{kg \cdot K}]$ compared to $2.67[\frac{kJ}{kg \cdot K}]$ for CO₂. This means that 1.56 times more energy is needed to heat the same mass of water by 1[K] than CO₂.

Unlike the BH pressure, WH temperature and WH pressure, which saw little to no change between comparable cycles over the duration of the simulations, the BH temperature continues to drop for the entirety of the simulation. Although the temperature drop between each comparable cycle is small, it confirms that the well is not in a thermal steady state even after 310 hours as seen in figure 47 in appendix E.3. Moreover, the 800 hour injection cycle simulations show that the well has not reached a thermally steady state even after 1600 hours of simulation. This highlights the long temperature time scales involved in cooling the rock formation surrounding injection wells.

While the BH temperature does not seem to stabilize fully, the changes occurring after the first injection cycle are small compared to the temperature drop during the first cycle. During the first CO₂ cycle in the 24 hour cycle simulation, the BH temperature drops from the pre-injection 32.6°C to 20.6°C. For comparison, the temperature at the end of the sixth 24 hour CO₂ cycle in figure 47 is 18.4°C (after 266 hours of WAG injection), meaning that 84.5% of the total temperature drop occurs over the first cycle.

Water as first injection medium Whether CO₂ or water was used as first injection medium had little to no impact on the WH temperature or BH pressure. However, some effects were seen on WH pressure and BH temperature. The BH temperature drops more rapidly over the first cycle (18.8°C over first two hours), and reaches 10.0°C at the end of the first cycle, com-

pared to 20.6°C with CO₂ as first injection medium. Only small temperature changes are seen over the following CO₂ and water cycles.

Figure 26 shows that the wellhead pressure drops by over 7[bar] during the first injection cycle when CO₂ is the first injection medium. Comparably, the WH pressure is constant throughout the first injection cycle when water is the first injection medium. This is likely due to the CO₂ density being more sensitive to temperature changes than water. As the fluid temperature drops significantly during the first injection cycle, the CO₂ density increases, thereby increasing the weight of the fluid column in the well. Although the water experiences a larger temperature drop, its density is far less affected by temperature changes, and hence the WH pressure is also less effected by the fluid temperature drop. As a supporting argument, tables of water and CO₂ densities at 80[bar] and 10-30°C have been included in appendix E.7. These tables show that at a pressure of 80[bar], a temperature change from 10-30°C causes $\Delta\rho_{CO_2} = 201 \frac{kg}{m^3}$ and $\Delta\rho_{H_2O} = 4 \frac{kg}{m^3}$.

Risk of Hydrate Formation When transporting water and CO₂ in the same well, the possible occurrence of hydrates must be taken into consideration. During the switch from water to CO₂ injection or vice-versa, the CO₂ will be in contact with free water and experiences with pipeline CO₂ transportation show that CO₂ hydrates can form at temperatures up to 10°C [12]. According to Gelein de Koeijer, co-author of reference [12], a rule of thumb is that CO₂ hydrates do not form at temperatures above 14°C [10]. Hydrates have caused plugging and equipment damage in pipelines, and is a threat to operational consistency. CO₂ injection wells are reliant on good reservoir injectivity, and hydrate plugging of well perforations or reservoir pores could cause significant problems. Hydrate formation is usually inhibited by reducing water content or injection of chemical inhibitors (e.g. MEG). As water is an innate element in the WAG process, chemical inhibitor injection is the most likely solution. As cold temperatures are necessary for hydrate formation, CCS operations in northern environments are more prone to hydrate formation. However, hydrate formation has not been reported at either Sleipner or Snøhvit, the two northernmost active CCS operations. This is due to Sleipner’s high WH fluid temperature ($\approx 25^\circ\text{C}$) and Snøhvit’s low water content (<50ppm).

In the OLGA WAG simulation, the injection WH temperature for both water and CO₂ is 4.4°C, and pressure is 36.5[bar] for water and 53.1[bar] for

CO₂. According to Li et.al. [37], these conditions are within the hydrate formation region. Based on this, special attention to hydrate formation and inhibition would have to be paid if a CO₂-EOR operation using the conditions of the simulation were to be designed. Moreover, the BH temperatures of water and CO₂ were shown to differ significantly in the simulation. A typical BH temperature for CO₂ was 18°C, while only 10°C for water. As a consequence of this, hydrates formed at the start of, or during, a CO₂ injection period would possibly "melt" by the time the fluid reached BH and hydrate formation conditions were no longer present. Comparatively, the same would not be the case during water injection, as fluid temperature do not rise above 10°C. Also, hydrates would be given much longer time to form during water injection, as the fluid is sub 10°C throughout its time in the well.

Risk of Corrosion During WAG injection, where both CO₂ and free water are present in the well, CO₂ can dissolve in water and form carbonic acid which is corrosive. According to Seiersten [52], the corrosion rates when free water is present can be in the order of $\frac{\text{mm}}{\text{yr}}$. In designing WAG-injection wells, this issue will have to be addressed. Some possible solutions are coating the well with a corrosion resistant alloy, or using a steel with high chrome content as was done at Sleipner according to Baklid et.al. [4].

6 Uncertainty Analysis

In this section the most prominent uncertainties associated with the work in this thesis will be discussed.

Several simplifications were made in the OLGA modeling of the State Charlton well. The length, geometry and tubing diameter of the well were modeled in accordance to information from the State Charlton final report, however the well's casing program was omitted from the simulation model. This could affect the model's calculation of heat transfer, as the thermal conductivity(k) of steel and cement in casings differ from "k" of the formation rock which in the OLGA model is located where the casings would be.

A simplified model of the formation rock surrounding the injection well was made for the OLGA simulation, as described in section 4.1. Rough estimates of the formation properties were made, based on the dominating rock type of that formation. Categorizing the properties of over 1[km] of formation rock solely based on a simplified model of each formation layer's primary rock type is unlikely to accurately replicate the conditions surrounding the well. The thermal conductivity of the formation rocks were later adjusted to 80% of the originally estimated value to better match the BH fluid temperature from the measured data, but formation rock density and heat capacity was kept constant.

All numerical simulations are subject to uncertainties. The results from a simulator are highly reliant on how well the underlying mathematical model describes the true physics of what is actually occurring in the well. Although OLGA is a validated and widely used simulation tool, numerical uncertainties can occur. The unexplained mass flow rate spikes seen in the WAG-simulations could be a product of numerical simulation errors, however this is hard to determine, especially without access to the OLGA source code.

The results from any numerical simulation are dependent on the time step size and spacial grid size used. For the simulation work in this thesis, an average grid length of 17[m] and maximum time step of 0.1[s] was used. These values were chose based on an analysis performed by Gjertsen [22]. It is possible that a finer grid might have resulted in somewhat improved results, but this has to be weighed up against the increased simulation times that this would require. Disregarding the flow rate spikes seen in the WAG-simualtions, no instabilities were observed during the simulation work. For the WAG-simulations it was attempted to lower the maximum time step to

0.01[s], but this did not change the simulation results or resolve the spike problems. Based on this and the consistency of the results, it is reasonable to assume that the chosen spacial and temporal grid were sufficient to perform accurate simulations.

The simulation results were matched against measured data from the State Charlton CO₂ injection well. This data, along with the description of the well, was taken from the State Charlton final report [31]. Faulty measurements from the gauges in the well is a possible source of error. It must also be considered that some of the information provided in the State Charlton report, on which the OLGA model is based, might be incorrect or misinterpreted.

In the State Charlton report it was noted that the injection rate was manually regulated during the Mechanical Integrity step-rate test, and that injection rates therefore were difficult to stabilize at lower rates. This implies that the injection rates reported, especially at lower rates, might not accurately reflect the actual injection rates.

7 Conclusion

The literature study showed that pressure fall-off analysis during shut-in of CO₂ injection wells have on multiple occasions successfully been used to deduce reservoir properties. In the offshore saline-aquifer Snøhvit injection well, regular short shut-ins were performed with the purpose of determining injection index and monitor changes in injection index and skin effects. Experiences from Snøhvit showed that the lack of BH gauges complicated the analysis of pressure fall-off analysis for shut-ins exceeding a couple of minutes. The pressure behavior in the well during the early stages of a shut-in was dominated by fluid density changes caused by heating of the CO₂. Due to the location of the gauges, a minimum of 100 hours of shut-in were required to have the well stabilize thermally, before reservoir behavior could be analyzed. The results from pressure fall-off analysis for shut-ins exceeding 100 hours were used in establishing the location of flow barriers in the reservoir.

Two experiences with step-rate tests from the State Charlton 4-30 saline aquifer CO₂ injection well were found. The two tests had significantly different BH pressure responses, and suggest that a certain amount of fluid should be injected before testing is commenced. This should be done in order to wash away potential near well skin effects and thermally stabilize the well and surrounding formation rock. The step-rate tests were found to provide insight on the "hydraulic behavior of the reservoir system" [25] and suggest a maximum possible injection rate for the well. Experiences from the State Charlton well indicated that pressure fall-off curves during shut-in provided "a better idea of overall reservoir behavior than step-rate and injection tests" [26]. The step-rate test results from State Charlton could be irregular due CO₂ phase change, manual control of injection rates, skin and other factors.

OLGA simulations were successful in replicating the BH conditions in one of the two State Charlton step-rate tests. The test for which it was not possible to match, measured BH pressure exhibited significant transient instabilities, possibly caused by skin-effects and reservoir heterogeneities, which OLGA's one-equation reservoir modeling is not designed to handle.

A comparison of step-rate test simulations with different degrees of thermal stability (i.e. heat transfer rates from the formation rock to the wellbore fluid) was performed. The simulation results suggested that the thermal stability of the well may not be an important factor for step-rate test pressure

analysis if the well has a BH pressure gauge. If the well does not have a BH sensors and fluid temperatures in the well have not stabilized, the simulation results suggested the injection rate should be stepped down, instead of up, as this will give more stable fluid temperatures during the test. This will minimize fluid density changes and thereby unwanted pressure changes.

An OLGA simulation of a shut-in performed in the State Charlton well was unable to match measured BH pressure or temperature data. The same heat modeling used to successfully match the BH temperature during the step-rate tests and constant injection period was used, but this led to a significant over-prediction of BH temperature during shut-in. Unsuccessful attempts at tweaking the heat modeling to match BH temperature during shut-ins were made. The linear reservoir modeling equation used was not able to match the measured pressure response of the reservoir. OLGA offers the possibility of using a one-equation quadratic model for reservoir modeling. It is however questionable if any one-equation model will be able to represent the reservoir well enough to make OLGA a viable simulator for shut-in simulations. OLGA is primarily designed to be a multiphase pipe flow simulator, and does not have the reservoir modeling capabilities of a dedicated reservoir simulator.

WAG simulations in OLGA were performed. The literature study did not find any published references of similar simulations, it can therefore be assumed that this is the first published attempt of WAG simulations in OLGA. The simulations highlight the different timescales on which pressure and temperature operate in a CO₂ injection well. No significant differences in pressure or temperature phenomena were found when comparing simulations with injection cycles ranging from 4 to 24 hours. It was also shown how the difference in heat capacity between water and CO₂ causes very different fluid temperature during injection. Using water as the first injection medium in a WAG sequence was found to give a more stable WH pressure during the first injection cycle.

Based on the work in this thesis, the following recommendation for future step-rate and shut-tests can be made:

- For shut-in pressure fall-off analysis it is advisable to have gauges installed as close to the BH as possible. This will negate the CO₂ density changes occurring in the well due to heating during shut-in and provide better data for analysis.
- Perform an extended period of injection before shut-in or step-rate tests are performed. This stabilize wellbore fluid temperature and cool

surrounding rock formation, limiting the fluid temperature and density changes that occur during shut-in and step-rate tests. Performing a period of injection before a step-rate test can also possibly help minimize skin effects during the test and improve results.

- It is questionable if OLGA can be used to successfully model injection well shut-ins, or if it is only able to model near-perfect reservoirs which can be described by a one-equation reservoir model.
- If a step-rate test is to be performed in a well that is not thermally stable and is not equipped with BH gauges, it is advisable to step injection rates down instead of up. This can help limit noise in the pressure measurements caused by fluid density changes.

8 Recommendations for Further Work

The simulations completed in this work were unable to match the measured BH pressure response to shut-in recorded in the State Charlton well. These simulations used the linear reservoir equation provided in OLGA for reservoir modeling. OLGA does have different reservoir modeling equations than linear and a natural progression in testing OLGA's ability to model shut-ins would be to perform history matching simulations with different reservoir modeling.

Due to a lack of published experiences and field data on CO₂ injection well leak-offs, it was decided not to go through with the OLGA leak-off simulations originally planned, but rather focus on shut-ins and step-rate tests. Leak-offs might still prove to be a useful tool in well and reservoir characterization and should be a subject for further studies, both through field experiments and simulations.

Depleted gas fields have shown promise as an option for geological storage of CO₂. The reservoir pressure of depleted gas fields are usually very low relative to aquifer storage, which might affect e.g. fluid phase behavior and thereby pressure and temperature response during shut-in and step-rate tests. No studies on these transient operations were found on injection wells to depleted gas reservoirs in the literature review. If depleted gas reservoirs are to be used in large scale CCS, research on transient operations (e.g. shut-in) for this type of reservoir could validate their usefulness and optimize operation execution.

The literature study found only one injection well where step-rate tests with CO₂ as injection fluid had been used for well and/or reservoir characterization. The tests in this case were found to provide useful information on the hydraulic behavior of the reservoir. However, as information from just one single well was found, further studies and performing step-rate tests in other CO₂ injection wells could help evaluate the operation's usefulness.

References

- [1] Carbon dioxide injection. [www.Statoil.com. http://www.statoil.com/en/technologyinnovation/optimizingreservoirrecovery/recoverymethods/co2injection/pages/co2injection.aspx](http://www.statoil.com/en/technologyinnovation/optimizingreservoirrecovery/recoverymethods/co2injection/pages/co2injection.aspx). Accessed: 23.01.2014.
- [2] R.J. Arts et.al. The feasibility of CO₂ storage in the depleted P18-4 gas field offshore the Netherlands (the ROAD project). *International Journal of Greenhouse Gas Control*, 11 Supplement:S10–S20, 2012.
- [3] P. Aursand, M. Hammer, S.T. Munkejord, and Ø. Wilhelmsen. Pipeline transport of CO₂ mixtures: Models for transient simulation. *International Journal of Greenhouse Gas Control*, 13:174–185, 2013.
- [4] A. Baklid, R. Korbøl, and G. Owren. Sleipner Vest CO₂ Disposal, CO₂ Injection into a Shallow Underground Aquifer. Conference Paper; 1996 SPE Annual Technical Conference, 1996. SPE 36600.
- [5] Kjell H. Bendiksen, Dag Malnes, Randi Moe, and Sven Nuland. The Dynamic Two-Fluid Model OLGA: Theory and Application. *SPE Production Engineering*, May 1991. SPE 19451.
- [6] Kevin Bullis. Skipping the Water in Fracking, MIT Technology Review. www.technologyreview.com/news/512656/skipping-the-water-in-fracking/, March 22nd 2013. Accessed: 31.01.2014.
- [7] G. Chen et.al. The genetic algorithm based back propagation neural network for MMP prediction in CO₂-EOR process, journal= Fuel, volume= 126, year= 2014, pages= 202-212,.
- [8] J.R. Christensen, E.H. Stenby, and A. Skauge. Review of WAG Field Experience. *SPE Reservoir Evaluation and Engineering*, 4(02):97–106, 2001. SPE 71203-PA.
- [9] T.J. Danielson, K.M. Bansal, R. Hansen, and E. Leporcher. LEDA: The Next Multiphase Flow Performance Simulator. In *12th International Conference on Multiphase Production Technology*. BHR Group, 2005. Document ID: BHR-2005-H4.
- [10] G. de Koeijer. Personal communication with G. de Koeijer, co-author of [12], year= 10.06.2014,.

- [11] J.O. de Sant'Anna Pizarro and C.C. Moreira Branco. Challenges in Implementing an EOR Project in the Pre-Salt Province in Deep Offshore Brasil. 2012.
- [12] E. de Visser et.al. Dynamis CO₂ quality recommendations. *International Journal of Greenhouse Gas Control*, 2(4):478–484, 2008.
- [13] Enhanced oil recovery. www.energy.gov/energy.gov/fe/science-innovation/oil-gas/enhanced-oil-recovery. Accessed: 20.01.2014.
- [14] U.S. Energy Information Administration [eia.gov](http://www.eia.gov). U.S. Shale Gas Production. http://www.eia.gov/dnav/ng/ng_prod_shalegas_s1_a.htm. Accessed: 31.01.2014.
- [15] O. Eiken, P. Ringrose, C. Hermanrud, and B. Nazarian. Lessons Learned from 14 years of CCS Operations: Sleipner, In Salah and Snøhvit. *Energy Procedia*, 4:5541–5548, 2011.
- [16] L.J.Pekot et.al. Simulation of Two-Phase Flow in Carbon Dioxide Injection Wells. *SPE*, SPE 144847, 2011.
- [17] Metz et.al. Carbon Dioxide Capture and Storage. Technical report, IPCC, 2005.
- [18] Robert C. Ferguson, Christopher Nichols, Tyler Van Leeuwen, and Vello A. Kuuskraa. Storing CO₂ with Enhanced Oil Recovery. *Energy Procedia*, 1:1986–1996, 2009.
- [19] M. Flett et.al. Subsurface development of CO₂ disposal for the Gorgon Project. *Energy Procedia*, 1:3031–3038, 2009.
- [20] Senate Department for Urban Development and the Environment. Geothermal potential: Specific conductivity and specific extraction capacity (Edition 2012). http://www.stadtentwicklung.berlin.de/umwelt/umweltatlas/e_text/ek218.doc. Accessed: 26.03.2014.
- [21] P. Garnham. Invited Keynote: From Longannet to Peterhead-the Goldeneye CCS project Continues to Move Forward, 2012. Third EAGE CO₂ Geological Storage Workshop.
- [22] Ole Kristian Gjertsen. Modeling of Transient Two-Phase Flow in CO₂ Injection Wells. Technical report, NTNU and Statoil, 2013. Project Thesis.

- [23] SPT Group. Olga 7 user manual. Software user manual.
- [24] SPT Group. Well Dynamics With OLGA, 2012. Training manual for OLGA.
- [25] N. Gupta, D. Ball, P. Jagucki, and J. Bradbury. Validating Geological Storage Potential in the Midwestern USA through Multiple Field Demonstrations. *Energy Procedia*, 1:2063–2069, 2009.
- [26] N. Gupta et.al. Geological storage field tests in multiple basins in Midwestern USA - lessons learned and implications for commercial deployment. *Energy Procedia*, 4:5565–5572, 2011.
- [27] O Hansen, O. Eiken, and T.O. Aasum. Tracing the path of carbon dioxide from a gas/condensate reservoir, through an amine plant and back into a subsurface aquifer - case study: The sleipner area, norwegian north sea. 2005. SPE 96742.
- [28] Olav R. Hansen. Personal communication with Olav R. Hansen. 26.05.2014.
- [29] O. Hansen et.al. Snøhvit: The history of injecting and storing 1 Mt CO₂ in the fluvial Tubåen Fm. *Energy Procedia*, 37:3565–3573, 2013.
- [30] F.P. Incropera, D.P. DeWitt, T.L. Bergman, and A.S. Lavine. *Fundamentals of Heat and Mass Transfer*. John Wiley & Sons, 6th edition, March 2006. ISBN13: 9780471457282.
- [31] Battelle Memorial Institute. Final Report - Michigan Basin Phase II Geologic CO₂ Sequestration Field Test. www.mrcsp.org/userdata/phase_II_reports/mrcspmibasinvalidationrpt_final.pdf, April 28 2011. Accessed: 24.03.2014.
- [32] T. Ishida, K. Aoyagi, T. Niwa, Y. Chen, S. Murata, Q. Chen, and Y. Nakayama. Acoustic emission monitoring of hydraulic fracturing laboratory experiment with supercritical and liquid CO₂. *Geophysical Research Letters*, 39(16), August 2012.
- [33] David M. Kargbo, Ron G. Wilhelm, and David J. Campbell. Natural gas plays in the marcellus shale: Challenges and potential opportunities. *Environmental Science and Technology*, 44(15):5679–5684, 2010.
- [34] Y. Kim. Equation of State for Carbon Dioxide. *Journal of Mechanical Science and Technology*, 21:791–796, 2007.

- [35] Vello A. Kuuskraa, Tyler Van Leewen, and Matt Wallace. Improving domestic energy security and lowering CO₂ emissions with "next generation" CO₂-enhanced oil recovery. Technical report, NETL, 2011.
- [36] B. Ladbroke et.al. CO₂ storage in depleted gas fields. Technical report, IEA GHG and Pyry Energy Consulting, June 2009. IEA Report No. 2009/1.
- [37] H. Li, J.P. Jakobsen, and J. Stang. Hydrate formation during CO₂ transport: Predicting water content in the fluid phase in equilibrium with the CO₂ hydrate. *International Journal of Greenhouse Gas Control*, 5:549–554, 2011.
- [38] H. Li, J.P. Jakobsen, Ø Wilhelmsen, and J. Yan. PVT_{xy} properties of CO₂ mixtures relevant for CO₂ capture, transport and storage: Review of available experimental data and theoretical models. *Applied Energy*, 88:3567–3579, 2011.
- [39] H. Li and J. Yan. Evaluating cubic equations of state for calculation of vapor-liquid equilibrium of CO₂ and CO₂-mixtures for CO₂ capture and storage processes. *Applied Energy*, 86:826–836, 2009.
- [40] E. Lindeberg. Modelling pressure and temperature profile in a CO₂ injection well. *Energy Procedia*, 4:3935–3941, 2011.
- [41] B.T. Løvfall. Research Scientist at SINTEF. Personal Communication. March 20th 2014.
- [42] T. Maldal and I.M. Tappel. CO₂ underground storage for Snøhvit gas field development. *Energy*, 29:1403–1411, 2004.
- [43] G.D. Nicoll. North Sea CO₂ Storage Activity outside the Norwegian Continental Shelf, 2012.
- [44] C.M. Oldenburg, K. Pruess, and S.M. Benson. Process modeling of CO₂ injection into natural gas reservoirs for carbon sequestration and enhanced gas recovery. *Energy & Fuels*, 15:293–298, 2001.
- [45] C.L. Pauchon and H. Dhulesia. TACITE: A Transient Tool for Multiphase Pipeline and Well Simulations. 1994. SPE-28545-MS.
- [46] A.M. Raaen, P. Horsrud, H. Kjørholt, and D. Økland. Improved routine estimation of the minimum horizontal stress component from extended leak-off tests. *International Journal of Rock Mechanics & Mining Sciences*, 43:37–48, 2006.

- [47] Philip S. Ringrose, 21.10.2013. Personal communication with P.S. Ringrose, lead author of [48].
- [48] P.S. Ringrose et.al. The In Salah CO₂ storage project: lessons learned and knowledge transfer. *Energy Procedia*, 37:6226–6236, 2013.
- [49] E.C. Robertson. United States Department of the Interior Geological Survey; Thermal Properties of Rocks. pubs.usgs.gov/of/1988/0441/report.pdf, 1988. Accessed: 26.03.2014.
- [50] D.S. Schechter et.al. CO₂ Pilot Design and Water Injection Performance in the Naturally Fractured Spraberry Trend Area, West Texas. Technical report, 2001. SPE 71605.
- [51] P.N. Seevam, J.M. Race, M.J Downie, and P. Hopkins. Transporting the Next Generation of CO₂ for Carbon, Capture and Storage: The Impact of Impurities on Supercritical CO₂ Pipelines. In *2008 7th International Pipeline Conference*, volume 1, pages 39–51. ASME, 2008. Paper No. IPC2008-64063, ISBN 978-0-7918-4857-9.
- [52] M. Seiersten. Material selection for separation, transportation and disposal of CO₂. In *Proceedings of the Corrosion 2001*. National Association of Corrosion Engineers, 2001. Paper 01042.
- [53] J. Sminchak, N. Gupta, and J. Gerst. Well test results and reservoir performance for a carbon dioxide injection test in the Bass Islands Dolomite in the Michigan Basin. *Environmental Geosciences*, 16(3), September 2009.
- [54] W.H. Somerton. *Thermal Properties and Temperature-Related Behaviour of Rock/Fluid Systems*. Elsevier Science, March 1992. ISBN-10: 044489017.
- [55] R. Span and W. Wagner. A New Equation of State for Carbon Dioxide Covering the Fluid Region From the Triple-Point Temperature of 1100K at Pressures up to 800MPa. *Journal of Physical and Chemical Reference Data*, 25:1509–1596, 1996.
- [56] S.A. Stevens, V.A. Kuuskraa, and J. Gale. Sequestration of CO₂ in depleted Oil & Gas Fields: Global Capacity, Costs, and Barriers. *GHGT-5, Conference Proceedings*, pages 278–283, 2001.
- [57] Eirik S. Thu. Modeling of Transient CO₂ Flow in Pipelines and Wells. Master’s thesis, NTNU, January 2013.

- [58] Ø Wilhelmsen et.al. Evaluation of spung[#] and other equations of state for use in carbon capture and storage modelling. *Energy Procedia*, 23:236–245, 2012.
- [59] EduMine www.edumine.com. Average specific gravity of various rock types. "<http://www.edumine.com/xtoolkit/tables/satables.htm>". Accessed: 26.03.2014.
- [60] www.engineeringtoolbox.com. A comprehensive list of some common solids as brick,cement,glass and many more - and their specific heats - imperial and SI units. www.engineeringtoolbox.com/specific-heat-solids-d_154.html. Accessed: 26.03.2014.
- [61] Global CCS Institute www.globalccsinstitute.com. Peterhead gas ccs project. "<http://www.globalccsinstitute.com/project/peterhead-gas-ccs-project>". Accessed: 10.06.2014.
- [62] International Energy Agency www.iea.org. Technology roadmap: Carbon capture and storage 2013. "<http://www.iea.org/publications/freepublications/publication/name,39359,en.html>". Accessed: 04.06.2014.
- [63] Kongsberg www.kongsberg.com. Ledaflow modelling. <http://www.kongsberg.com/en/kogt/offerings/software/ledaflow/ledaflowmodeling/>. Accessed: 28.02.2014.

List of Figures

| | | |
|----|---|----|
| 1 | U.S. Shale Gas Production 2007-2011. [14] | 13 |
| 3 | Phase diagram for pure CO ₂ . Taken from Pekot et.al. [16] | 26 |
| 4 | State Charlton Injection well(4-30) downhole temperature log. From Michigan Basin Phase II Final Report [31] | 34 |
| 5 | State Charlton Injection well(4-30) and monitoring well(3-30) lithology. From Michigan Basin Phase II Final Report [31] | 35 |
| 6 | Bottom hole pressure and temperature data from the State Charlton 4-30 mechanical integrity test. From State Charlton Final Report [31] | 40 |
| 7 | Bottom hole pressure and injection rate data from the State Charlton 4-30 step rate test. From Michigan Basin Phase II Final Report [31] | 40 |
| 8 | Pressure data from the State Charlton 4-30 shut-in test. From State Charlton Final Report [31] | 41 |
| 9 | WH pressure, flow rate, annulus pressure and WH temper- ature data from the State Charlton 4-30 2nd step rate test performed March 5th. From State Charlton Final Report [31] | 42 |
| 10 | BH pressure and temperature data from the State Charlton 4-30 2nd step rate test performed March 5th. From State Charlton Final Report [31] | 43 |
| 11 | Mechanical integrity test simulation with original reservoir equation and rock properties. Simulated versus measured BH pressure. Linear reservoir equation constants from equation 3 | 47 |
| 12 | Mechanical integrity test simulation with original reservoir equation and rock properties. Simulated versus measured BH temperature. Linear reservoir equation constants from equa- tion 3 | 48 |
| 13 | Measured and simulated BH pressure. Modified reservoir equa- tion and rock conductivity. | 48 |
| 14 | Measured and simulated BH pressure. Modified reservoir equa- tion and rock conductivity. | 49 |
| 15 | Measured and simulated BH pressure, step rate test zoom-in. Modified reservoir equation and rock conductivity. | 49 |
| 16 | "A" values used in "Variable Reservoir Equation" simulation. | 50 |
| 17 | Measured and simulated BH pressure from "Variable Reservoir Equation" simulation. | 51 |
| 18 | Comparison of shut-ins with different different reservoir tem- perature and rock properties to the measured BH temperature response to shut-in. | 52 |

| | | |
|----|--|-----|
| 19 | Shut-in BH temperature comparison of measured data to simulation with reservoir temperature of 18°C, and dolomite and limestone $k=1.5 \frac{W}{m \cdot K}$ | 53 |
| 20 | MIT BH temperature comparison of measured data to simulation with reservoir temperature of 18°C, and dolomite and limestone $k=1.5 \frac{W}{m \cdot K}$ | 54 |
| 21 | Measured and simulated bottom hole temperature and pressure for March 5th step rate test simulation. | 55 |
| 22 | Simulated and measured wellhead pressure for March 5th step rate test simulation. | 55 |
| 23 | BH temperature comparison of second step-rate test simulations with different heat transfer. | 57 |
| 24 | WH pressure comparison of second step-rate test simulations with different heat transfer. | 58 |
| 25 | BH pressure comparison of second step-rate test simulations with different heat transfer. | 59 |
| 26 | Wellhead pressure, 24 hours injection cycle simulation. | 71 |
| 27 | Bottom hole temperature, 24 hours injection cycle simulation. | 72 |
| 28 | Bottom hole temperature, 4 hours injection cycle simulation. | 72 |
| 29 | Bottom hole temperature, 800 hours injection cycle simulation. | 73 |
| 30 | Bottom hole temperature, water as first injection medium, 24 hour injection cycle simulation. | 74 |
| 31 | Wellhead pressure, water as first injection medium, 24 hour injection cycle simulation. | 74 |
| 32 | Mechanical injection test simulation with modified heat transfer coefficient for dolomite. | 95 |
| 33 | Profile plot showing the extent of the two-phase gas liquid region 1.9hours into the simulation. Measured in gas volume fraction | 95 |
| 34 | Profile plot showing the extent of the two-phase gas liquid region 3.9hours into the simulation. Measured in gas volume fraction | 96 |
| 35 | Profile plot showing the fluid temperature along the length of the well right before shut-in, and 11 and 22 hours into shut-in. | 97 |
| 36 | Profile plot of BH Temperature during shut-in, with modified rock heat capacity. Red line(top):2x Cp of what was given in 4. Black line(bottom): 0.5x Cp of 4. | 98 |
| 37 | Excel re-make of figure 8. BH pressure of the MIT shut-in. | 99 |
| 38 | Excel re-make of figure 7. BH pressure of the MIT step-rate test. | 100 |

| | | |
|----|---|-----|
| 39 | Excel re-make of figure 6. BH pressure and temperature of the MIT. | 100 |
| 40 | Excel re-make of figure 10. BH pressure and temperature of the second step-rate test. | 101 |
| 41 | Excel re-make of figure 9 WH pressure of the second step-rate test. | 101 |
| 42 | BH pressure and temperature comparison for simulations with different EOSs. Span-Wagner and SRK-Peneloux | 102 |
| 43 | BH temperature comparison. Measured versus simulated(with modified rock conductivity, from table 8.) | 102 |
| 44 | WH temperature. 24 hour injection cycle simulation. | 103 |
| 45 | Mass flow rate. 24 hour injection cycle simulation. | 103 |
| 46 | BH Pressure. 24 hour injection cycle simulation. | 104 |
| 47 | BH Temperature. 24 hour injection cycle, extended simulation. | 104 |
| 48 | WH temperature. 4 hour injection cycle simulation. | 105 |
| 49 | WH pressure. 24 hour injection cycle simulation. | 105 |
| 50 | BH pressure. 4 hour injection cycle simulation. | 106 |
| 51 | WH pressure. Water shut-in, followed by CO ₂ shut-in. | 107 |
| 52 | Wellhead temperature, water as first injection medium, 24 hour injection cycle simulation. | 108 |
| 53 | Bottom-hole pressure, water as first injection medium, 24 hour injection cycle simulation. | 108 |
| 54 | H ₂ O densities. From webbook.nist.gov/chemistry/fluid/ . Accessed 22.05.14 | 109 |
| 55 | CO ₂ densities. From webbook.nist.gov/chemistry/fluid/ . Calculator uses Span-Wagner EoS. Accessed 22.05.14 | 109 |

List of Tables

| | | |
|----|--|----|
| 1 | Table of common impurities from some anthropogenic CO ₂ sources. From reference [38] | 28 |
| 2 | Impurity concentrations. From reference [38]. | 28 |
| 3 | Existing long distance CO ₂ pipelines with naturally sourced CO ₂ . From reference [51] | 29 |
| 4 | CO ₂ stream content at Sleipner. From de Visser et.al. [12]. a) The non-condensable content is not expected to increase above 3% during normal operation, even though 5% non-condensable is stated as design basis. | 29 |
| 5 | Properties of AISI 304 Stainless Steel. From Incropera et.al. [30] | 37 |
| 6 | Simplified lithology of St.Charlton Injection well | 37 |
| 7 | WH pressure, BH pressure and flow rate of March 5th step rate test. Taken from figure 10 and 9. | 43 |
| 8 | Modified rock thermal conductivity. Modified k-values=80% of original k-values | 45 |
| 9 | "A" value for simulation "Variable Reservoir Equation". Shut-in commences at 74 hours simulation time. | 51 |
| 10 | Approximate WH and BH pressures for the given injection rate, from step rate test simulation. Measured values in the two right columns. | 56 |
| 11 | Comparison of simulated and measured bottom hole temperature values during step rate test and constant injection. | 60 |
| 12 | Comparison of measured to simulated BH pressure response to mass flow step down. | 63 |
| 13 | Comparison of the measured and simulated values of the WH pressure during March 5th step rate test. | 64 |
| 14 | Comparison of measured to simulated WH pressure response to mass flow step down. | 65 |

A Appendix

A.1 Mechanical Injection Test

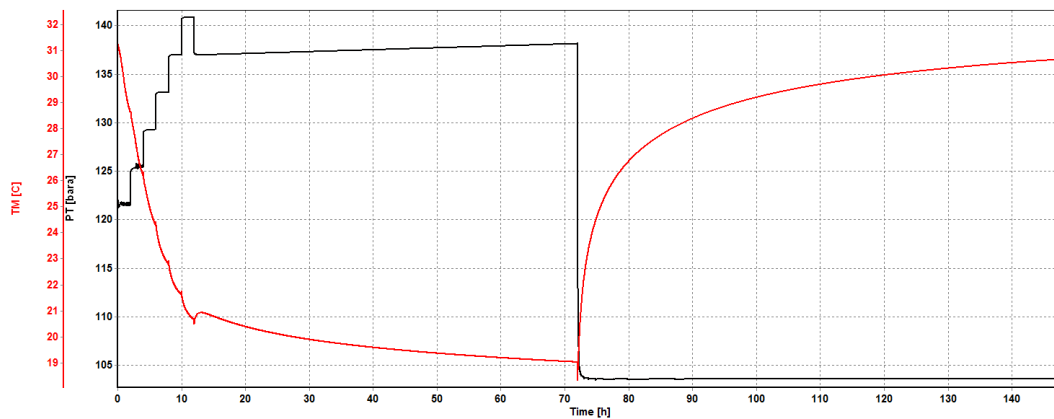


Figure 32: Mechanical injection test simulation with modified heat transfer coefficient for dolomite.

B

B.1 Two-phase profile plot

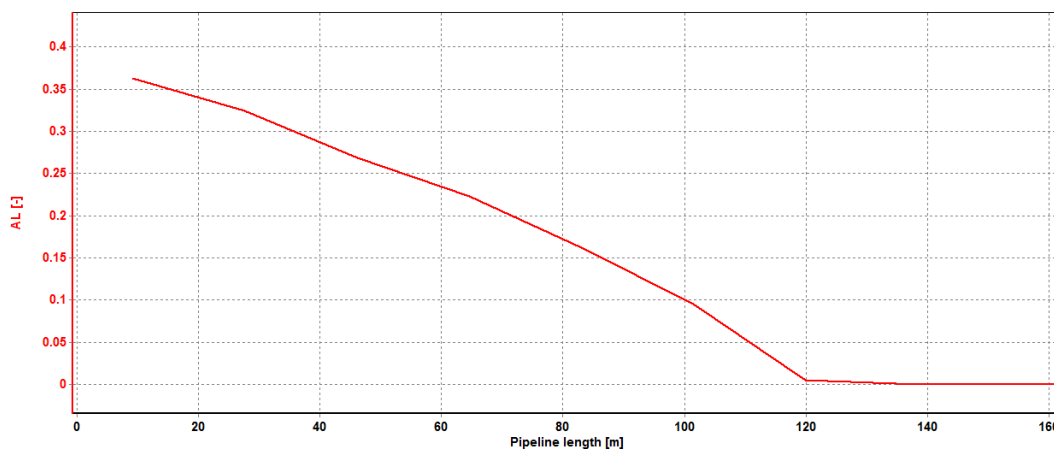


Figure 33: Profile plot showing the extent of the two-phase gas liquid region 1.9 hours into the simulation. Measured in gas volume fraction

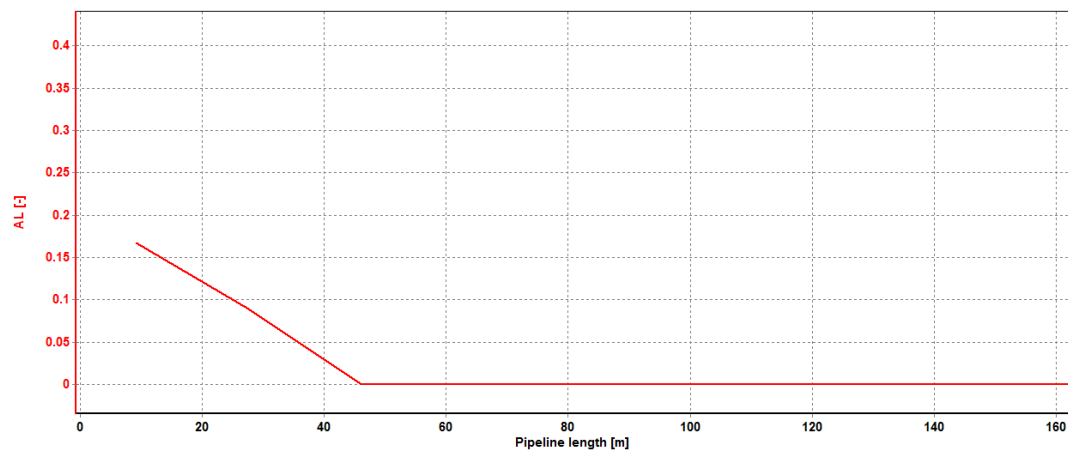


Figure 34: Profile plot showing the extent of the two-phase gas liquid region 3.9 hours into the simulation. Measured in gas volume fraction

B.2 Temperature profile plot of shut-in

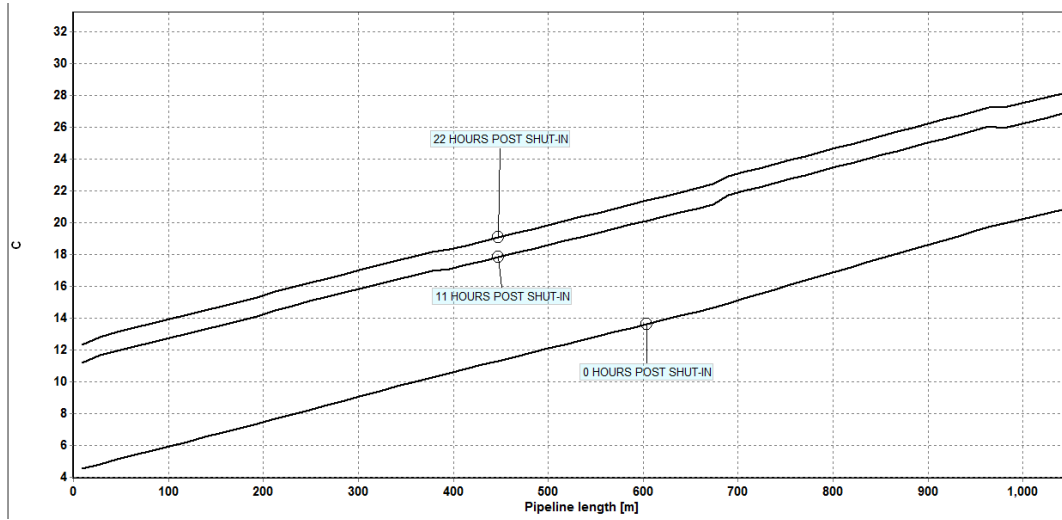


Figure 35: Profile plot showing the fluid temperature along the length of the well right before shut-in, and 11 and 22 hours into shut-in.

C

C.1 BH Temperature Response Shut-In, Variable Cp

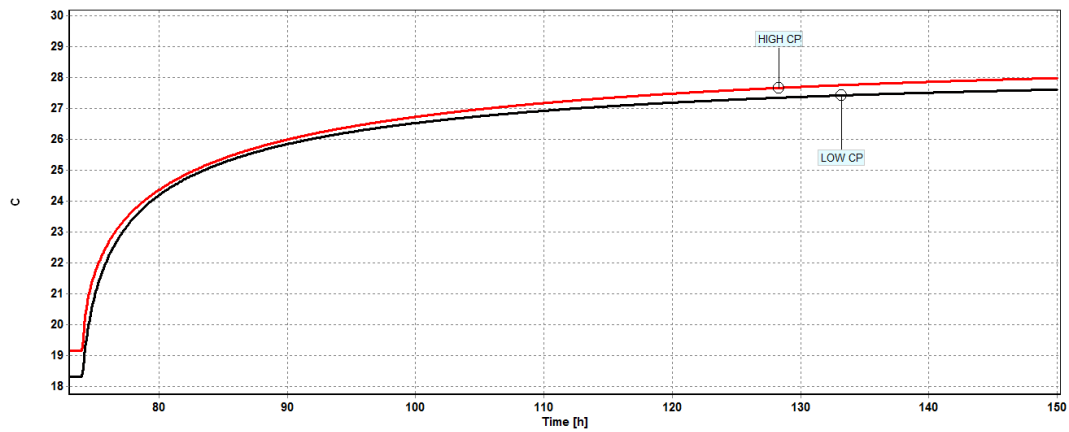


Figure 36: Profile plot of BH Temperature during shut-in, with modified rock heat capacity. Red line(top):2x Cp of what was given in 4. Black line(bottom): 0.5x Cp of 4.

D

D.1 Excel-graph re-make

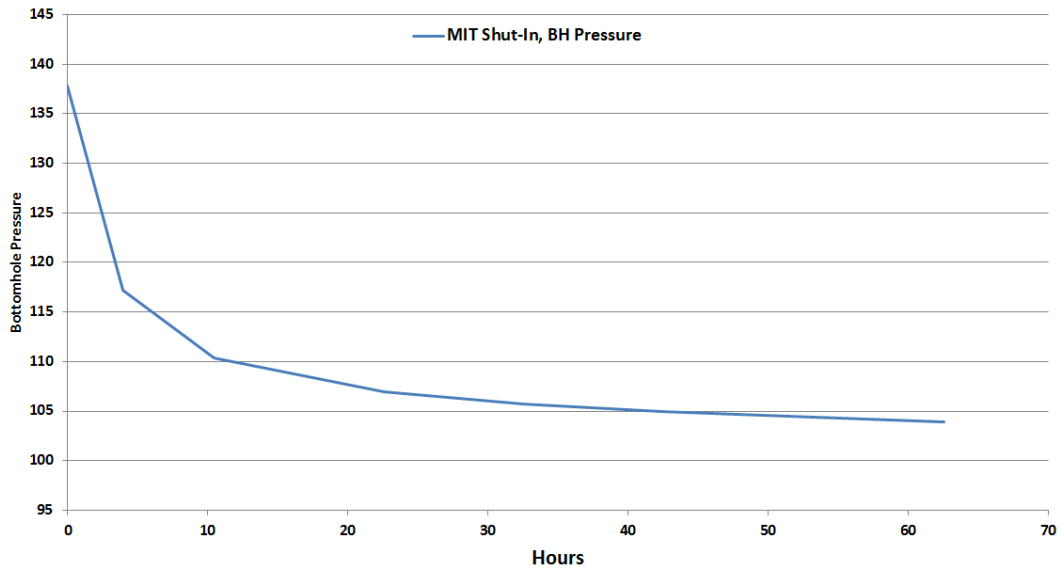


Figure 37: Excel re-make of figure 8. BH pressure of the MIT shut-in.

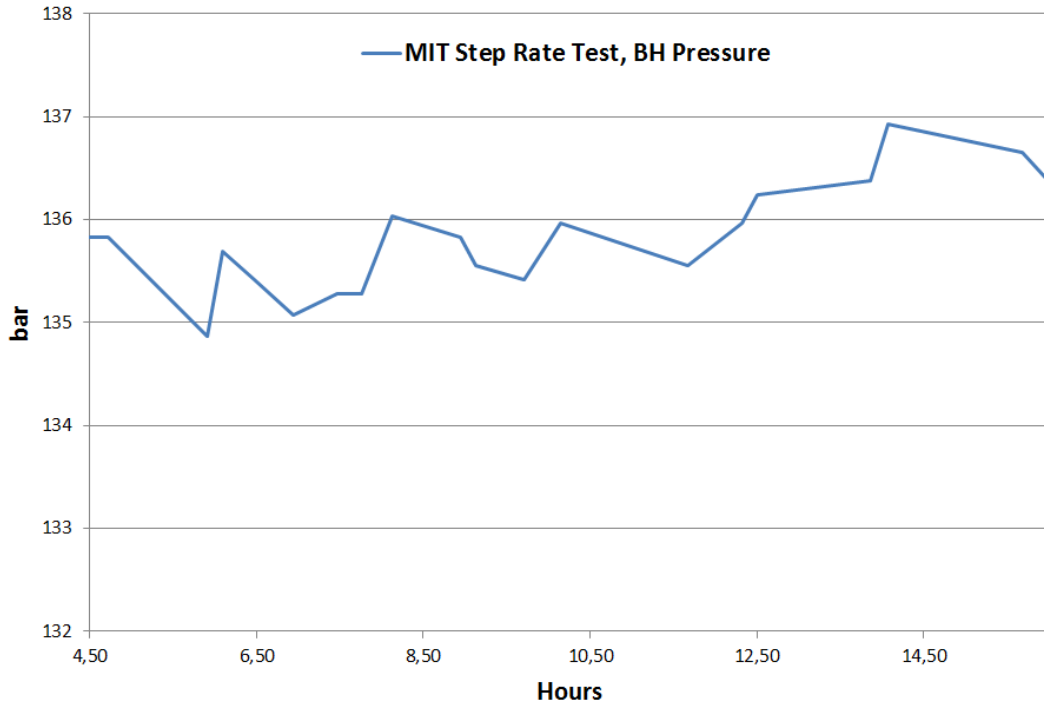


Figure 38: Excel re-make of figure 7. BH pressure of the MIT step-rate test.

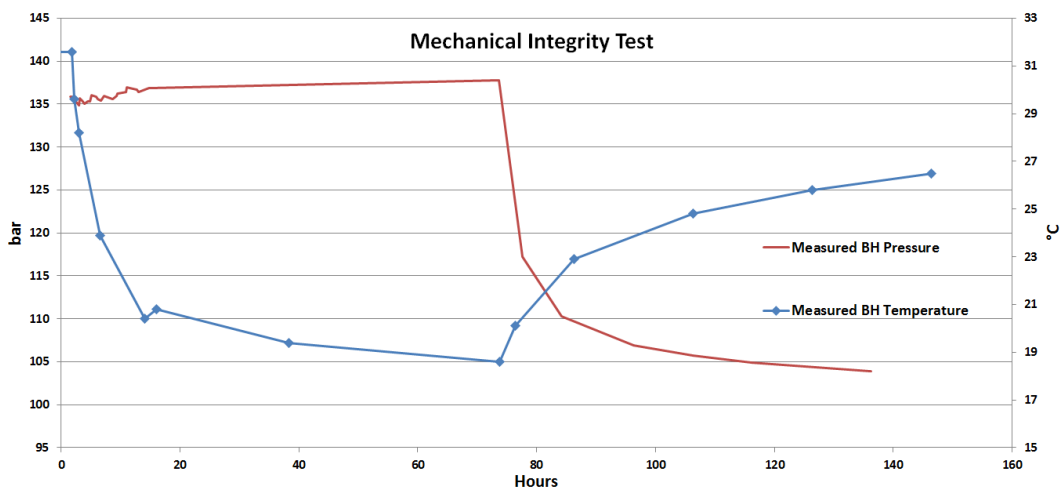


Figure 39: Excel re-make of figure 6. BH pressure and temperature of the MIT.

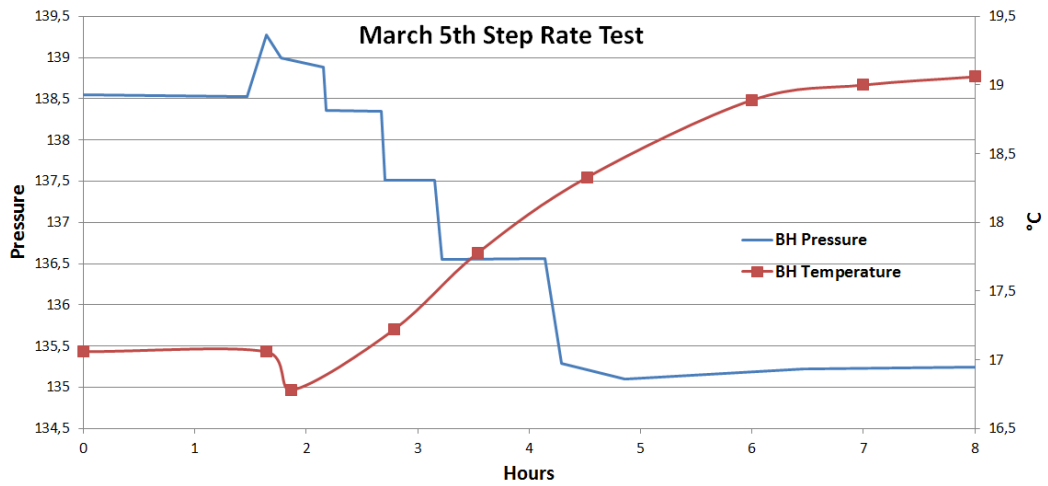


Figure 40: Excel re-make of figure 10. BH pressure and temperature of the second step-rate test.

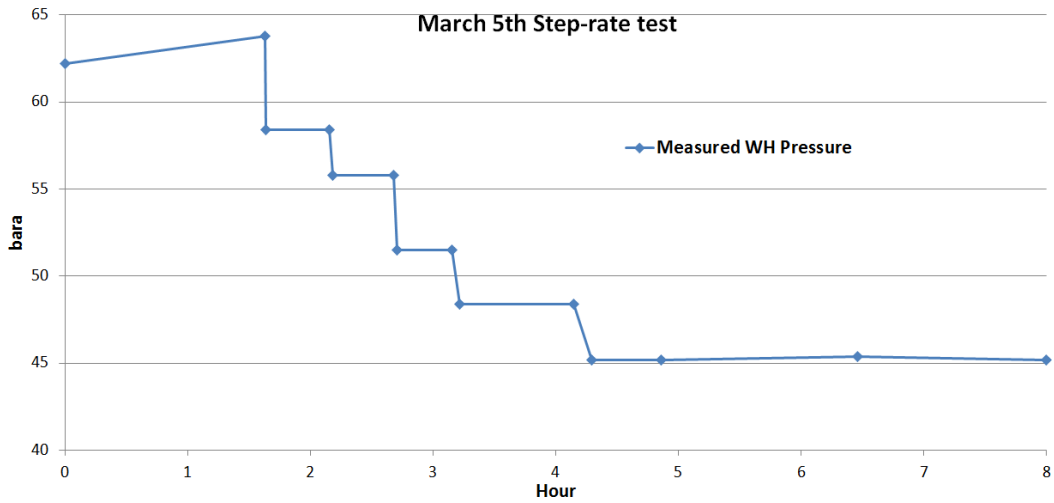


Figure 41: Excel re-make of figure 9 WH pressure of the second step-rate test.

E EOR

E.1 EOS Comparison

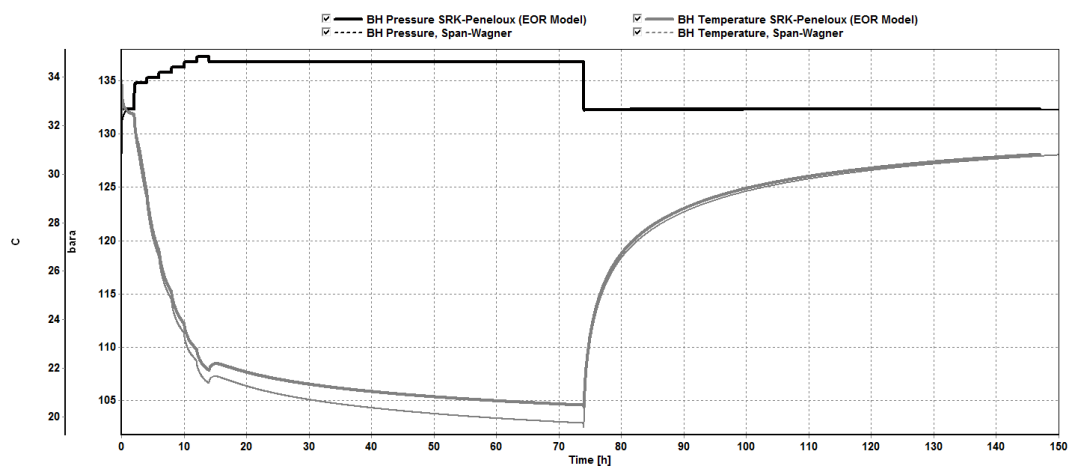


Figure 42: BH pressure and temperature comparison for simulations with different EOSs. Span-Wagner and SRK-Peneloux

E.2 BH Temperature comparison MIT

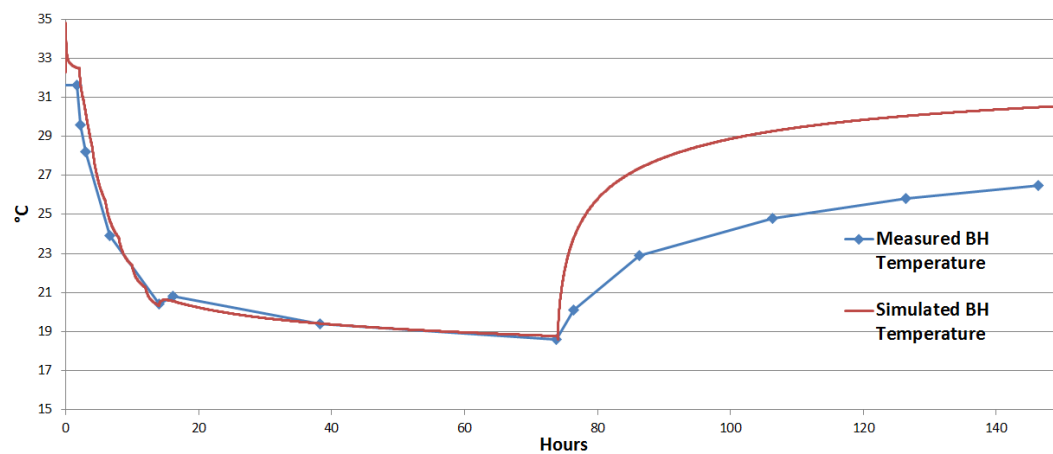


Figure 43: BH temperature comparison. Measured versus simulated (with modified rock conductivity, from table 8.)

E.3 24hour injection cycle

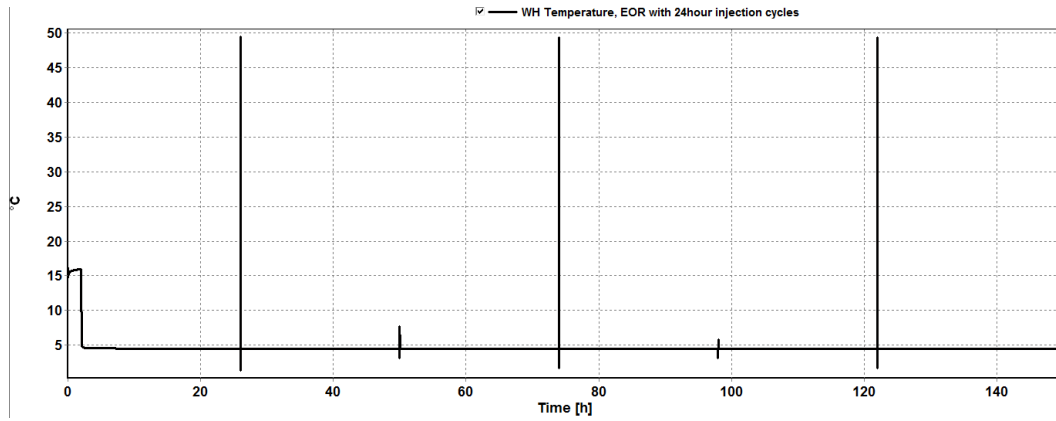


Figure 44: WH temperature. 24 hour injection cycle simulation.

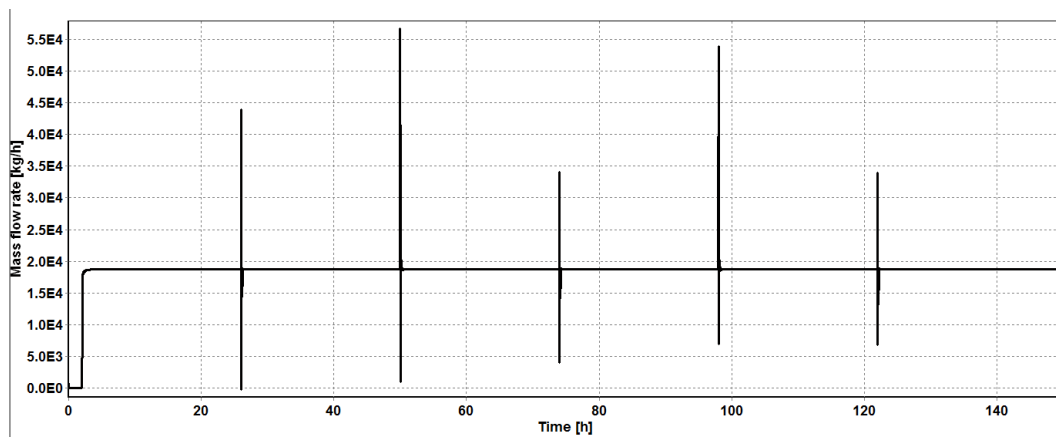


Figure 45: Mass flow rate. 24 hour injection cycle simulation.

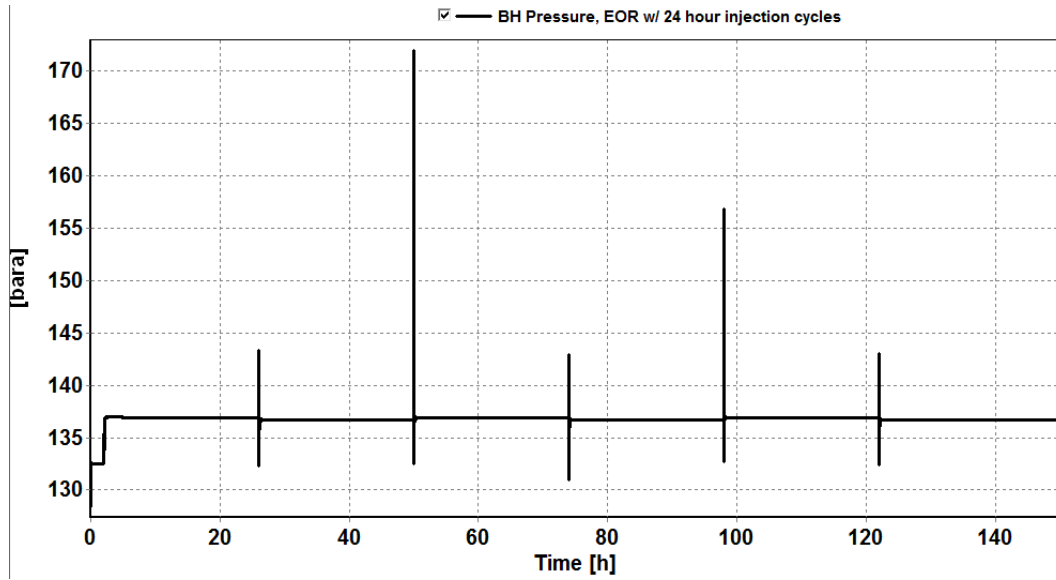


Figure 46: BH Pressure. 24 hour injection cycle simulation.

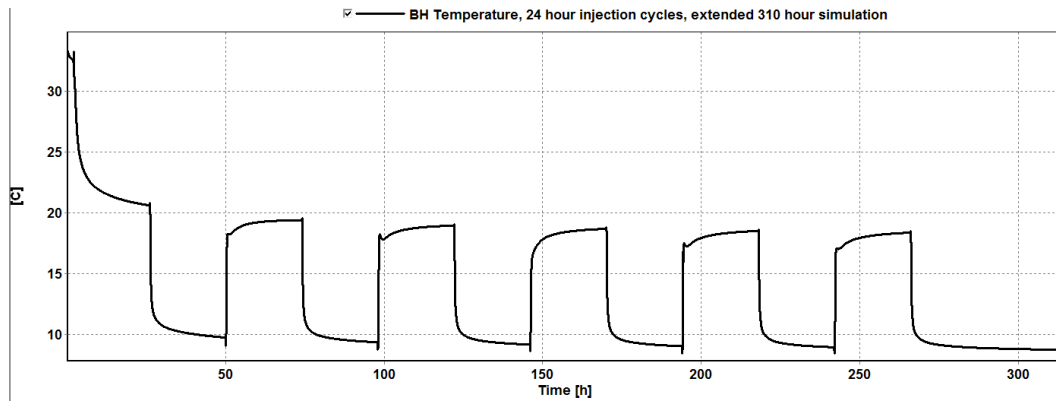


Figure 47: BH Temperature. 24 hour injection cycle, extended simulation.

E.4 4 hour injection cycle

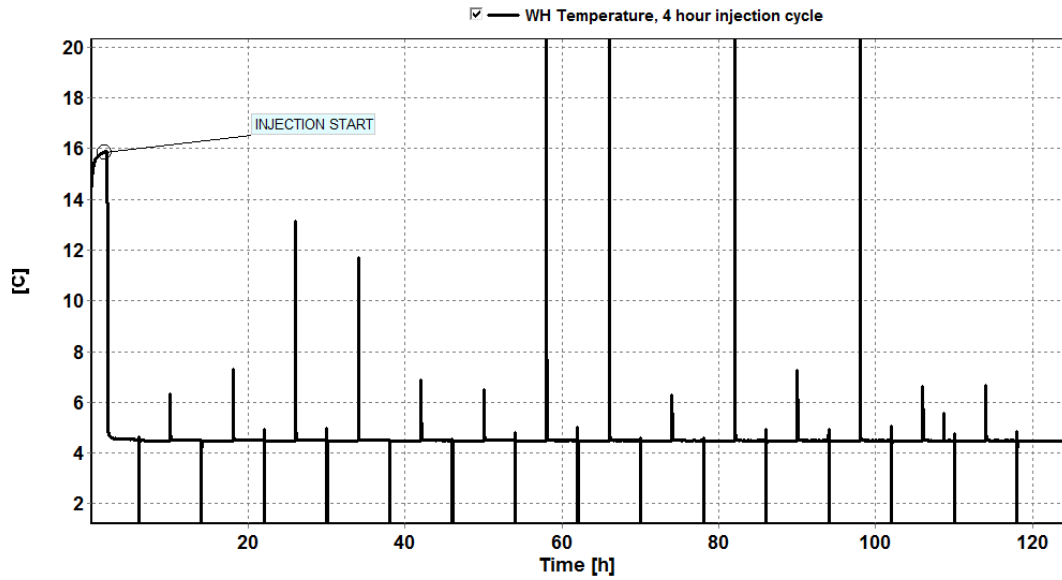


Figure 48: WH temperature. 4 hour injection cycle simulation.

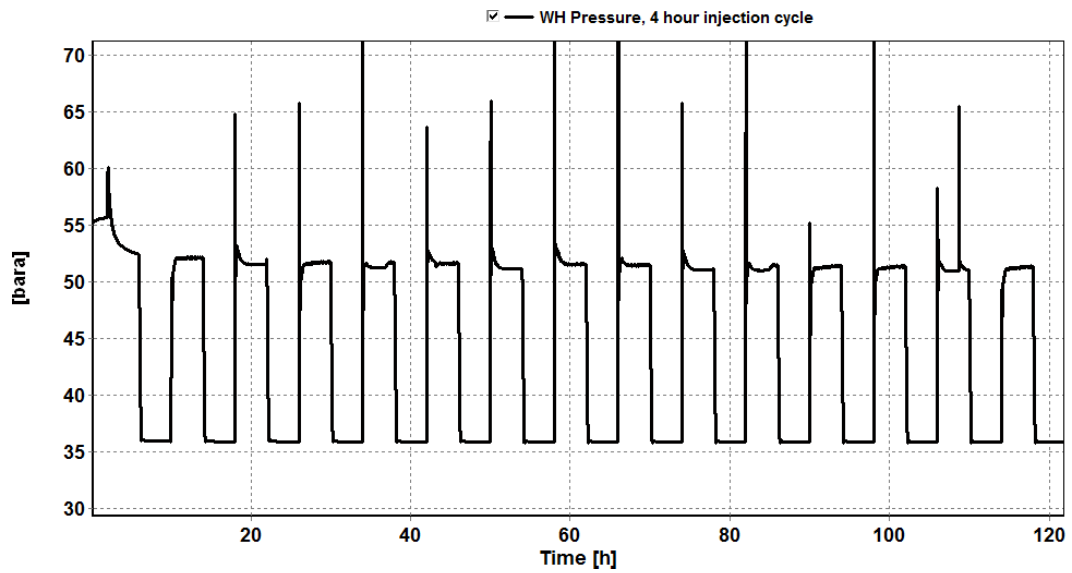


Figure 49: WH pressure. 24 hour injection cycle simulation.

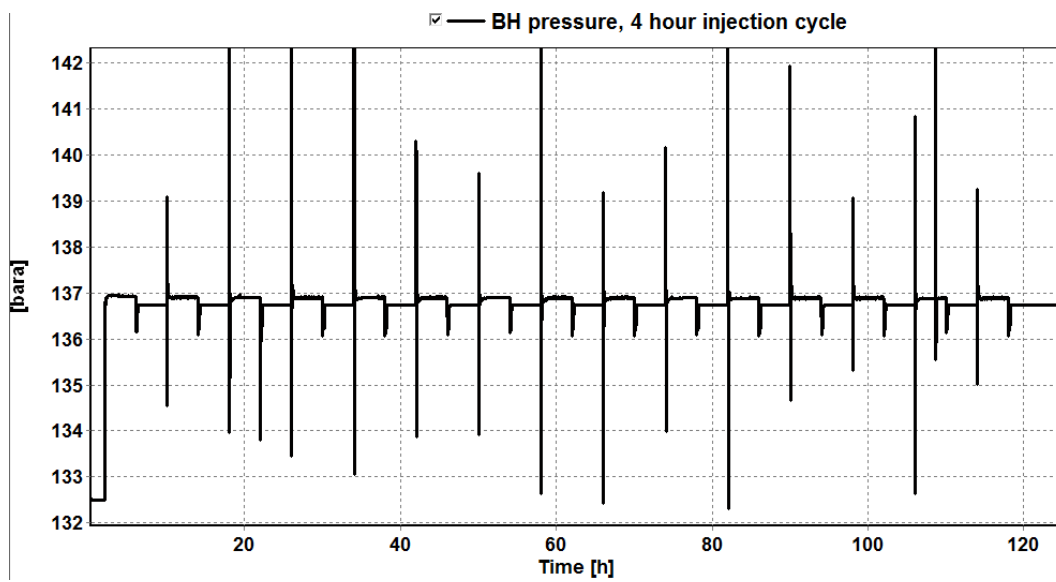


Figure 50: BH pressure. 4 hour injection cycle simulation.

E.5 WAG Shut-in

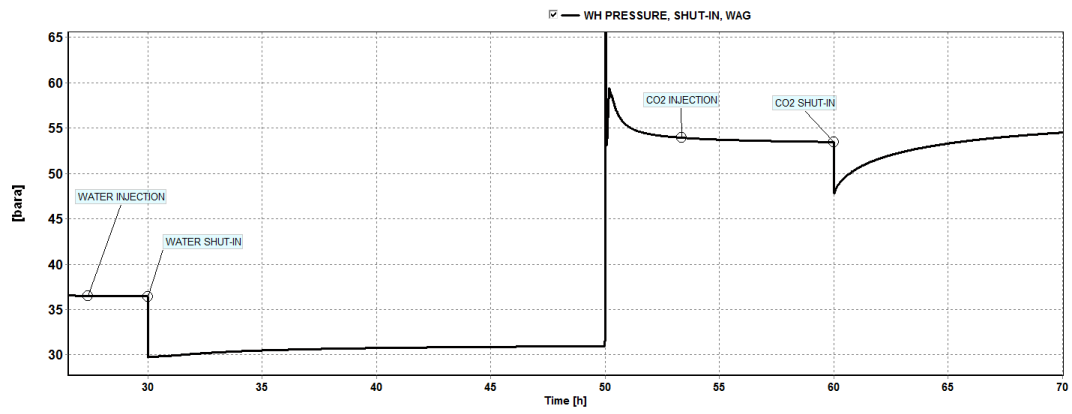


Figure 51: WH pressure. Water shut-in, followed by CO₂ shut-in.

E.6 WAG, Water as first injection medium

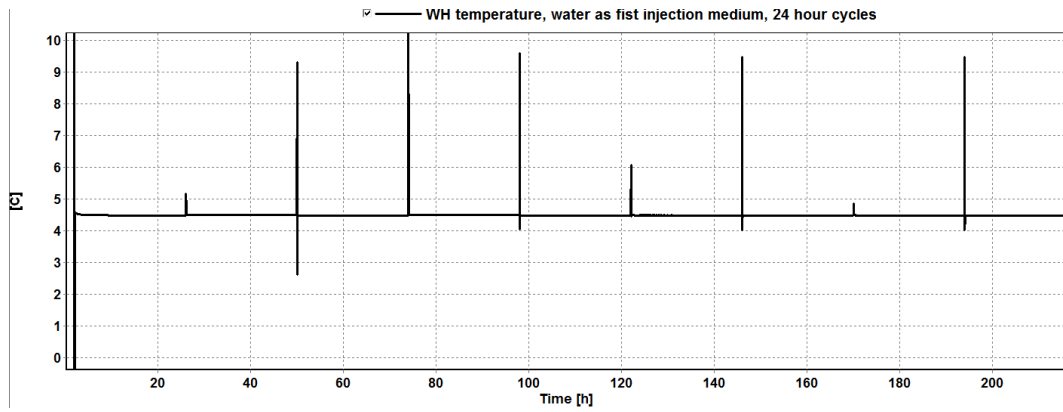


Figure 52: Wellhead temperature, water as first injection medium, 24 hour injection cycle simulation.

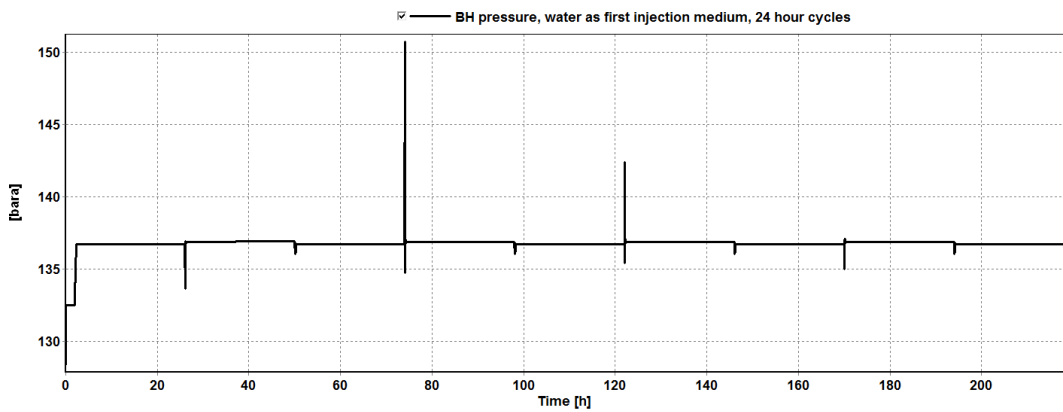


Figure 53: Bottom-hole pressure, water as first injection medium, 24 hour injection cycle simulation.

E.7 H₂O and CO₂ densities. 80[bar], 10-30°C.

| Temperature (C) | Pressure (bar) | Density (kg/m ³) |
|-----------------|----------------|------------------------------|
| 10.000 | 80.000 | 1003.4 |
| 15.000 | 80.000 | 1002.8 |
| 20.000 | 80.000 | 1001.8 |
| 25.000 | 80.000 | 1000.6 |
| 30.000 | 80.000 | 999.14 |

Figure 54: H₂O densities. From webbook.nist.gov/chemistry/fluid/ . Accessed 22.05.14

| Temperature (C) | Pressure (bar) | Density (kg/m ³) |
|-----------------|----------------|------------------------------|
| 10.000 | 80.000 | 903.13 |
| 15.000 | 80.000 | 868.40 |
| 20.000 | 80.000 | 827.71 |
| 25.000 | 80.000 | 776.64 |
| 30.000 | 80.000 | 701.72 |

Figure 55: CO₂ densities. From webbook.nist.gov/chemistry/fluid/ . Calculator uses Span-Wagner EoS. Accessed 22.05.14

E.8 OLGA Input Specifications Report

1. Introduction

| | |
|------------------|-----------------------|
| Project | |
| Case description | |
| Date | |
| Author | Ole Kristian Gjertsen |
| Compressor File | |
| Feed File | |
| Pump File | |
| PVT File | |
| Wax File | |
| Restart File | |

2. Simulation Options

| | | |
|-----------------|----------------------|----------|
| Overall setting | Flow model | OLGA |
| | Mass eq scheme | 1STORDER |
| | Compositional model | SINGLE |
| | Debug | ON |
| | Drilling | OFF |
| | Phase | THREE |
| | Elastic walls | OFF |
| | Void in slug | SINTEF |
| | Steady state | OFF |
| | User defined plug-in | OFF |
| | Temp. calc. | WALL |
| | Wax deposition | OFF |
| | Restart | OFF |
| Integration | Simulation starttime | 0 |
| | Simulation stoptime | 140 h |
| | Minimum time step | 1E-10 |
| | Maximum time step | 0.1 |

3. System Layout - Graphics



4. System Layout - Table

4.1 Summary

4.1.1 Overall

| No. of Branches | No. of Pipes | No. of Sections |
|-----------------|--------------|-----------------|
| 1 | 6 | 63 |

4.1.2 Flows

| Branches | No. of Pipes | No. of Sections | Min. Section Length | At | Max. Section Length | At |
|---------------|--------------|-----------------|---------------------|--------|---------------------|--------|
| StateCharlton | 6 | 63 | 11.5 M | PIPE-6 | 18.4545454545455 M | PIPE-1 |

4.2 Layout

| Pipe no. | Branch | Label | Diameter | Roughness | XEnd | YEND | Wall |
|----------|---------------|--------|----------|-----------|------|---------|------------------|
| 1 - 1 | StateCharlton | PIPE-1 | 0.073 M | 1E-05 M | 0 M | -203 M | well+GlacialTill |
| 1 - 2 | StateCharlton | PIPE-2 | 0.073 M | 1E-05 M | 0 M | -387 M | well+shale |
| 1 - 3 | StateCharlton | PIPE-3 | 0.073 M | 1E-05 M | 0 M | -682 M | well+limestone |
| 1 - 4 | StateCharlton | PIPE-4 | 0.073 M | 1E-05 M | 0 M | -972 M | well+dolomite |
| 1 - 5 | StateCharlton | PIPE-5 | 0.073 M | 1E-05 M | 0 M | -1049 M | well+limestone |
| 1 - 6 | StateCharlton | PIPE-6 | 0.073 M | 1E-05 M | 0 M | -1072 M | well+dolomite |

5. Insulation and Walls

5.1 Material

| Label | Density | Conductivity | Heat Capacity | E-modulus |
|--------------|---------|--------------|---------------|-----------|
| AISI 304 | 7900 | 14.9 | 477 | |
| Glacial till | 2000 | 2.9 W/m-K | 1000 J/kg-K | |
| Shale | 2600 | 3.4 | 795 | |
| Limestone | 2500 | 2.9 | 836.8 | |
| Dolomite | 2850 | 4.5 | 920 | |

5.2 Walls

| Label | Material | Wall thickness | Elastic |
|------------------|--------------|----------------|---------|
| well+GlacialTill | AISI 304 | 0.02 | OFF |
| | Glacial till | 0.05 | |
| | Glacial till | 0.1 | |
| | Glacial till | 0.2 | |
| | Glacial till | 0.4 | |
| | Glacial till | 0.8 | |
| | Glacial till | 1.6 | |
| | Glacial till | 3.5 | |
| | Glacial till | 7 | |
| | Glacial till | 14 | |
| | Glacial till | 28 | |
| | Glacial till | 56 | |
| well+shale | AISI 304 | 0.02 | OFF |
| | Shale | 0.05 | |
| | Shale | 0.1 | |
| | Shale | 0.2 | |
| | Shale | 0.4 | |
| | Shale | 0.8 | |
| | Shale | 1.6 | |
| | Shale | 3.5 | |
| Shale | 7 | | |

| | | | | |
|----------------|-----------|------|--|-----|
| | Shale | 14 | | |
| | Shale | 28 | | |
| | Shale | 56 | | |
| well+limestone | AISI 304 | 0.02 | | OFF |
| | Limestone | 0.05 | | |
| | Limestone | 0.1 | | |
| | Limestone | 0.2 | | |
| | Limestone | 0.4 | | |
| | Limestone | 0.8 | | |
| | Limestone | 1.6 | | |
| | Limestone | 3.5 | | |
| | Limestone | 7 | | |
| | Limestone | 14 | | |
| | Limestone | 28 | | |
| | Limestone | 56 | | |
| well+dolomite | AISI 304 | 0.02 | | OFF |
| | Dolomite | 0.05 | | |
| | Dolomite | 0.1 | | |
| | Dolomite | 0.2 | | |
| | Dolomite | 0.4 | | |
| | Dolomite | 0.8 | | |
| | Dolomite | 1.6 | | |
| | Dolomite | 3.5 | | |
| | Dolomite | 7 | | |
| | Dolomite | 14 | | |
| | Dolomite | 28 | | |
| | Dolomite | 56 | | |

6. Boundary Conditions

6.1 Nodes

| Label | Type | GMF |
|-------|--------|-----|
| WH | CLOSED | -1 |
| BH | CLOSED | -1 |

6.2 Heattransfer

| Branch | Pipe | Interpolation | Houteroption. | Hambient |
|---------------|------|---------------|---------------|----------|
| StateCharlton | ALL | LENGTH | HGIVEN | 100 |

6.3 Initial Conditions

| Branch | Pipe | Mass Flow | WaterCu t |
|---------------|------|-----------|--------------|
| StateCharlton | ALL | 0 | 0 |

6. 4 Sources

| Label | Abs. Pos. | Branch | Pipe | Section | Massflow | Type | Time | Temperature | GMF | Gas fraction eq | Oil fraction eq | water fraction eq |
|-----------|-----------|---------------|--------|---------|--|------|---|--|--|-----------------|-----------------|-------------------|
| CO2Source | | StateCharlton | PIPE-1 | 1 | (25000, 25000, 28125, 28125, 25000, 25000, 20833, 20833, 16666.67, 16666.67, 12500, 12500, 0) kg/h | MASS | (0, 101.5, 101.51, 102.07, 102.08, 102.58, 102.59, 103.02, 103.03, 104.02, 104.03, 108, 108.02) h | (4.44, 4.44, 4.44, 4.44, 4.44, 4.44, 4.44, 4.44, 4.44, 4.44, 4.44) | (-1, -1, -1, -1, -1, -1, -1, -1, -1, -1, -1, -1, -1) | 1 | 1 | 1 |

6. 5 Wells

| Label | Abs. Pos. | Branch | GMF | Inj. option | Prod. option |
|--------|-----------|---------------|-----|-------------|--------------|
| WELL-1 | 1050 | StateCharlton | -1 | LINEAR | LINEAR |

7. Equipment

7. 1 Position

| Label | Branch | Abs. Pos. |
|------------------|---------------|-----------|
| StartPerforation | StateCharlton | 1049 |
| EndPerforation | StateCharlton | 1071 |
| BHGauge | StateCharlton | 1048 |